Published in final edited form as:
*Compr Physiol*. 2013 October ; 3(4): 1553–1567. doi:10.1002/cphy.c130003.

# Mechanical Properties of Respiratory Muscles

**Gary C. Sieck, Ph.D.**[1,2], **Leonardo F. Ferreira, Ph.D.**[3], **Michael B. Reid, Ph.D.**[3], and **Carlos B. Mantilla, M.D., Ph.D.**[1,2]

[1]Department of Physiology & Biomedical Engineering, Mayo Clinic, Rochester, MN 55905

[2]Department of Anesthesiology, Mayo Clinic, Rochester, MN 55905

[3]Department of Physiology, University of Kentucky, Lexington, KY

## Abstract

Striated respiratory muscles are necessary for lung ventilation and to maintain the patency of the upper airway. The basic structural and functional properties of respiratory muscles are similar to those of other striated muscles (both skeletal and cardiac). The sarcomere is the fundamental organizational unit of striated muscles and sarcomeric proteins underlie the passive and active mechanical properties of muscle fibers. In this respect, the functional categorization of different fiber types provides a conceptual framework to understand the physiological properties of respiratory muscles. Within the sarcomere, the interaction between the thick and thin filaments at the level of cross-bridges provides the elementary unit of force generation and contraction. Key to an understanding of the unique functional differences across muscle fiber types are differences in cross-bridge recruitment and cycling that relate to the expression of different myosin heavy chain isoforms in the thick filament. The active mechanical properties of muscle fibers are characterized by the relationship between myoplasmic $Ca^{2+}$ and cross-bridge recruitment, force generation and sarcomere length (also cross-bridge recruitment), external load and shortening velocity (cross-bridge cycling rate), and cross-bridge cycling rate and ATP consumption. Passive mechanical properties are also important reflecting viscoelastic elements within sarcomeres as well as the extracellular matrix. Conditions that affect respiratory muscle performance may have a range of underlying pathophysiological causes, but their manifestations will depend on their impact on these basic elemental structures.

### Keywords

Muscle physiology; Respiratory physiology; Contraction; Skeletal muscle; Fatigue

---

This review is part of an initiative by the American Physiological Society that extends the classic *Handbook of Physiology* series. The original *Handbook* was created almost a half-century ago to provide "…a critical, comprehensive presentation of physiological knowledge and concepts" (112). The respiratory muscles were mentioned in chapters on respiratory system anatomy, mechanics, and neural regulation. Existing information was largely limited to respiratory muscle structure and function at the whole-body and tissue levels. Two decades later, the *Handbook* was revised and expanded (253). New chapters were dedicated to the mechanical and electrical properties of respiratory muscle, respiratory muscle energetics, and inspiratory muscle fatigue. Traditional concepts of muscle cell biology – fiber type, metabolic properties, sarcolemmal excitability – were integrated with data from intact animals and humans to broaden our understanding of respiratory muscle function.

Since then, interest in respiratory muscles has exploded. A search of the PubMed data base (http://www.ncbi.nlm.nih.gov/pubmed) using the term 'respiratory muscle' identified fewer

than 11,000 reports published in the century prior to 1985. In the succeeding 24-year period, from 1986-2010, over 25,000 manuscripts on respiratory muscles have been published. This shows that investigators recognize the critical importance of respiratory muscles in health and disease. Researchers have learned that the functional properties of respiratory muscles and their limits to performance can differ markedly from limb muscles. The cellular physiology of respiratory muscles has become a major focus of research. Emerging technologies and contemporary biological tools have allowed investigation of the biochemical and molecular mechanisms that define respiratory muscle mechanics. In this review, discoveries made over the last quarter century have been combined with concepts of enduring value to provide a comprehensive perspective on respiratory muscle mechanics.

## Respiratory Muscle Types

### Pump muscles

Breathing is mediated by the concerted action of "pump" muscles of the chest wall (i.e., the thorax and the abdomen) that change intrathoracic pressure. The pump muscles act to change transthoracic pressure thereby altering lung volume, causing air to flow in or out of the lungs. The pump muscles are essential for breathing and are major determinants of respiratory mechanics.

The pump muscles consistently active with inspiratory or expiratory efforts are categorized as "primary" respiratory muscles. Those muscles recruited only occasionally with increased inspiratory or expiratory efforts are termed accessory respiratory muscles. Classification of primary and accessory respiratory muscles can vary across species. In humans, the primary inspiratory pump muscles include the diaphragm and parasternal intercostal muscles that act to expand the chest wall. Muscles such as the sternocleidomastoid, scalenes and triangularis sterni that also act on the chest wall are accessory, since they are recruited only with increased inspiratory effort. In fact, activation of these accessory inspiratory muscles is an important clinical sign of inspiratory loading.

In humans, expiration is typically passive requiring no muscle activity, but driven by the elastic recoil of the lung and chest wall. During forced expiration, abdominal muscles are activated to increase intraabdominal pressure (184, 254, 310). Accordingly, abdominal muscles are classified as accessory respiratory muscles, and their recruitment is also used in the clinical setting as an indicator of respiratory loading.

### Upper airway muscles

Dilator muscles of the pharynx and larynx minimize upper airway resistance during inspiration, thus facilitating airflow into and out of the lungs (87, 257, 447, 448, 450). The pharynx is collapsible and subatmospheric pressures generated in the airway lumen during inspiration can cause airway narrowing and in some cases occlusion (e.g., obstructive sleep apnea) (443, 448, 472). Airway patency is maintained during breathing by tightly coordinated co-activation of respiratory pump muscles and muscles of the upper airways.

The main airway dilator muscle of the pharynx is the genioglossus. Contraction of the genioglossus muscle depresses and protrudes the tongue, thereby opposing obstruction of the posterior pharynx during breathing (368). However, contraction of the genioglossus alone is not sufficient to prevent narrowing of the upper airway in humans (87, 307, 308).

The position of the hyoid bone strongly influences upper airway resistance. The hyoid is not connected directly to any other skeletal structure; thus, making it highly mobile (442). If posterior movement of the hyoid is not opposed during inspiration, it can increase airway resistance and limit airflow. However, contraction of some of the extrinsic muscles of the

neck including the sternothyroid, thyrohyoid, sternohyoid, and geniohyoid results in dilation of the upper airways (447). For example, simultaneous contraction of the sternohyoid and geniohyoid move the hyoid bone in the anterior direction, thus dilating the upper airway (306, 448, 472). The mylohyoid and digastrics are non-dilator muscles (306), while contraction of the omohyoid muscle is likely to constrict the upper airway through posterior displacement of the hyoid bone.

In the larynx, the posterior cricoarytenoid muscle abducts the arytenoid cartilages and separates the vocal cords, thereby increasing glottal diameter and facilitating airflow (17, 81, 201). Other non-dilator and constrictor muscles play important roles in non-respiratory actions of the upper airways, e.g., swallowing and phonation (447).

Twitch and tetanic mechanical characteristics have been determined for the geniohyoid, sternohyoid, and genioglossus muscles (70, 449, 451-453). Other studies have established the fiber type composition and metabolic characteristics of upper airway dilator muscles in animals and humans (51, 183, 247, 306, 368, 450, 454, 457, 480). Overall, muscles of the upper airways have faster twitch characteristics than the diaphragm. During normal breathing, upper airway muscles contract isometrically (448) and maintain patency of the upper airway with approximately the same diameter as in the absence of respiratory drive. Measurements of whole muscle mechanics are consistent with histochemical analyses that show a predominance of type II fibers in the genioglossus, geniohyoid, and sternohyoid muscles (51, 306, 451). Single fiber function from non-dilator (vocal) laryngeal muscles is consistent with those of skeletal muscles in general (81). To our knowledge, the mechanical properties of upper airway muscles have not been studied at the single fiber level.

This article addresses the mechanical properties of respiratory pump muscles, with a special focus on the diaphragm as the primary muscle of inspiration. Other respiratory muscles will be discussed where differences among muscles may illustrate useful concepts or influence the mechanics of breathing.

## Respiratory Muscle Structure

Three major regions of the diaphragm muscle are recognized by the origin of their muscle fibers. Muscle fibers in the sternal region originate from the xyphisternal junction. Fibers in the costal region originate from the lower rib cage. Fibers in the crural region originate from the upper lumbar vertebrae. In each of these diaphragm muscle regions, fibers insert into the central tendon. In the sternal region, the orientation of fibers is generally parallel. In the costal region, the circumference of the costal margin is longer than that of the central tendon insertion, thus, the orientation of fibers radiate outward from the central tendon. The orientation of fibers in the crural region is far more complex as they encompass the esophagus, serving as an esophageal sphincter. Of physiological importance is the fact that the descending aorta and inferior vena are not encompassed by diaphragm muscle fibers as they traverse between thoracic and abdominal cavities. In smaller animals such as rats and mice, diaphragm muscle fibers extend from origin to insertion reaching lengths exceeding 20 mm. In larger species such as cats, dogs, and humans, diaphragm muscle fibers do not extend the full length of the muscle but instead, have intramuscular tendinous insertions (147, 375).

Mechanical effects of fiber activation in different regions of the diaphragm muscle depend on the specific origins and insertions of fibers, and the varying loads imposed by ribcage and abdominal displacement (43, 86). Differences between mechanical effects of different diaphragm regions led to the suggestion that the costal and crural regions are actually different muscles, with different embryonic origins and neural innervation (85, 86). With respect to embryonic origin, Greer and colleagues reported an elegant series of studies

clearly demonstrating that all regions of the diaphragm muscle have similar embryonic origin (4, 11, 165). A systematic evaluation of diaphragm innervation using glycogen depletion techniques clearly demonstrated considerable overlap in the cervical segmental innervation of diaphragm fibers across regions (117, 386, 391). For example, phrenic nerve axons from higher cervical levels innervate more ventral aspects of the costal and crural regions, while axons from lower cervical levels innervate more dorsal aspects of both diaphragm regions (Figure 1).

## Sarcomeric structure and contractile proteins

The basic structural unit of a skeletal muscle fiber is the sarcomere, comprising thick (myosin) and thin (actin) filaments aligned in an interdigitating, crystalline structure. The sarcomere itself is bounded at each end by a dense Z-disc (Z-line) from which the actin filaments project toward the midline, while thick filaments are situated in the middle of the sarcomere (Figure 2). Myosin molecules of the thick filaments bind with actin molecules of the thin filament to form cross-bridges that are the essential units of force generation and contraction – the two primary functions of muscle fibers. The Z-disc runs perpendicular to the filaments and connects neighboring sarcomeres, creating a functional unit that permits transmission of lateral and longitudinal force during contraction. The dimension of each sarcomere is approximately 1 μm in diameter and ~2.5 μm in length (Z-line to Z-line). The overlap between thick and thin filaments determines the number of cross-bridges that can be formed during muscle contraction. The thick filament has a relatively fixed length of ~1.6 μm, while the thin filament length ranges between 1.0-1.3 μm and is species and fiber type-dependent. During muscle fiber contraction, the intrinsic lengths of both the thick and thin filaments does not change, but the binding of the myosin head to actin pulls the Z-line of the sarcomere toward the midline thus increasing the overlap between thick and thin filaments. The number of sarcomeres in series can vary but generally does not exceed ~20 mm (~8,000 sarcomeres in series).

The structural organization of the sarcomere appears crystalline with a fixed stoichiometry between the number of thick and thin filaments. This crystalline structure of the sarcomere is evident in electron microscopic images and by X-ray diffraction. In cross-sections of skeletal muscle fibers, each myosin filament is surrounded by six actin filaments, which are further surrounded by six myosin filaments. The spacing between each myosin and actin filament is relatively fixed in a lattice structure. Thus, this arrangement creates a double hexagonal array forming a myofilament lattice (Figure 2). Understanding the thick and thin filament spacing in this myofilament lattice is key to understanding the interactions between thick and thin filaments during skeletal muscle force generation and contraction. The filament lattice provides stability to the sarcomere and balances radial and axial forces placed upon it. Since the sarcomere is encompassed by the sarcolemma, muscle fiber osmolarity shifts caused by changes in ion concentrations across the membrane can result in osmotic compression of the lattice and change the spacing between thin and thick filaments. Under hypertonic conditions, lattice spacing and muscle force generation are decreased. Conversely, under hypotonic conditions, lattice spacing increases and may lead to a decrease in force.

**Myosin Heavy Chain (MyHC)—**The myosin molecule is a hexameric protein with two heavy and four light chains. At its C-terminus, the two heavy chains dimerize into an alpha-helical tail and at the N-terminus, the heavy chains separate and form two distinct heads that serve both as the actin binding and catalytic domains (79, 340). Several MyHC isoforms exist, encoded by a highly conserved family located on chromosome 17 (human) or 11 (mouse) (367). The MyHC isoform composition of muscle fibers forms the basis for fiber type classification with a general correlation to histochemical classification based on the pH

lability of myofibrillar adenosine triphosphatase (mATPase) (15, 148, 365, 430). Rates of ATP hydrolysis vary across MyHC isoforms, contributing to fiber type differences in cross-bridge cycling kinetics (393-395, 412).

**Myosin Light Chain—**Myosin light chains are divided into essential ($MyLC_{20}$) and regulatory ($MyLC_{17}$) proteins that provide structural support and modulation of mechanical performance, respectively (339, 349). The extent of the regulatory role of $MyLC_{17}$ remains controversial, but there is evidence that $MLC_{17}$ phosphorylation and perhaps $Ca^{2+}$ binding may modulate MyHC ATPase activity and thus, cross-bridge cycling kinetics and velocity of shortening (91, 161, 162, 319, 324).

**Thin filament proteins—**Thin filaments attach to the Z-line and serve as the insertion point for muscle contraction. In skeletal and cardiac muscle fibers, $Ca^{2+}$ binding to the regulatory protein troponin C (TnC) removes the steric hindrance that prevents binding of the myosin head (MyHC) to actin, and thus, cross bridge formation and force generation. Thus, $Ca^{2+}$ binding to TnC underlies excitation-contraction coupling and the dependency of force on myoplasmic $Ca^{2+}$ concentration [$Ca^{2+}$]. The number of $Ca^{2+}$ binding sites differ between fast (TnC-f – 2 binding sites) and slow (TnC-s 1 binding) TnC isoforms. Accordingly, there are differences in $Ca^{2+}$ binding affinities between TnC isoforms that are reflected in fiber type differences in force/[$Ca^{2+}$] relationships. For example, the force/[$Ca^{2+}$] relationship of slow fibers is less steep and is shifted to the left (higher $Ca^{2+}$ sensitivity) when compared to that of fast fibers (130, 131). It has been shown that when the TnC-f present in fast (rabbit psoas) fibers is substituted with the TnC-s isoform, the force/pCa relationship of these fibers is altered to reflect the newly constituted TnC-s isoform (52, 296). Other troponin subunits (TnI or TnT) may also contribute to the regulation of muscle contractility, but their role is not clear (58, 482). Both slow and fast isoforms of TnI and TnT are present in skeletal muscle and their expression is coupled to that of TnC. Thus, fibers expressing slow TnI and TnT isoforms have higher $Ca^{2+}$ sensitivity than fibers containing fast TnI and TnT isoforms. However, whether this properly reflects the individual properties of the different subunits or results from the coupled expression across troponin subunit isoforms has not been elucidated.

## Fiber type classification

**Myofibrillar ATPase—**In adults, skeletal muscle fibers can be classified using histochemical techniques that are based on the pH lability of staining for myofibrillar ATPase. After preincubating muscle sections at acid vs. alkaline pH, there are differences in myofibrillar ATPase staining across muscle fibers, allowing classification as type I, IIa and IIb fibers (37, 56, 375). As mentioned above, this histochemical classification has been shown to correlate with MyHC isoform content of muscle fibers in both immunohistochemical and single fiber biochemical studies (358, 384, 386, 387).

**Metabolic activity—**An earlier histochemical classification scheme relied on differences in fiber staining for metabolic enzymes related to oxidative or glycolytic capacities. Accordingly, fibers were initially classified as slow (type S) or fast (type F) based on differences in myofibrillar ATPase staining, with further subclassification of type F fibers based on relative differences in staining for oxidative and glycolytic enzymes (325). In this classification scheme, type S fibers display more intense staining for oxidative enzymes but lower staining intensity for glycolytic enzymes; thereby classified as slow-twitch oxidative (SO) fibers. Type F fibers display higher staining for glycolytic enzymes but vary in their staining for oxidative enzymes. Accordingly, type F fibers that display higher relative staining intensity for oxidative enzymes are classified as fast-twitch-oxidative-glycolytic (FOG) whereas type F fibers that display lower relative staining for oxidative enzymes are

classified as fast-twitch-glycolytic (FG) (325). One major problem with this classification scheme is the subjective nature of assessing relative staining for oxidative and glycolytic enzymes. In this regard, methods were developed to quantify both actomyosin ATPase and succinate dehydrogenase activities (35, 37, 275). Using these quantitative techniques, a number of studies have shown that the metabolic properties of diaphragm muscle fibers are continuous and highly plastic under a variety of conditions (36, 204, 237, 377, 381, 389, 390, 466).

**Myosin heavy chain isoform expression—**The histochemical classification schemes generally correlate with the expression of different MyHC isoforms in muscle fibers such that fibers classified as type I (or type S) express the $MyHC_{Slow}$ isoform, whereas fibers classified as type IIa (type FOG) express $MyHC_{2A}$, fibers classified as type IIx (type FOG or FG) express $MyHC_{2x}$, and fibers classified as type IIb (type FG) express either $MyHC_{2B}$ alone or together with $MyHC_{2X}$ (15, 149, 366, 367, 380, 387, 389). In particular, the classification of type II fibers is challenging with histochemical techniques. Specific antibodies for all adult MyHC isoforms exist except for the $MyHC_{2X}$ isoform (365). Immunoreactivity for MyHC antibodies is now the method of choice to classify fiber types since it is less ambiguous and relates back to the molecular basis for differences in mechanical properties of different fiber types.

Using Western blot analysis, it has been shown that under normal conditions rat diaphragm muscle fibers generally express a single MyHC isoform, with one exception: the frequent co-expression of $MyHC_{2X}$ and $MyHC_{2B}$ (Figure 3). However, with aging or under pathophysiological conditions, the incidence of MyHC isoform co-expression increases, and classification of a unique “fiber type” becomes more difficult (135, 151, 206, 262, 397, 455, 466, 468). Under these conditions, single fiber analyses have generally shown a higher incidence of certain patterns of MyHC isoform co-expression; for example, $MyHC_{Slow}$ together with $MyHC_{2A}$, $MyHC_{2A}$ together with $MyHC_{2X}$ and $MyHC_{2X}$ together with $MyHC_{2B}$ (400).

**Fiber type composition of the diaphragm muscle—**In a number of species, the diaphragm muscle has been shown to comprise all fiber types, but the relative proportions vary (116, 208, 360, 380, 389). There are relatively few studies that have examined fiber type distribution in the human diaphragm muscle. These studies employed immunohistochemical techniques (235, 303), and surprisingly reported expression of neonatal and embryonic MyHC isoforms in adult biopsies. Unfortunately, these studies were not systematic, relying on limited sampling of biopsy material in relatively few subjects. The expression of neonatal and embryonic MyHC isoforms in the adult human diaphragm muscle needs to be further explored since it is inconsistent with all other mammalian species that have been examined.

**Fiber type classification during postnatal development—**During fetal and early postnatal development classification of muscle fiber types is more difficult. During this period there are transitions in MyHC isoform expression, with a high incidence of co-expression of MyHC isoforms that precludes clear distinction of muscle fiber types (231, 232, 465, 468). In the fetal mouse and rat diaphragm muscle, an embryonic MyHC isoform ($MyHC_{Emb}$) is abundantly expressed together with $MyHC_{Slow}$ and $MyHC_{2A}$ isoforms. During the perinatal period, there is a transient increase in expression of a neonatal MyHC isoform ($MyHC_{Neo}$), while expression of the $MyHC_{Emb}$ decreases. Subsequently, expression of the $MyHC_{Neo}$ gradually disappears in the mouse and rat diaphragm muscle and is totally absent by postnatal day 28. Expression of the adult $MyHC_{2X}$ and $MyHC_{2B}$ isoforms appears only by the second postnatal week in both the mouse and rat diaphragm muscle, and the proportion of fibers expressing these isoforms increases until the fourth

postnatal week, when the adult pattern of MyHC isoform expression is fully established (136). These postnatal transitions in MyHC isoform expression in the rodent diaphragm muscle are accompanied by changes in muscle contractile properties – most notably an increase in maximum specific force and shortening velocity (132, 151). After weaning at postnatal day 21, the relative growth of fibers expressing $MyHC_{2X}$ and $MyHC_{2B}$ is far greater than that of fibers expressing $MyHC_{Slow}$ and $MyHC_{2A}$ isoforms (206, 330). Thus, the relative contributions of these fiber types to total diaphragm muscle mass increases (132, 136). It is likely that the pattern of innervation exerts a major influence on the differentiation and growth of diaphragm muscle fibers either directly (e.g., activation patterns) or indirectly (e.g., release of neurotrophic factors) (397). However, the precise mechanisms by which activation history and/or neurotrophic factors affect diaphragm muscle development are poorly understood.

Among the many factors that may influence muscle fiber type differentiation, it has been suggested that class II histone de-acetylases (HDACs) may contribute by inhibiting the myocyte enhancer factor-2 (MEF2) family of transcription factors (283). MEF2 mediated gene transcription is regulated by p38 MAP kinase signaling, but the role of MEF2 in the developmental determination of muscle fiber type is still unknown. Recently, postnatal changes in MyHC isoform mRNA transcription were found to be regulated by a natural antisense transcript (bII NAT) such that expression of $MyHC_{Neo}$ is positively correlated with expression of bII NAT whereas expression of $MyHC_{2B}$ is negatively correlated. Thus, postnatally expression of bII NAT can play a critical role in coordinating the transition from $MyHC_{Neo}$ to adult $MyHC_{2B}$ (and possibly $MyHC_{2X}$) isoforms (315). Recently, it was shown that postnatal changes in MyHC isoform mRNA expression in the rat diaphragm muscle do not match the changes in MyHC protein expression, suggesting that changes in MyHC isoform expression in the developing rat diaphragm muscle are not driven solely by changes in mRNA expression (136). Furthermore, myonuclear domain size (reflecting the volume of myoplasm under transcriptional control by a single myonucleus) increased postnatally as fiber cross-sectional area increased, indicating that changes in transcriptional activity (although present) do not exclusively determine the postnatal growth of diaphragm muscle fibers (136, 262).

**Fiber type classification and motor unit organization—**In adults, muscle fiber types are functionally organized by their motor innervation into different motor units, defined as a single motoneuron and the group of muscle fibers it innervates (92, 245). Normally, muscle fibers within a motor unit are a single type, sharing similar contractile protein composition and metabolic enzyme activities that influence the contractile and fatigue properties of motor units (Figure 4) (63, 380, 390). Diaphragm motor units that comprise type I fibers (expressing $MyHC_{Slow}$ with high oxidative enzyme activity) display slower contractile properties and are more fatigue resistant. Motor units comprising type IIa fibers (expressing $MyHC_{2A}$ with higher oxidative and glycolytic enzyme activities) display faster contractile properties and are also more fatigue resistant. Motor units comprising type IIx fibers (expressing $MyHC_{2X}$ with higher glycolytic enzyme activity but lower oxidative enzyme activity) display faster contractile properties but are more susceptible to fatigue. Finally, motor units comprising type IIb fibers (expressing $MyHC_{2B}$ usually in combination with $MyHC_{2X}$ with higher glycolytic capacity but the lowest oxidative enzyme activity) display faster contractile properties but are the most susceptible to fatigue (389). Studies examining the mechanical properties of single permeabilized diaphragm muscle fibers have clearly demonstrated an association between MyHC isoform composition, specific force and shortening velocity (130, 131, 394).

### Structural Proteins

**Z-line proteins—**The most obvious element of the striated structure of skeletal and cardiac muscle is the Z-lines as the densest sarcomeric component. It takes its name for the German "Zwischenscheibe", meaning spacer in the case of muscle fibers between sarcomeric contractile elements. The Z-line splits the I (isotropic) band which is made of thin filaments, as opposed to the M-line which binds thick filaments together in the A (anisotropic) band. The major proteins in the Z-line include the actin-binding α-actinin, the actin-capping protein CapZ, as well as Z-nin, Z protein, zeugmatin and myozenin (417, 425). Other filament proteins including titin, which extends from the M line to the Z line, and nebulin, which forms inextensible filaments associated with thin filaments, also insert at the Z-line. Titin and nebulin may contribute to passive properties of striated muscle by providing both elastic and inextensible templates for thick and thin filaments, respectively. Titin interacts with many sarcomeric proteins including telethonin and α-actinin at the Z-line, calpain and obscurin in the I-band region and myosin-binding protein C, calmodulin 1, CAPN3, and MURF1 within the A-band and at the M-line (14). Within the I-band, titin contains IgG and proline-glutamate-valine-lysine (PEVK) regions that confer extensibility. Based on its insertion and elastic "spring-like" properties, titin helps stabilize myosin filaments in a central location relative to the thin filaments during contraction (125). Changes in titin expression or stiffness may contribute to developmental adaptations in mechanical properties (314) and impaired diaphragm muscle function in adult patients with COPD (312).

## Cross-bridge Formation and Muscle Fiber Mechanical Properties

### Sliding filament theory

The sliding filament theory resulted from independent seminal observations in the labs of A.F Huxley and H.E. Huxley in 1954 in which they used interference light microscopy to observed a decrease in sarcomere length and most notably, in I-band length during muscle contraction (191, 195). Subsequently, the cross-bridge model for muscle contraction was proposed (192, 194) in which cross-bridges cycle between two functional states: 1) A force generating state in which myosin heads (MyHC cross-bridges) are strongly attached to actin and via a power stroke generate force; and 2) A non-force generating or detached state in which the myosin head is detached from actin. Thus, a cross-bridge is the essential element of force generation and movement. Relaxation results from cross-bridges detaching from actin and thereby transitioning to a non force generating state. This is a grossly simplified model, but it is useful in assessing force generation and contraction of muscle fibers.

**Conceptual framework for force generation—**The transitions between functional cross-bridge states can be simply described by two apparent rate constants (Figure 5): one for cross-bridge attachment ($f_{app}$) and a second for cross-bridge detachment ($g_{app}$). With an increase in myoplasmic [$Ca^{2+}$], the binding site for MyHC on the actin filament is exposed by removal of steric hindrance leading to the attachment of cross-bridges and force generation (described by $f_{app}$). With the removal of myoplasmic [$Ca^{2+}$] and ATP hydrolysis (actomyosin ATPase), cross-bridges transition to a non-force-generating state (described by $g_{app}$).

Although the transduction of chemical to mechanical energy during the cross-bridge cycle is likely to involve multiple steps, Brenner proposed a simpler analytical framework that is based on Huxley's two-state model (53-55). In this analytical framework, the steady-state fraction of strongly-bound cross-bridges in the force generating state ($\alpha_{fs}$) is given by:

$$\alpha_{fs}=f_{app}/(f_{app}+g_{app})$$

Geiger et al (131) estimated $\alpha_{fs}$ during maximum $Ca^{2+}$ activation in single permeabilized fibers in the rat diaphragm muscle by imposing small amplitude sinusoidal length perturbations (0.2% of optimal length at 2 kHz) and measuring the recoil force (fiber stiffness). In the absence of ATP (rigor condition), it was assumed that all available cross-bridges would be attached and that maximum stiffness would be achieved. By normalizing to this maximum stiffness, it was observed that $\alpha_{fs}$ during maximum $Ca^{2+}$ activation was approximately 75-80% with no difference across fiber types.

Taking into account the number of myosin heads in parallel per half sarcomere or MyHC content per half sarcomere (n), and the mean force per cross-bridge (*F*), the force generated by a muscle fiber can be described by:

$$\text{Force}=n \cdot F \cdot \alpha_{fs}$$

With an increase in fiber cross-sectional area the MyHC content per half sarcomere (n) increases and thus the number of potential cross-bridges per half sarcomere increases. To account for this relationship, it is common practice to normalize the force generated by a muscle fiber by the cross-sectional area of the muscle (specific force). However, this assumes that MyHC content per half-sarcomere is directly proportional to fiber cross-sectional area. This assumption was challenged by direct measurements of MyHC content per half-sarcomere in the rat diaphragm muscle (131). In this study, it was shown that type I and IIa fibers had similar MyHC contents per half-sarcomere and that these were lower than those of type IIx and IIb fibers. When maximum force was normalized for MyHC content per half-sarcomere, the force of type I fibers was lower than that of all type II fibers and there were no differences in normalized force across type II fibers. Force normalized for MyHC content per half-sarcomere thus reflects the average force per cross-bridge (*F*).

In single muscle fibers, the number of myosin heads per half sarcomere (n) can be estimated based on electrophoretic separation of MyHC from a known volume of muscle fiber to determine MyHC concentration. If the length and cross-sectional area of the single fiber segment is measured (to determine fiber volume), and the number of sarcomeres in series are counted, MyHC content per half sarcomere can be derived (131). This relatively simple measure can be extrapolated further by assuming parameters for the length of the thick filament and the distance between myosin heads, which yields approximately 300 myosin heads per myosin filament. With relatively fixed thick-thin lattice spacing in muscle fibers, the number of myosin heads can be calculated. For example, in a muscle fiber with a cross-sectional area of 1,500 $\mu m^2$, there are approximately 1 million myosin filaments and 300 million myosin heads. Thus, the MyHC content (number of myosin heads) per half sarcomere volume (n) was estimated to be ~400 myosin heads per $\mu m^3$ half sarcomere volume.

The specific force of single permeabilized diaphragm muscle fibers during maximum $Ca^{2+}$ activation at 37°C is ~30 $Ncm^{-2}$. Based on the estimated number of myosin heads per half sarcomere (n), and an $\alpha_{fs}$ of 80%, the force per myosin head or cross-bridge (*F*) is ~0.5 pN. However, the estimated force per cross-bridge is ~45% lower in type I fibers compared to all fast fiber types (131). The molecular basis for this fiber type difference in force per cross-bridge is unclear.

The force generated by a muscle fiber is primarily regulated by affecting the fraction of cross-bridges recruited (changing $\alpha_{fs}$) either by changing muscle fiber length or intracellular $Ca^{2+}$ concentration ($[Ca^{2+}]_i$). The fraction of cross-bridges in a strongly-bound state ($\alpha_{fs}$) can be estimated by measuring muscle fiber stiffness (131-134, 174). As the number of cross-bridges formed increases, longitudinal stiffness of the muscle fiber also increases. Stiffness is determined by stretching single muscle fibers using high frequency (2 kHz), small amplitude (0.01% of $L_o$) length oscillations and then measuring recoil force (Figure 6). Such small amplitude length perturbations do not disrupt cross-bridge binding, and the high frequency oscillations exceed the cross-bridge cycling rate, thereby minimizing hysteresis. Under these conditions, muscle fiber stiffness reflects the number of strongly bound cross-bridges, at different muscle fiber lengths and/or $Ca^{2+}$ activation conditions that affect cross-bridge recruitment and $\alpha_{fs}$. To induce maximum recruitment of strongly bound cross-bridges, permeabilized muscle fibers are exposed to a “rigor” solution that contains higher $Ca^{2+}$ concentration (e.g., pCa of >4.0) but does not contain ATP. Muscle fiber stiffness is then normalized to the maximum rigor condition. Using this approach, ~75-80% of cross-bridges are recruited during optimal conditions of $L_o$ and maximum $Ca^{2+}$ activation. Muscle fiber stiffness can also be measured under submaximal conditions of fiber length or $Ca^{2+}$ activation, and generally measurements of fiber stiffness parallel measures of muscle force generation. There are no apparent differences in $\alpha_{fs}$ across fiber types during maximum or submaximal $Ca^{2+}$ activation.

Muscle weakness under a variety of conditions, is reflected by a decrease in specific force. For example, the diaphragm muscle is generally weaker (reduced specific force) during early postnatal development (132, 206, 385, 392, 464, 468, 485) and during old age (99, 151) compared to adults. Similarly, diaphragm muscle specific force is reduced following muscle denervation (133, 240, 386, 397, 484) and under conditions of sepsis (39, 83, 473), hypothyroidism (134, 154, 263) and corticosteroid treatment (237, 241, 445). In these conditions, the simplified two-state model of force generation provides a conceptual framework to assess possible underlying mechanisms for muscle weakness. For example, diaphragm muscle fiber weakness induced by denervation is associated with reduced MyHC content per half sarcomere (n) and a decrease in the average force per cross-bridge (*F*) (133). However, $\alpha_{fs}$ is not affected by denervation. Similarly, hypothyroidism results in reduced MyHC content per half sarcomere but no change in the average force per cross-bridge or $\alpha_{fs}$ (134). Obviously, the balance between MyHC protein synthesis and degradation is extremely important in respiratory muscles and underlies functional changes leading to muscle weakness under a variety of conditions.

**Fiber type differences in atrophy and muscle weakness—**It is well known that under a variety of conditions, diaphragm muscle fiber cross-sectional area can change (hypertrophy or atrophy); however the change in MyHC content per half-sarcomere has received little attention. Disproportionate changes in MyHC content per half-sarcomere may underlie changes in specific force that are often noted. For example, during postnatal development there is an increase in diaphragm muscle specific force concurrent with substantial growth in diaphragm muscle fibers. The increase in the cross-sectional area in the developing rat diaphragm muscle is disproportionate across fiber types, with a larger increase for type IIx and IIb fibers compared to type I or IIa fibers (132). Of more importance, during postnatal growth of the rat diaphragm muscle, there is a disproportionate increase in MyHC content per half-sarcomere in type IIx and IIb fibers compared to type I or IIa fibers leading to a greater increase in normalized force (per MyHC content per half-sarcomere) in these fibers. Similarly in the adult diaphragm muscle, phrenic nerve denervation leads to selective atrophy of type IIx and IIb fibers and a disproportionate decrease in MyHC content per half-sarcomere (133). Specific force (normalized per cross sectional area) does not reflect the reduction in contractile protein content but force

normalized per MyHC content per half-sarcomere does unveil a fundamental effect on force per cross-bridge. A change in MyHC content per half-sarcomere in diaphragm muscle fibers may underlie reductions in force generation in other pathophysiological conditions as well – e.g., hypothyroidism (134).

## Fiber type differences in $Ca^{2+}$ sensitivity of force generation

As mentioned above, force generation depends on myoplasmic $Ca^{2+}$ concentration, and this dependency is evident in permeabilized muscle fibers by the force/pCa (-log [$Ca^{2+}$]) relationship (Figure 7). A leftward shift in this force/pCa relationship as is evident in diaphragm muscle fibers expressing $MyHC_{Slow}$ indicates a greater $Ca^{2+}$ sensitivity (130). It should be noted that all diaphragm muscle fibers expressing fast MyHC isoforms have similar force/pCa relationships. The pCa at which 50% of maximum force is generated ($PCa_{50}$) is commonly used as an index of the $Ca^{2+}$ sensitivity of muscle fiber force generation. In diaphragm muscle, fibers expressing $MyHC_{Slow}$ are more sensitive to $Ca^{2+}$ (lower $pCa_{50}$) compared to fibers expressing fast MyHC isoforms (130). Again, the simplified two-state model of force generation provides a valuable conceptual framework to interpret differences in $Ca^{2+}$ sensitivity across fiber types. In this model, the fraction of cross-bridges in a strongly bound state ($\alpha_{fs}$) depends on myoplasmic $Ca^{2+}$ concentration and this can be observed by changes in muscle fiber stiffness.

In skeletal muscle, myoplasmic $Ca^{2+}$ binds to troponin C (TnC), which is part of the troponin protein regulatory process on the thin filament that exposes the actin binding site to the myosin head. Thus, $Ca^{2+}$ binding to TnC simply acts to increase the probability of cross bridge formation by unmasking myosin binding sites on actin. There are different TnC isoforms in muscle fibers expressing fast MyHC (TnC-f) versus slow MyHC (TnC-s). The TnC-f isoform has two regulatory binding sites for $Ca^{2+}$ compared to one binding site for TnC-s. Fiber type differences also exist in the binding affinities of TnC for $Ca^{2+}$. These essential differences in TnC isoforms underlie fiber type differences in $Ca^{2+}$ sensitivity. For example, when TnC-f normally expressed in rabbit psoas muscle fibers is substituted with TnC-s, the force/pCa relationship shifts leftward indicating grater $Ca^{2+}$ sensitivity (52, 296).

In addition to TnC, the troponin complex also comprises TnI or TnT subunits. Ca2+ binding to TnC induces conformation changes in both TnI and TnT, which are required to remove the steric hindrance that tropomyosin presents for the myosin binding site on actin. Both slow and fast isoforms of TnI and TnT exist, generally conforming with TnC-s and TnC-f expression, and it has been reported that muscle fibers comprising slow TnI and TnT have greater $Ca^{2+}$ sensitivity than fibers expressing fast TnI and TnT isoforms (58).

**Fiber type differences in excitation-contraction coupling—**Excitation-contraction coupling in skeletal muscles, including the diaphragm and other respiratory muscles, begins with neuromuscular transmission, in which the motor neuron action potential is transmitted to muscle fiber to induce a transient increase in myoplasmic [$Ca^{2+}$]. Depolarization-induced release of ACh from the presynaptic nerve terminal causes depolarization of the postsynaptic motor endplate via binding of ACh to cholinergic receptors. The morphology of pre- and postsynaptic elements of the neuromuscular junction differs across fiber types in the diaphragm muscle. It has been clearly demonstrated that the diaphragm muscle is susceptible to neuromuscular transmission failure with repetitive nerve stimulation (2, 101, 205, 225, 258, 259, 264, 268, 332, 374, 396, 475), and that this susceptibility increases with the rate of nerve stimulation. In addition, the diaphragm is more susceptible to neuromuscular transmission failure in old age (226, 267, 331, 401), and under different pathophysiological conditions. At the single fiber level, it has been demonstrated that quantal release of ACh varies across fiber types, with quantal content being higher at type

IIx and/or IIb diaphragm fibers (100, 258, 359). The quantal release of ACh decreases rapidly with repetitive stimulation, and this may at least partially underlie fiber type differences in susceptibility to neuromuscular transmission. Type IIx and or IIb fibers are muscle more susceptible to neuromuscular transmission failure compared to type I or IIa fibers (205, 359).

With successful neuromuscular transmission, depolarization at the endplate generates propagating muscle fiber action potentials that are passively transmitted down transverse tubules (T-tubules) resulting in activation of voltage-gated $Ca^{2+}$ (dihydropyridine receptor - DHPR) channels in the T-tubules (115, 119, 193). The DHPR channels are associated with ryanodine receptor (RyR1) channels of the sarcoplasmic reticulum (SR) and depolarization-induced activation of DHPR channels allosterically activates RyR1 channel opening and SR $Ca^{2+}$ release and a transient increase in myoplasmic [$Ca^{2+}$]. The subsequent decrease in myoplasmic [$Ca^{2+}$] is mediated by a sarcoplasmic/endoplasmic reticulum $Ca^{2+}$ ATPase (SERCA) that actively pumps $Ca^{2+}$ back into the SR. In skeletal muscle, the protein phospholamban is associated with SERCA and serves to regulate the rate of $Ca^{2+}$ reuptake into the SR via phosphorylation (323). When phospholamban is not phosphorylated it is more closely associated with SERCA and the rate of SR $Ca^{2+}$ reuptake is reduced. Phosphorylation of phospholamban leads to its dissociation from SERCA, causing the rate of SR $Ca^{2+}$ reuptake to increase. Thus, the duration of the myoplasmic $Ca^{2+}$ transient can be modulated by the state of phospholamban phosphorylation, and the effect on force relaxation will affect the force-frequency response of the muscle fiber. Another SR protein, calsequestrin, binds $Ca^{2+}$ and thereby reduces the concentration of free $Ca^{2+}$ within the SR (120). The $Ca^{2+}$ concentration in the SR is normally much higher than the myoplasmic $Ca^{2+}$ concentration (10,000-fold). Thus, the SERCA pump must act against this large concentration gradient, and calsequestrin facilitates the activity of SERCA.

Fiber type differences in E-C coupling obviously exist, as evidenced by differences in contractile properties (145). Varying expression of DHPR and RyR isoforms and calsequestrin are reported across muscles of different fiber type composition, throughout the lifespan and in response to altered use (82, 122, 322). Most of these studies, however, have conducted analyses at the whole muscle and thus whether these differences reflect issues specifically related to fiber type is not clear.

## Muscle fiber shortening velocity

In addition to force generation, contraction or shortening is also a fundamental outcome of muscle fiber activation. As external load on a muscle increases, the velocity of shortening decreases. When the force generated by a muscle equals the external load, no shortening occurs, but maximum force is generated ($F_{max}$ or $P_o$) assuming optimal sarcomere length.

**Conceptual framework based on thermodynamics—**In his classic paper A.V. Hill described the hyperbolic relationship between the force generated by muscle and velocity of shortening (181). The initial focus of his study was to understand the relationship between the heat produced by muscle during shortening under constant load conditions. Experimentally, Hill systematically measured muscle shortening velocity under varying constant load (isotonic) conditions. Maximum muscle force generation occurs during isometric (no shortening) conditions at optimal fiber length, while maximum velocity ($V_{max}$) occurs under unloaded conditions (no force generation). Since it is difficult to achieve truly unloaded conditions, the force-velocity curve is typically extrapolated to zero load using Hill's model for muscle contraction, which is based on a mathematical description for a rectangular hyperbola:

$$(F+a)\,v=b\,(F_{max}\,F)$$

where *v* is the velocity of muscle shortening, F is the force generated by a muscle (or the load opposing muscle shortening), and $F_{max}$ is the maximum isometric force. In the equation there are two constants, *a* termed the coefficient of shortening heat and *b* equal to $a{\cdot}V_{max}/F_{max}$. Solving the equation gives units of energy dissipation, reflecting its derivation based on thermodynamic principles. Since the curve is hyperbolic, with higher loads opposing muscle shortening, shortening velocity becomes slower. Similarly, faster shortening velocities are achieved only with lower loads and less force generation by the muscle.

**Force-velocity relationship—**As in the studies by Hill, maximal shortening velocity can be calculated from the force-velocity relationship, where isotonic loads are systematically varied. Unfortunately, using this technique it is not possible to achieve zero load conditions experimentally; thus, it is necessary to extrapolate the curve to obtain an estimate of $V_{max}$. Alternatively, another method was developed in which during maximal activation, muscle fiber length is rapidly shortened to varying fractions of optimal length, thereby releasing external loading while the muscle fiber shortens against zero external load ("slack" test) (6, 73, 94, 290). The time required before force redevelops depends on the extent of "slack" (% $L_o$) and the maximum unloaded shortening velocity ($V_o$) of the fiber. In single muscle fibers, $V_{max}$ and $V_o$ should match, although some differences may be associated with errors introduced by extrapolation in the $V_{max}$ measurement. For this reason, most single fiber studies employ the "slack" test. However, there may be concern regarding the possibility of shortening inactivation as a result of the quickly imposed slack in the muscle fiber. If anything, this would prolong force redevelopment, with an underestimation of $V_o$. Shortening inactivation is not necessarily obviated by measuring isotonic shortening by a quick release to varying loads. In muscle bundles, especially those with mixed fiber type composition, $V_{max}$ and $V_o$ are not the same, since fibers with faster $V_o$ (type IIx and/or IIb) will predominate. Accordingly, the $V_{max}$ measurement in muscle bundles will reflect an average of the shortening velocities for all fibers within the bundle (74).

**Fiber type differences in $V_o$—**In diaphragm muscle, there are differences in $V_o$ across fibers expressing different MyHC isoforms. Fibers expressing $MyHC_{2B}$ display the fastest $V_o$ followed by fibers expressing $MyHC_{2X}$, $MyHC_{2A}$, and $MyHC_{Slow}$ (93, 394, 395, 399, 400). In the rat diaphragm muscle at 15°C, fibers expressing $MyHC_{Slow}$ and $MyHC_{2A}$ display $V_o$ of 1.2 ± 0.2 and 2.0 ± 0.2 $L_o s^{-1}$, respectively, compared to 5.1 ± 0.2 $L_o s^{-1}$ for fibers expressing $MyHC_{2X}$ and/or $MyHC_{2B}$ (394). Comparable results were obtained across all studies and these differences in $V_o$ can be generally attributed to the lower actomyosin ATPase activities of fibers expressing $MyHC_{Slow}$ and $MyHC_{2A}$ compared to those of fibers expressing $MyHC_{2X}$ and/or $MyHC_{2B}$ (394, 395, 399, 400). In "hybrid" fibers where MyHC isoforms are co-expressed, there is likely an impact on $V_o$, but this has not been thoroughly explored. This is important since the incidence of hybrid fibers increases in many pathophysiological conditions.

## Muscle fiber energetic properties – ATP consumption

Brenner's two-state conceptual framework for cross-bridge cycling can also be used to evaluate changes in muscle fiber energetic properties during activation. Assuming that one ATP molecule is hydrolyzed by each cross-bridge during the cross-bridge cycle, ATP consumption rate can be described by:

$$\text{ATP Consumption Rate} = n \cdot b \cdot g_{app} \cdot \alpha_{fs}$$

Since during activation, ATP consumption occurs throughout the muscle fiber, the total number of cross-bridges must be considered; thus, ATP consumption will also depend on the number of half-sarcomeres in series (b) and the fraction that are in the strongly bound force-generating state ($\alpha_{fs}$). At any given level of $Ca^{2+}$ activation, where $\alpha_{fs}$ remains constant, ATP consumption within the fiber is thus directly proportional to $g_{app}$ reflecting the fact that cross-bridge detachment is dependent on ATP hydrolysis.

The maximum velocity of the biochemical actomyosin ATPase reaction ($V_{max}$ ATPase) in single diaphragm muscle fibers has been measured using a quantitative histochemical procedure (37, 394, 395). As might be expected, type IIx and/or IIb fibers in the rat diaphragm have the highest $V_{max}$ ATPase followed by type IIa and type I fibers. The ATP consumption rate of single permeabilized fibers in rat diaphragm muscle during maximum isometric activation ($ATP_{iso}$), was measured using an NADH-linked fluorometric procedure (394, 395, 400). In the rat diaphragm muscle, $ATP_{iso}$ was also dependent on fiber type (type IIb>IIx>IIa>I). Across all fibers $ATP_{iso}$ was significantly lower than $V_{max}$ ATPase. In addition, $ATP_{iso}$ varies with velocity of shortening reaching a maximum at ~33% maximum unloaded shortening velocity. This is consistent with the well-known fact that ATP consumption rate increases in proportion to work – the Fenn effect (110, 111). Accordingly, maximum ATP consumption rate was observed during diaphragm muscle contraction at an isovelocity rate that approximated 1/3 maximum shortening velocity and 1/3 maximum force. Differences in ATP consumption across diaphragm muscle fibers may contribute, at least in part, to the differences in fatigability that exist (394, 395).

## Force-Length Relationship

### Passive length-tension relationship

Under passive conditions, tension increases exponentially as muscle fibers are lengthened beyond optimal length. Respiratory muscle length is closely related to lung volume *in vivo*. As lung volume increases, inspiratory muscles shorten and expiratory muscles lengthen. Passive tension in inspiratory muscles decreases, while passive tension in expiratory muscles increases accordingly. This opposing change in passive tension can be measured as the transmural pressure gradient across intact respiratory muscles.

Beyond the diaphragm, other respiratory muscles appear to vary in their resting lengths. The resting length of rectus abdominis and intercostal muscles (internal and external) are similar to Lo measured in vitro (103, 106). In contrast, resting lengths of the external oblique and parasternal muscles are 20% shorter than $L_o$ and longer than $L_o$, respectively (103, 106).

**Passive tension—**Skeletal muscles develop nearly no passive tension below or at $L_o$, with passive tension increasing exponentially as sarcomere length exceeds $L_o$ (Figure 8) (142, 146, 329). This effect is seen in limb and respiratory muscles (102, 272, 279, 282, 343). Across muscles and species, the relationship between passive tension and sarcomere length can vary. For example, rabbit diaphragm muscle fiber bundles develop passive tension when sarcomere length is 2.3 μm or greater (329); mice, rat and human diaphragm single fibers develop passive tension when sarcomere length is 2.5 μm or greater (175, 223, 293, 313). However, there is controversy regarding the relationship between passive tension developed by the diaphragm muscle *in vivo* and $L_o$ For example, it has been reported that passive tension in the diaphragm muscle develops at lengths estimated to be 70-80% of $L_o$ in sheep (168, 169) and dogs (274) vs. 110% $L_o$ in rabbits (483). This discrepancy between

*in vitro* and *in vivo* measurements of passive tension in relation to sarcomere length may reflect species differences and/or experimental techniques. Another possibility is that the diaphragm is exposed to biaxial loading *in vivo*, i.e., tension is developed both longitudinally and transversely with respect to the direction of muscle fibers (274). Biaxial loading *in vitro* elicits an increase in passive tension at sarcomere lengths shorter than $L_o$ (168, 169) and may account for the apparently greater passive stiffness of the diaphragm muscle *in vivo* compared to *in vitro* measurements under uniaxial loading conditions (274). However, it remains unresolved whether the diaphragm muscle is exposed to significant biaxial loading and passive tension during ventilatory behaviors, and if so, whether or not higher passive tension affects the performance of these behaviors.

Passive tension exerted by respiratory muscles varies among muscle groups. Parasternal, internal and external intercostals, and rectus abdominis muscles are stiffer than the diaphragm (103, 106), while the external oblique muscle of the abdomen is less stiff than the diaphragm (106). It is worth noting that these comparisons among respiratory muscle groups were performed *in vitro* using muscle segments during uniaxial loading. Thus, mechanical properties of either the myocyte and/or connective tissue may account for differences in muscle stiffness.

**Molecular basis of passive tension in muscle—**In the diaphragm, like in limb muscles (188), stiffness is highest in the (central) tendon, followed by the myotendinous junction, and muscle fibers (196). The central tendon is composed largely of collagen fibers that are stiff and non-distensible within the range of forces developed during breathing (196). Connective tissue in the endomysium, perimysium, and epimysium contribute to diaphragm stiffness. Collagen digestion of diaphragm strips reduces stiffness by roughly 40% *in vitro* (357). Aging increases diaphragm and intercostal stiffness (210), in part, due to heightened collagen concentration and cross-linking content in the diaphragm (152). Another extra-myocyte structure that contributes to diaphragm stiffness is a fascia-like membrane of high elastin content that lies over the thoracic surface of the diaphragm (168, 169). This structure is responsible for approximately 50% of passive tension at a sarcomere length near functional residual capacity (FRC), a contribution that lessens progressively as sarcomere length increases.

Under relaxed conditions, stiffness is less in diaphragm muscle fiber bundles than limb muscles (329). This likely reflects differences in sarcomeric proteins that influence passive tension. A potential source of passive tension is cross-bridges that may exist in a weakly bound, non-force generating state. This concept remains a matter of debate (298, 334) with some studies suggesting that cycling weakly bound cross-bridges contribute substantially to passive tension (66, 158, 159) and others indicating there is no effect (12, 18, 299). Early microscopic studies suggest nebulin is not a determinant of passive tension (459, 481). However, this structural protein may contribute to passive tension by enhancing cross-bridge cycling kinetics and thin filament activation (71).

As mentioned above, titin is a primary determinant of passive stiffness in diaphragm muscle (329). Titin acts as a molecular spring that helps to keep the thick filaments centered during stretch and shortening (contraction) cycles (186). In this manner, titin can be considered a determinant of the active length-tension relationship. Titin is a large protein with molecular weight >3.0 MDa (121, 157, 329). Little is known about the molecular structure of titin in respiratory muscles. The size of titin size (3.6 – 3.7 MDa) (223, 329) and titin-based passive stiffness (329) are similar in rabbit diaphragm and soleus muscles. It is likely that the spring elements of titin in the diaphragm muscle have a molecular composition similar to that of titin in the soleus muscle (329). Thus, the ensuing discussion of the structure and function of titin is based on data from limb muscles with focus on the diaphragm whenever appropriate.

The I-band region of skeletal muscle titin contains spring elements that are responsible for the elasticity of titin: two blocks of tandem immunoglobulin (Ig) segments separated by a domain rich in proline (P), glutamate (E), valine (V), and lysine (K) (PEVK), and the N2A element (Figure 9) (121, 157, 159, 460, 461). The spring elements of titin are differentially expressed (splice variants) among muscles (438), which lead to variations in titin-based passive stiffness (329). Titin-based passive stiffness can be assessed based on molecular events in the tandem Ig and PEVK segment, which behave as entropic springs in series (437). The Ig segment is less stiff than the PEVK domain. Consequently, stretch of sarcomeres beyond slack length initially extends Ig segments (157, 289, 438, 461) followed by extension of the PEVK segment at intermediate to long sarcomere length (157, 438, 460). Upon sarcomere lengthening, fractional extension of tandem Ig and PEVK segments with longer contour lengths (diaphragm and soleus) is lower than muscles with shorter contour lengths (e.g., psoas) (121). The contour lengths of Ig and PEVK segments of soleus muscle titin are, respectively, ~100 nm and ~400 nm longer than psoas muscle (121) – contour lengths in the diaphragm are possibly the longest among skeletal muscles (329). Therefore, titin-based passive force is higher in the psoas than the diaphragm (and soleus) muscle. However, the psoas muscle is not representative of limb muscles – it has one the smallest titin sizes reported in skeletal muscles (121, 329).

Titin-based stiffness of striated muscles can be modulated by interaction with thin filaments, titin phosphorylation, and calcium concentration (157, 160). Interaction between F-actin and the PEVK segment increases passive stiffness in cardiomyocytes (227, 478). However, skeletal muscle PEVK segment does not bind actin (478). Titin in the diaphragm muscle can be phosphorylated mainly at serine residues (407), a modification expected to decrease passive tension. Titin phosphorylation by PKA lowers passive tension in cardiomyocytes (124, 223). Diaphragm stiffness is unaffected by PKA-induced phosphorylation of titin (223). PKA may phosphorylate diaphragm titin at residues located in the A-band (non-elastic) region. The possibility of modulation of titin-based passive stiffness in the diaphragm by phosphorylation of (serine/threonine (407)) residues in the spring elements cannot be ruled out. Titin-based stiffness is also calcium sensitive. The PEVK segment has high affinity for calcium (427) – an effect that requires E-rich exons (123, 229, 230). The PEVK segment of mouse skeletal (soleus) muscle contains 9 E-rich exons (123, 229). Exposure of skinned soleus muscle fibers to $Ca^{2+}$ (10 μM) increases passive tension in the absence of actomyosin interaction (post-gelsolin treatment) (229). Importantly, titin-based passive stiffness is not the sole determinant of total passive stiffness. The soleus and diaphragm muscles have similar titin-based passive stiffness, but soleus fiber bundles are roughly twice the stiffness of diaphragm fiber bundles (329). This emphasizes the relevance of extra-myofibrillar sources to total passive stiffness in skeletal muscles.

**Extramyofibrillar contribution to passive tension—**Extra-myofibrillar sources are responsible for a significant portion of passive tension in diaphragm muscle fiber bundles (329). These extra-myofibrillar sources include proteins of the intermediate filaments, extracellular matrix (ECM), and sarcolemma. Tension in the intermediate filaments of rabbit psoas muscle fibers increases at lengths beyond a sarcomere length of 4.5 μm (159, 460, 461). Therefore, in the physiological range of sarcomere lengths, intermediate filaments do not seem to contribute to passive tension during uniaxial loading. However, deficiency of the intermediate filament protein desmin increases stiffness in mouse soleus muscle (7). Desmin deficiency has no effect on diaphragm longitudinal stiffness (tension exerted along the axis of the fibers), but decreases diaphragm transversal stiffness (46). The role of the intermediate filament protein vimentin on skeletal muscle stiffness is unknown. Vimentin contributes to stiffness in smooth muscles: decreased vimentin content lowers passive tension upon stretch (462).

Proteins of the extracellular matrix are fundamental for force transmission along the muscle fibers. The contribution of extracellular matrix proteins to passive tension is evident in animals deficient in individual proteins. Dystrophin deficiency in *mdx* mice decreases diaphragm muscle stiffness (228). Stiffness is also reduced in the diaphragm muscle of mice lacking the transmembrane protein $\alpha_7$-integrin (248). In a counter-intuitive manner, merosin or α-sarcoglycan deficiency increase passive stiffness of diaphragm muscle fiber bundles (200, 320). However, caution should be exercised when interpreting findings from muscles deficient in extracellular matrix proteins. These deficiencies are often accompanied by increased collagen content (200) and can cause muscle degenerative disorders, e.g., Duchenne and limb girdle muscular dystrophies (228, 248, 320).

**Viscoelastic characteristics—**Upon deformation, viscous materials develop tension that is proportional to the rate of shape change. Elastic materials develop tension that is proportional to the magnitude of shape change and return to their original shape when the deforming input is released. Skeletal muscles display both viscous and elastic properties, i.e., muscles are viscoelastic (295, 440). General viscoelastic characteristic of muscle include stress relaxation, creep, and static elasticity (440). A key property of viscoelastic material is hysteresis in the stress-strain relationship, i.e., at any muscle length, tension developed during passive stretch will exceed the tension during passive shortening (Figure 10) (200, 320, 333, 423). In hysteresis, both viscous and elastic forces resist passive lengthening; elastic recoil causes passive shortening and is opposed by viscous forces. Thus, energy is lost during stretch-shortening cycles. Hysteresis is observed in intact muscles and isolated single fibers, and is affected by the history of stretch-shortening cycles (Figure 10) (66, 67, 297). The diaphragm exhibits hysteresis that is dependent on cycle frequency, strain, initial muscle length, and direction of tension (200, 228, 320, 423). Viscous and elastic forces are increased in the rat diaphragm when stretch-shortening cycles start at longer muscle lengths (Figure 10) (423). In addition, viscous resistance is proportional to the rate of strain (299, 423). Viscous resistance is greater for tension applied to the long axis of diaphragm and abdominal muscle fibers than for tension applied transversely (200, 228, 320). Biaxial loading decreases the magnitude of hysteresis in intact diaphragm and abdominal muscles (196, 200, 320).

Viscoelasticity is determined by the mechanical properties of extracellular and intracellular proteins. Collagen is viscoelastic (336) and partially responsible for tissue hysteresis. Removal of the basement membrane of frog semitendinosus muscle fibers with collagenase and hyaluronidase reduces hysteresis by 85% (432). However, these findings do not exclude contributions from intracellular components. The cytoplasm (or sarcoplasm), as a fluid, has viscous properties (27, 249). Viscous properties of muscle fibers could arise from shearing forces in the sarcoplasm between the sliding thin and thick filaments (295). Proteins of the thin, thick, and intermediate filaments are also directly involved in viscoelastic characteristics of muscles. As shown for the whole diaphragm muscle in Figure 10 (423) and for single diaphragm fibers in Figure 11 (LF Ferreira, KS Campbell, and MB Reid; unpublished observations), hysteresis is present in the passive length-tension relationship. Hysteresis nearly disappears in muscle fibers after extraction of thick and thin filaments using KCl/KI (438, 460), but is unchanged after selective extraction of thin filaments using gelsolin (158, 438). These results, along with computer simulations (297, 338), suggest a role for thick filaments in the viscoelasticity of skeletal muscles. Single titin molecules display viscoelastic properties (84) and exhibit hysteresis in lengthening-shortening cycles (441). The viscous component of titin has been attributed to distension of Ig domains, which dictate slow stress-relaxation. Elastic properties of titin are determined by the PEVK segment of titin (437, 438, 441, 461). The intermediate filament protein desmin dissipates mechanical force in the diaphragm. Stress-relaxation upon stretch is decreased in diaphragm muscle fiber bundles of desmin-deficient mice (46). The molecular mechanisms proposed by

Boriek et al. (46) to explain dissipation of energy by desmin include distension of coiled-coil domains and/or alignment of filaments in the longitudinal and transverse planes. Actomyosin cross-bridges may also contribute to hysteresis. The mechanical behavior of rapid cycling cross-bridges, modeled as linear springs with a single rate of attachment and detachment, have been shown to mimic a viscoelastic system (369).

Hysteresis is affected by the history of lengthening-shortening and stretch velocities. This history dependence has been termed 'thixotropy' (66, 67, 233) and is evident in single muscle fibers. In a series of lengthening-shortening cycles, hysteresis (or energy loss) of an individual fiber is greater in the first cycle than in subsequent cycles (Figure 11; Ferreira LF, Reid MB, Campbell KS, unpublished observations) (12, 67, 182). This thixotropic behavior is determined by a short-range elastic component that appears to stem from the number of attached cross-bridges (67, 68) (see refs. 12, 13, 297 for an opposing view on this topic). At the molecular level, titin also exhibits thixotropic behavior; prior stretches decrease the stiffness of this protein (209, 289). The intact respiratory system displays thixotropy that is considered to reflect history dependence of inspiratory muscles (185, 198). Assuming that diaphragm muscle is similar to limb muscles, the short-range elastic component of diaphragm muscle fibers will contribute to hysteresis of lengthening-shortening cycles and affect the mechanics of breathing. Indeed, end-expiratory lung volume increases following respiratory efforts above or below FRC (185, 198, 199). These changes have been linked to temporary perturbations in the mechanics of respiratory muscle cells following movement (199).

The hysteretic properties of respiratory muscle are physiologically relevant. However, experimental results from isolated muscle tissue and single muscle fibers should be interpreted with caution. Stretch velocities are important determinants of the viscoelastic characteristics of any material. Fast stretches in experiments, if outside the physiological range of lengthening-shortening rate, will overestimate energy loss due to viscous resistance and underestimate the contribution of thixotropy to viscoelastic characteristics. The influence of thixotropy on hysteresis of respiratory muscles during breathing should be greater in large mammals than in small mammals where breathing frequencies can range from 5 breaths·min$^{-1}$ in the Asian elephant (197) to 230 breaths·min$^{-1}$ in mice (220). Viscous resistance of respiratory muscles during breathing is expected to scale inversely with body size. Another confounding factor in the quantification of viscoelastic properties is temperature. Viscosity and elasticity of a material decreases when temperature is elevated, a concept valid for skeletal muscles (224, 295). Accordingly, *in vitro* experiments performed at temperatures <25°C will overestimate viscosity and hysteresis relative to respiratory muscles that operate at 37°C *in vivo*. Nevertheless, viscoelastic characteristics of respiratory muscles are evident in experiments performed at 37°C (46, 196, 200, 320) suggesting that these properties influence the mechanics of breathing.

## Active force-length relationship of muscle

The active force-length relationship measured in diaphragm bundles *in vitro* is bell shaped, plateauing at lengths ranging from 90 to 110% $L_o$ (105, 272, 279, 343); a feature consistent among several mammalian species (Figure 8) (279). The ascending limb of the force-relationship is shifted to the right for intercostals (external and internal) and abdominal muscles compared to the diaphragm (103, 106). In single muscle fibers, the bell-shaped profile is dictated by the classical description of thick-thin filament overlap that gave rise to the sliding-filament theory of muscle contraction (Figure 8) (146).

**Optimal sarcomere length and cross-bridge recruitment—**The optimal sarcomere length ($L_o$) at which single diaphragm muscle fibers generate maximal force is ~2.5-2.7 μm.

At this sarcomere length, the maximum number of myosin heads per half sarcomere (n) overlap with the thin filament and thus, the maximum number of cross-bridge can form during $Ca^{2+}$ activation (maximal $\alpha_{fs}$). As muscle fibers shorten or stretch beyond $L_o$, fewer myosin heads can bind to the actin filament; thus fewer cross-bridges can form and force is reduced ($\alpha_{fs}$ decreases).

Additional factors related to muscle fiber length may also affect force generation. Myofibril bending (or wavy myofibrils) has been reported in frog sarcomeres allowed to shorten below 2.0 μm (59, 429). Sarcomere shortening below slack length stretches the extensible region of titin in a direction opposite to elongation, creating restoring forces that counteract active tension development at short sarcomere lengths (160). Inward transmission of depolarization in the T-tubules may also be less effective or incomplete at short sarcomere lengths, thereby affecting the release of $Ca^{2+}$ from the SR and excitation-contraction coupling (337, 429).

**Active force in respiratory muscles—**The force-length relationship of respiratory muscles is a fundamental component of the mechanics of breathing. The general features of force development as a function of muscle length determined *in vivo* are also evident in diaphragm muscle fiber bundles and single fibers examined *in vitro*. This uniformity implies that the relationship between muscle force (or trans-diaphragmatic pressure) and muscle length (or lung volume) is predominantly determined at the cellular level.

During active force (pressure) generation, the intact diaphragm muscle of supine quadrupeds (dogs, sheep) generally produces the highest trans-diaphragmatic pressure (Pdi) at a lung volume near FRC (168, 169, 273, 353). However, one study suggested that active Pdi is highest when muscle length is 10-30% longer than at supine FRC (216). Posture is an important consideration for data from quadrupeds. Some studies assessed animals in the supine position whereas, in the prone position, FRC is larger and intact diaphragm length is shorter than at supine FRC. In the rabbit diaphragm muscle, *in vivo* passive length changes were measured in the sternal and midcostal regions using sonomicrometry (483). Changes in diaphragm muscle length during the respiratory cycle were then compared to optimal muscle fiber length ($L_o$) measured *in vitro*. Resting length of the sternal region of the diaphragm muscle (at FRC) was ~78% of $L_o$, whereas resting length of the midcostal region was ~95% of $L_o$. It should be noted, that in both diaphragm regions, these resting lengths were not associated with any appreciable passive tension.

During conditions of lung hyperinflation, the diaphragm muscle is chronically shortened. In response, there is a decrease in the number of sarcomeres in series, thereby maintaining optimal overlap of thick and thin filaments. This length adaptation has been demonstrated in a number of models of emphysema (212, 238). Thus, length adaptation would lead to a decreased muscle mass while fiber cross-sectional area may be unaffected.

## Plyometric contraction-induced muscle injury

Application of an external load that is greater than the force generated by a muscle results in lengthening of activated muscle. Such maneuvers are termed plyometric or eccentric contractions or more correctly lengthening activation. Respiratory muscles routinely undergo plyometric contractions. Inspiratory and expiratory muscle groups have opposing actions and are co-activated to regulate air flow, maintain posture, or stabilize the trunk. Increased activation of one muscle group exerts increased force (or load) on the opposing group, causing it to actively lengthen.

For a given level of activation, muscle force is higher during plyometric contractions than during isometric (fixed length) activation. This principle, first defined in limb muscles, was later demonstrated for human inspiratory muscles by Topulos, et al. (436) who showed that

healthy volunteers develop higher mouth pressures during maximum plyometric maneuvers than during maximum static efforts against an occluded airway. More recently, Tzelepis and associates (444) reported that plyometric contractions performed immediately before an inspiratory effort can augment maximum inspiratory power, mimicking limb muscle performance in a stretch-shortening cycle (50).

Plyometric contractions can be damaging to muscle fibers. In limb muscles, plyometric exercise causes tissue injury characterized by myofibrillar disruption, sarcolemmal damage, and decrements in force (109, 280). The mechanism of injury involves mechanical overload at the cellular level that is exacerbated by loss of $Ca^{2+}$ regulation (251) and increased free radical activity (278).

Less is known about plyometric injury of respiratory muscles. Subjects tested by Topulos and co-workers (436) perceived no deleterious consequences following maximal inspiratory efforts under plyometric conditions. However, subsequent studies confirmed that plyometric contractions can injure respiratory muscles. For example, myofibrillar disruption has been reported in the rat diaphragm during plyometric contractions (467). Analyses of excised tissue by Gea and associates (129) demonstrated sarcomeric and sarcolemmal damage and depressed force in canine diaphragm subjected to maximum plyometric contractions. Clinical reports further suggest that expiratory muscles of the abdominal wall may by injured by plyometric contractions during athletic activity (271).

## Isotropic and Anisotropic Force Transmission

### Functional relevance

The diaphragm and abdominal muscles are subjected to mechanical loading along multiple axes. These forces can alter muscle dimensions, i.e., produce strain. In isotropic materials, the tension-strain relationship is independent of the direction that force is applied. Conversely, anisotropic materials have mechanical properties that are non-uniform; strain varies with the direction of force. The central tendon is nearly isotropic (47, 49, 196) and inextensible (47). The diaphragm and internal abdominal muscles are anisotropic. Stiffness is less when force is oriented along the longitudinal axis of muscle fibers compared to force is applied in the perpendicular (transverse) direction (45, 196, 274, 320, 418). For example, in the intact diaphragm, longitudinal stress is 2-4 times greater than transverse stress during passive loading (45) and breathing (274). The anisotropic tissue characteristics and three-dimensional distribution of forces have major implications for respiratory muscle mechanics.

The description of skeletal muscle architecture in traditional and modern textbooks suggests that muscle fibers span the full length of the muscle and are connected to tendons at their origin and insertion through myotendinous junctions (173, 252). However, several skeletal muscles – including the diaphragm of larger mammals – have a substantial fraction of fibers with tapered, non-myotendinous ends that terminate within muscle fascicles (44, 45, 335, 439). In the canine diaphragm, nearly 80% of muscle fibers do not span the entire muscle length (48). Thus, forces generated by the diaphragm muscle during breathing are transmitted from chest wall to central tendon mainly through adjacent non-spanning fibers. Experiments using frog muscle show that 75-100% of the tension generated by a single fiber is transmitted laterally to neighboring fibers through shear forces (416). The relevance of lateral force transmission to diaphragm function is emphasized by studies showing that $P_o$ is increased by 10-20% when tension is applied transverse to the fiber orientation (200, 248, 320). Thus, contractile forces in the axial dimension are increased by mechanically loading the structures that transmit lateral forces. These include proteins of the costamere, extracellular matrix, and connective tissue (188, 217, 292).

### Molecular determinants

The term costamere refers to a cluster of transmembrane proteins that anchor sarcomeric proteins and the sarcolemma near the Z- and M-lines of myofibrils (Figure 12) (24, 69, 75, 316). The costamere is part of the cytoskeleton, which consists of several proteins whose functions remain elusive. Proteins of the costamere that may be involved in lateral force transmission include vinculin, laminin, integrin, and the dystrophin-associated glycoprotein complex (24, 38, 321). Consistent with the notion that costameric proteins play a role in force transmission, maximal tetanic stress of diaphragm muscle fiber bundles is depressed in mice lacking $\alpha_7$-integrin (248), merosin ($\alpha_2$-laminin) (200), α-sarcoglycan (component of dystrophin-associated complex; (320)), and dystrophin (*mdx* mice; (166)). In addition, muscles of mice deficient in α-sarcoglycan do not exhibit augmented maximal tetanic stress during transverse loading (320). Vinculin is a promising candidate for lateral force transmission (292, 316). However, establishment of the role of vinculin has been hindered by the fact that vinculin deficiency is embryonically lethal (477). Linking sarcomeric proteins to the sarcolemma, desmin is also expected to participate in lateral transmission of force (431). Desmin-deficient diaphragm muscle generates higher $P_o$ than control muscle but lacks the increase in $P_o$ with transverse loading (46). Boriek and colleagues (46) proposed that desmin might dissipate lateral forces. The greater $P_o$ generated the diaphragm muscle of desmin-deficient mice contrasts with the weakness observed in the soleus muscle of such mice (244). Compensatory adaptations to desmin deficiency must be examined before a definitive conclusion can be reached regarding the role of desmin in lateral force transmission.

The extracellular matrix consists mainly of proteoglycans, laminin, and type IV collagen (172, 217, 246, 433, 434). With the exception of laminin (see above), there is relatively little information regarding the role of extracellular matrix components in lateral force transmission within respiratory muscles. The endo, peri, and epimysium are composed of several collagen types but types I and III collagen predominate (246). Types I and III collagen are thought to confer rigidity and elasticity, respectively, to connective tissues (see references in 152). mRNA levels of type III collagen are 2-fold higher than mRNA of type I collagen in rat diaphragm (153). Immunohistochemistry using antibodies for type I collagen reveals a dense network of connective tissue in the diaphragm muscle (78). Visual inspection of immunohistochemistry images suggest the diaphragm perimysium is composed largely of type I collagen (78) – consistent with limb muscles (217, 246). Perhaps, the higher levels of type III collagen mRNA (153) result in enhanced type III collagen in the endomysium (318). Hydroxyproline is found in collagen and elastin (302) and is higher in the mouse diaphragm muscle compared to the gastrocnemius muscle (155). The collagen content of diaphragm muscle does not change during development but cross-linking of collagen fibrils increases from birth to adulthood (150) and with aging (152). The increase in collagen cross-linking presumably leads to stiffening of the diaphragm (152, 210).

### Structural organization

Architecture and molecular composition are important determinants of the mechanical properties of a multifibril network. The endomysium contains elastin and type IV collagen (246, 318) that have low stiffness (255, 335). The endomysium is also characterized by a mesh of collagen fibrils oriented in multiple directions (mean angle 60°) – a structure that confers lower passive stiffness (335). Collagen fibrils of the endomysium are oriented along the longitudinal axis of myofibers (217). Purslow & Trotter (335) proposed that the low stiffness makes the endomysium unsuitable for lateral force transmission. However, once the muscle is stretched, endomysial fibers oriented longitudinally may facilitate lateral force transmission among muscle fibers (335, 439).

The perimysium, which is connected to the endomysium, is another important site of lateral force transmission in skeletal muscles (188, 292, 318). Collagen fibrils of the perimysium are oriented in a plane perpendicular to the long axis of muscle fibers (217). This fibril distribution makes perimysium collagen a potential structure for the distribution of transverse tension, increasing diaphragm $P_o$. It is reasonable to suppose that transverse tension stretches collagen fibrils of the endomysium and perimysium in the diaphragm muscle; thus, promoting the transmission of force from rib to central tendon. This speculation is supported by the observation that collagenase treatment diminishes passive stiffness of the diaphragm (357).

## Isometric Force-Frequency Relationship

Skeletal muscle force increases with an increase stimulus frequency reaching a plateau that corresponds to maximum tetanic force. The relationship between force and stimulus frequency is sigmoidal and the shape of this relationship is primarily determined by the rate of force relaxation (one-half relaxation time: ½RT) during a twitch contraction. Tetanic fusion of force occurs at lower frequencies of stimulation in muscle fibers and motor units with slower ½RT (Figure 13) (116, 380). Consequently, skeletal muscles primarily composed of slow-twitch (type I) fibers have a force-frequency relationship that is shifted leftward compared to fast-twitch (type II) muscle fibers (219, 250). The force-frequency curve is also affected by temperature such that at room-temperature (22-25°C) the curve is shifted leftward compared to the force-frequency relationship at 35-37°C (89, 287, 343) – ½RT nearly doubles with every 10°C increase in temperature, i.e., $Q_{10}$ ~2.0 (287). The force-frequency relationship of the diaphragm muscle has a sigmoidal shape in humans, dogs (103, 105), and rodents (89, 113, 114, 215, 250, 343, 421). Canine abdominal, sternomastoid, scalene, intercostal, and parasternal muscles also have a sigmoidal force-frequency relationship that is right-shifted in relation to the diaphragm muscle (103, 104, 106). The differences in shape and position of the force-frequency relationship among respiratory muscles may arise from distinct fiber type composition and contractile properties of individual muscle fibers that scales with animal size.

### Twitch characteristics

Muscle twitch force can be characterized by three parameters: peak twitch force ($P_t$), time to peak tension (TPT), and ½RT. These parameters vary among species and follow closely with the muscle fiber type composition of a muscle (Table 1). Canine abdominal and intercostal muscles reach $P_t$ approximately 10-15 ms faster than the diaphragm muscle (106). The ½RT follows a species- and muscle-specific pattern similar to TPT (Table 1). The ½RT of canine intercostals is similar to the diaphragm, except for external intercostals (½RT ~ 40 ms) (103). These twitch characteristics are determined by rates of cross-bridge attachment ($f_{app}$) and detachment ($g_{app}$), and intracellular $Ca^{2+}$ dynamics.

### Maximum tetanic force ($P_o$)

Maximal specific force (force per cross-sectional area) of the diaphragm is commonly measured using isolated muscle fiber bundles *in vitro* or *in situ*. The advantage of this preparation is that diaphragm fibers are oriented perpendicular to the rib and follow a straight line to the central tendon (46, 347). Using the dissection method first introduced by Bulbring (62) and modified by Goffart & Ritchie (141), the cross-sectional area of fiber bundles can be estimated from $L_o$ and bundle weight (based on a muscle specific density of 1.06 $g \cdot cm^{-3}$) to calculate specific force (force per cross-sectional area) (77). Since diaphragm muscle fibers run parallel, the calculation does not require correction for physiological cross-sectional area based on the angle of pennation of fibers (57). The $P_o$ of the diaphragm muscle measured *in vitro* is 20-30 $Ncm^{-2}$ in a variety of species (102, 105,

108, 113, 151, 175, 187, 236, 238, 239, 241, 269, 272, 279, 294, 311, 344, 345, 351, 364, 373, 408, 420, 423) and is consistent with values reported for limb muscles (57). The maximum specific force generated by single muscle fibers is relatively consistent across species and muscles. Thus, it is likely that differences among muscles examined *in vitro* reflect limitations of the technical procedures involved in the experiment.

## Molecular Determinants of Muscle Protein Balance

In all cells, including skeletal muscle fibers, proteins are continuously synthesized and degraded with this balance determining net protein loss or gain. Changes in protein synthesis and degradation rates thus determine whether there is muscle fiber atrophy or hypertrophy. For example, following unilateral denervation of the diaphragm muscle, both protein synthesis and protein degradation increase, with a net decrease in protein balance by 5 days (8). Recent developments in molecular and cell biology guide our understanding of the mechanisms regulating protein balance in muscle fibers. However, specific information regarding protein balance across many diseases or physiological states is lacking. The complexity of the signaling pathways likely reflects redundancy in maintaining essential cellular functions (e.g., in muscle contractile protein expression and metabolic support) (9, 362, 363, 413). This complexity precludes unambiguous interpretation of studies that examine only one mechanism. For example, hypertrophy can result from either an increase in protein synthesis and/or a decrease in protein degradation. Similarly, atrophy reflects a decrease in the net protein balance that may involve changes in both protein synthesis and degradation. Muscle fiber hypertrophy and atrophy are not synonymous with an increase in protein synthesis and degradation, respectively.

The Akt signaling pathway is thought to be critical in triggering an increase in protein synthesis under a variety of conditions (139, 363). This signaling cascade is initiated by Akt phosphorylation (41, 355, 356, 426) with downstream activation of the mammalian target of rapamycin (mTOR), glycogen synthase kinase-3β (GSK3β) and p70S6 kinase (p70S6K) (10). Among a number of extracellular signals, phosphorylation of Akt is induced by IGF-1 and insulin (178, 356). Binding to their receptors activates phosphoinositide-3 kinase (PI3K), which targets Akt to the plasma membrane where PI3K phosphorylates Akt. Akt signaling involves phosphorylation of a variety of substrates, involved in protein synthesis, gene transcription, glucose metabolism, cell proliferation, and regulation of apoptosis (276, 456). Ultimately, the extent of protein synthesis depends on translation initiation factors such as eukaryotic initiation factor 2B (eIF2B), eukaryotic initiation factor 4E (eIF4E), and eIF4E-binding protein 1 (4EBP1) (218, 463). The Akt signaling pathway has been evaluated in diaphragm muscle under conditions of hypertrophy and atrophy of muscle fibers. For example, following unilateral denervation of the diaphragm muscle there is an initial phase of muscle hypertrophy followed by subsequent muscle atrophy (156, 240, 290, 358, 484). Of note, following denervation, Akt phosphorylation with downstream activation of mTOR and p70S6K is unchanged but protein degradation rate decreases leading to a net positive protein balance and transient fiber hypertrophy (9). Subsequently, Akt signaling pathways contribute to elevated protein synthesis but this is more than offset by a marked increase in protein degradation with consequent net negative protein balance and fiber atrophy. In the condition of acute short-term nutritional deprivation, Akt phosphorylation and activation of mTOR and p70S6K decrease in the diaphragm muscle, consistent with reduced protein synthesis (242, 243). Since there is muscle fiber atrophy, this change in Akt signaling does not appear to be offset by a decrease in protein degradation. Indeed, it is likely that protein degradation also increases. These examples highlight the complexity of assessing both aspects of protein balance in concert.

Signaling pathways involved in protein degradation in muscle fibers include the ubiquitin ligases atrogin-1/MAFbx and MuRF1 which increase protein degradation via the ubiquitin-proteasome system (40, 144). In addition, protein degradation can be mediated via autophagy-lysosome pathways and by regulation of metabolic processes. The "forkhead box" family of transcription factors FoxO is regulated by Akt via phosphorylation of FoxO and export of FoxO from the nucleus (28, 29, 60, 402). Thus, Akt terminates transcriptional activity exerted by FoxO. In conditions of muscle atrophy (e.g., following fasting or glucocorticoid treatment), Akt and FoxO are dephosphorylated with upregulation of atrogin-1/MAFbx (362, 405). Following denervation of the diaphragm muscle, there is an immediate decrease in Akt phosphorylation followed by nuclear translocation of FoxO1 protein, and increased total protein ubiquitination with subsequent increase in protein degradation (8, 9).

Activation of nuclear factor κB (NF-κB) transcription factors is also involved in muscle atrophy under a variety of conditions (65, 189, 190, 207, 370, 446). NF-κB-mediated muscle atrophy is likely due to its transcriptional regulation of MuRF1 (65). Inhibition of both NF-κB and FoxO transcription factors is necessary to prevent muscle atrophy after immobilization (341). Importantly, MuRF1 and MAFbx, encode ubiquitin ligases responsible for targeting proteins for degradation in the proteasome (40). Three distinct enzymes (E1 ubiquitin-activating enzyme, E2 ubiquitin-conjugating enzyme, and E3 ubiquitin-ligating enzyme) regulate the addition of the short peptide ubiquitin to specific protein substrates. The proteasome complex comprises more than 50 subunits (19) that execute protein breakdown into small peptides (326). Inhibiting the proteasome prevents increased protein breakdown associated with several atrophy conditions (428). Notably, MyHC is degraded by the ubiquitin-proteasome pathway via MuRF1 (76, 406).

Autophagy and activation of the lysosome system also contribute to protein degradation given their role in removing dysfunctional organelles and unfolded proteins (363). Indeed, lysosomal proteases are upregulated in various conditions associated with muscle atrophy (88, 127, 234, 291). The interplay between protein degradation pathways is exemplified by the FoxO3-mediated interaction between ubiquitin-proteasome and autophagy-lysosome pathways. FoxO3 regulates expression of several autophagy-related genes and activates autophagic protein breakdown (256, 486).

Metabolic processes may also contribute to the regulation of protein balance. In particular, AMPK inhibits protein synthesis by downregulating mTOR (42, 128, 410) while promoting protein degradation via FoxO and atrogin-1/MAFbx expression (80, 163, 164, 301, 305, 435). However, following denervation of the diaphragm muscle, there was no evidence of AMPK activation at a time of markedly increased protein degradation (9). Mitochondrial remodeling is also associated with muscle atrophy, likely via activation of AMPK (354). Mitochondria are crucial for energy production and respond to environmental stressors via the balance between fusion and fission processes. It is thought that mitochondrial fission may be important in isolating dysfunctional components from mitochondria, targeting them for repair or removal via autophagy (23). Mitochondrial fission can subsequently activate AMPK, triggering FoxO-mediated signaling and activation of ubiquitin-proteasome and autophagy-lysosome pathways (354).

## Muscle Fatigue and Endurance

Muscle fatigue is defined as a decline in the ability of a muscle to generate an expected or required level of force (95), and is typically apparent as a decline in force with repetitive activation of muscle fibers. What distinguishes muscle fatigue from muscle weakness is that fatigue is reversible; i.e., the muscle recovers from fatigue in a relatively short period of

time; thus muscle fatigue is temporary. Muscle endurance is the ability of a muscle to sustain a given level of force during repeated activation, and endurance is usually presented in units of time. Although muscle fatigue and endurance may be related to each other, they are not the same and the terms should not be used interchangeably.

In the entire neuromotor system, there are several potential sites where failure may occur leading to a decline in muscle force (fatigue) and a decrease in endurance. These potential sites have been generally categorized as being either "central" (i.e., central nervous system – CNS) or "peripheral" origin (32). If a motor neuron fails to generate an action potential, the innervated muscle fibers will not be activated and a "central fatigue" of force generation will result (214). This failure to activate a motor neuron may result from reduced synaptic drive (213, 214). It is important to note that "central fatigue" does not reflect an inability of the muscle per se to generate force. In other words, it is not a form of intrinsic muscle fatigue.

Peripheral fatigue may result from a failure at several potential sites including: axonal propagation especially at nerve branch points (388), neuromuscular transmission, muscle fiber action potential propagation, T-tubule depolarization, excitation-contraction coupling, sarcoplasmic reticulum release of $Ca^{2+}$, $Ca^{2+}$-mediated thin filament regulation ($Ca^{2+}$ sensitivity), cross-bridge recruitment (affecting $\alpha_{fs}$), average force per cross-bridge ($F$), or ATP production within muscle fibers. Central fatigue is bypassed by stimulating the motor nerve to activate the muscle; however, it is far more difficult to discriminate among the various potential sites of peripheral fatigue. Toward this end, direct muscle stimulation eliminates the potential neural sites of failure and focuses on intrinsic muscle fatigue.

Susceptibility to fatigue is an important property that defines muscle fiber types similar to shortening velocity (e.g., fast vs. slow; fatigable vs. fatigue resistant). The susceptibility of muscle fibers to fatigue varies across the motor unit types they comprise (116, 380). For example, fatigue resistant slow- and fast-twitch motor units display little change in force during repetitive stimulation (<25% decline in force during repetitive stimulation at 40-Hz in 330-ms duration trains repeated every s for a 2-min period). It has been shown that these motor units comprise type I and IIa muscle fibers that higher oxidative metabolic capacities and are therefore capable of producing higher levels of ATP to meet the metabolic demands of increased activity (98, 390). In contrast, more fatigable fast-twitch motor units display substantial force decline (>75%) using the same 2-min stimulation paradigm. The type IIx and/or IIb muscle fibers that comprise these more fatigable fast-twitch motor units have lower oxidative metabolic capacities for energy production. This has led some investigators to suggest a relationship between intrinsic fatigue of muscle fibers and their oxidative capacities (386).

## Axonal propagation and neuromuscular transmission failure

A number of studies have clearly demonstrated that both axonal propagation failure and neuromuscular transmission failure can contribute to "peripheral" muscle fatigue. In either case, this would result in fewer muscle fibers being activated, and therefore, a decline in force generation. However, the underlying mechanisms differ between axonal propagation failure and neuromuscular transmission failure, but both would appear as what was formerly termed "peripheral" fatigue. In reality, both reflect a central nervous system mechanism of fatigue rather than intrinsic muscle fatigue.

**Axonal propagation failure—**In 1935, Barron and Mathews (16) first demonstrated that in response to electrical stimulation action potentials sometimes failed to propagate along each branch of a motor axon. With repetitive stimulation of the phrenic nerve, Krnjevic and Miledi (221, 222) observed that action potential propagation failure occurred, and that the incidence of this failure increased at higher stimulation rates (222). They attributed this to a

failure of propagation at axonal branch points. Since then, the incidence of axonal propagation failure has been clearly demonstrated in a variety of species (34, 171, 176, 317). In the abductor muscle of the crayfish, Smith (403) showed that axonal branch point failure of action potential propagation occurred first in more peripheral branches and then progressed centrally to regions where axons were larger. Accordingly, the probability of axonal branch point failure is greater in larger motor units, where the innervation ratio (number of muscle fibers per motor unit) is greater. This would explain the increased incidence of axonal branch point failure in larger type FF and FInt motor units.

Associated with a failure of axonal action potential propagation, there is also a prolonged depolarization of the axonal membrane and a decrease in inward $Na^+$ current (176). It was also shown that axonal propagation failure could be reversed by hyperpolarization of the axon or by exposing the axon to a low $K^+$ solution. Accordingly, it was suggested that axonal propagation failure results from a prolonged refractory period of the axon that was more prevalent at axonal branch points. Stimulation-induced alterations in $Na^+$ and $K^+$ concentrations around the axon may also underlie axonal propagation failure (1, 171, 404). Alterations in $N^+$ and $K^+$ concentrations are more likely at smaller axonal sizes, where the surface-to-volume ratio is higher (403).

A number of theoretical models have examined the relationship of axonal geometry on action potential propagation (143, 414, 415, 422, 469). These models indicate that changes in axonal membrane excitability due to differences in axonal geometry may result in propagation failure in smaller axons, depending on action potential frequency in the parent axon (414, 415). For example, at an axonal branch point, higher axial resistance and lower membrane capacitance in one of the daughter branches results in a frequency dependent propagation failure along that smaller daughter branch compared to the larger daughter branch. Even small differences in axonal resistance (length of axon branches) and membrane capacitance (diameter of axon branches) of daughter branches may result in higher probabilities of axonal propagation failure especially at higher stimulation frequencies. Clinical neurophysiological recording of single muscle fiber action potentials has identified neuromuscular “jitter” (increased variability of interval between single fiber action potentials) that is attributed, at least in part, to axonal branch point failure. The incidence of neuromuscular jitter increases with age and in neuromotor diseases. Thus, the complex interactions between changes in axonal branching geometry and susceptibility to action potential propagation failure may underlie “peripheral” fatigue under a variety of conditions.

Axonal propagation failure has been demonstrated in the diaphragm muscle by the inability to consistently evoke muscle fiber action potentials by phrenic nerve stimulation (118). In adult rat diaphragm muscle, the incidence of propagation failure depends on stimulation frequency, with lower probability with stimulation rates below 75 Hz (118). In contrast, in the neonatal diaphragm muscle the incidence of propagation failure is much higher across all stimulation frequencies, but it is particularly prevalent at higher stimulation rates. Importantly, the neonatal diaphragm displays polyneuronal innervation, such that a muscle fiber initially receives input from multiple phrenic motor neurons (61, 261). Accordingly, the extent of axonal branching is much greater in the neonate compared to the adult. Thus, it is possible that the higher incidence of axonal failure in neonates reflects the increased axonal branching associated with polyneuronal innervation of muscle fibers.

In a study of the adult cat diaphragm, susceptibility to axonal propagation failure was assessed by changes in evoked muscle unit action potentials (MUAP) (382). Fatigue resistant type S and FR motor units displayed consistent evoked MUAP during repetitive stimulation at 40 Hz. In contrast, more fatigable FF and FInt units occasionally displayed an abrupt decrease in evoked MUAP amplitude consistent with a failure to activate a subset of

muscle fibers within the motor unit (e.g., as might occur with axonal branch point failure). Similar abrupt changes in MUAP amplitude were observed in cat medial gastrocnemius muscle motor units during repetitive stimulation (361). These investigators showed that such abrupt changes in MUAP waveform were associated with a failure to evoke action potentials in some motor unit fibers.

**Neuromuscular transmission failure—**Neuromuscular transmission failure is distinct from axonal propagation failure and is defined as inability of a nerve impulse to elicit a muscle fiber action potential. This may occur at the presynaptic terminal with inadequate release of ACh (decreased quantal content) or postsynaptically with an inadequate excitatory postsynaptic potential (EPP) response. The fact that neuromuscular transmission failure occurs under experimental conditions is indisputable, but its contribution to muscle fatigue during normal motor behaviors remains controversial. Neuromuscular transmission failure has been assessed using three techniques: 1) comparison of the forces induced by repetitive nerve vs. superimposed direct muscle stimulation, thereby bypassing neuromuscular transmission; 2) assessment of evoked compound muscle action potentials (e.g., M wave) during motor behaviors; and 3) electrophysiological assessment of neuromuscular transmission including quantal content and EPP responses.

With repetitive nerve stimulation, muscle fibers that are not activated due to neuromuscular transmission failure are spared from intrinsic muscle fatigue. Accordingly, with increasing extent of neuromuscular transmission failure, the difference between forces induced by nerve vs. direct muscle stimulation will become greater (Figure 14). Using this nerve vs. direct muscle stimulation technique, a number of studies have demonstrated neuromuscular transmission failure in the diaphragm muscle under a variety of conditions (2, 101, 205, 211, 225, 258, 259, 264, 268, 290, 332, 374, 396, 475). The relative extent of neuromuscular transmission failure in the diaphragm muscle varies with stimulation rate (225). At a stimulation rate of 20 Hz (33% duty cycle, 1 s duration train repeated each s), neuromuscular transmission failure contributes approximately 16% to diaphragm fatigue after a 2 min period. With the same duty cycle and train duration but with stimulation at 40 Hz, neuromuscular transmission failure contributes approximately 35%, and at 75 Hz approximately 42%. Thus, in the adult rat diaphragm, most of the peripheral fatigue appears to be intrinsic to the muscle rather than a failure of neural activation. However, there is a difference in the susceptibility of different diaphragm muscle fiber types to neuromuscular transmission failure. By comparing the pattern of muscle fiber glycogen depletion induced by repetitive direct muscle stimulation versus phrenic nerve stimulation, it was shown that type IIx and IIb fibers are most susceptible to neuromuscular transmission failure (205).

Merton introduced the assessment of evoked muscle electrophysiological response (compound action potentials termed M waves) as a means of estimating the extent of neuromuscular transmission failure during voluntary contractions in 1954 (286). If the M wave amplitude decreased during voluntary contractions, the decline in force (or fatigue) was attributed to neuromuscular transmission failure rather than intrinsic muscle fatigue. In the human adductor pollicis muscle, Merton observed no change in the M wave amplitude despite substantial force decline during maximum voluntary contractions (286). Accordingly, he concluded that neuromuscular transmission failure does not contribute to fatigue during maximum voluntary contractions; a conclusion that has been reached in a number of subsequent studies in human muscles (22, 30, 31, 33, 281). However, not all investigators agree, as some have reported significant declines in M wave amplitude of the human adductor pollicis during fatiguing maximum voluntary contractions (300) as well as the first dorsal interosseus (409). With repeated electrical stimulation of the ulnar nerve to activate the first dorsal interosseus muscle, Grob (170) reported that at frequencies greater than 25 Hz there was a parallel reduction in M wave amplitude and tetanic force, indicating

significant neuromuscular transmission failure. A parallel reduction in M wave amplitude and force was shown during inspiratory loaded breathing in anesthetized rabbits (3) and in unanesthetized sheep (20), also suggesting significant neuromuscular transmission failure in the diaphragm muscle. During inspiratory loaded breathing in anesthetized rabbits (309) and piglets (277), there was no change in M wave amplitude or measures of diaphragm force (Pdi) during inspiratory loaded breathing despite terminal task failure. Unfortunately, inspiratory loaded breathing involves submaximal activation of the diaphragm muscle and it is thus unclear whether in the latter two studies any fatigue occurred since task failure may not relate to muscle fatigue. Using repetitive stimulation of the hypoglossal nerve to elicit tongue protrusion or retraction, Fuller and Fregosi (126) reported that there was little change in either force or M wave amplitude during normoxic conditions in anesthetized rats. However, during hypoxia (15% $O_2$), there was a parallel reduction in both M wave amplitude and force suggesting neuromuscular transmission failure. Very few studies currently use the M wave to assess neuromuscular transmission failure as it is an indirect measurement that is influenced by a number of other variables, which may account for the discrepant results in the literature. In contrast, direct electrophysiological assessment of neuromuscular transmission provides a direct measure although it cannot be performed in vivo during motor behaviors.

Adequate synaptic vesicle release at the presynaptic terminal is essential to sustain neuromuscular transmission. Synaptic vesicles are distributed throughout the presynaptic terminal and their location is an important determinant of their probability of release with a nerve impulse. One group of synaptic vesicles is docked at active zones, and therefore, these vesicles are readily available for release (defined as the “readily releasable” pool - RRP) (350, 352). However, only a fraction of these RRP vesicles are released with each neural impulse. Another group of synaptic vesicles is located in close proximity to active zones and can be cycled into the RRP; thus, these synaptic vesicles comprise a “cycling” pool (487). Another group of synaptic vesicles are located at some distance from active zones and constitute a “reserve” pool of vesicles that may be recruited to the “cycling” pool or RRP sustained neuromuscular transmission with repeated stimulation. Once released, synaptic vesicles can be recycled returning to the RRP, “cycling” or “reserve” pool of vesicles (350, 419). Although a number of studies have described the distribution of these synaptic vesicle pools at the presynaptic terminal (96, 258, 327, 342, 359, 474), the mechanisms regulating the distribution of synaptic vesicles and their release during repeated stimulation are not well understood.

Activity-dependent neuroplasticity can improve the efficacy synaptic neurotransmission (177). Using fluorescent styryl dyes to label recycling synaptic vesicles at rat soleus (predominantly comprising type I and IIa fibers) and extensor digitorum longus (EDL - predominantly comprising type IIx and IIb fibers), Reid and colleagues (342) reported fiber type differences in vesicle cycling, which they attributed to differences activation history. Electrophysiological studies demonstrated that presynaptic terminals at EDL muscle fibers have a higher initial quantal content compared to terminals at soleus muscle fibers (137, 342, 476). Because of their more frequent activation, the total number of synaptic vesicles cycled into the RRP or cycling pools would need to be higher at type I or IIa fiber terminals compared to type IIx and IIb terminals (205, 379). In agreement, during repetitive phrenic nerve stimulation, vesicle recycling, as measured by styryl dye uptake (FM4-64), was significantly greater at type I or IIa fiber terminals in the diaphragm muscle compared to type IIx and IIb terminals (258, 260, 359). Similar findings were obtained in limb muscles that comprise a more homogenous fiber type (26, 288, 342, 411). Thus, it is likely that fiber type differences in synaptic vesicle release and recycling reflect the activation history of these fibers.

As the major pump muscle for breathing, the diaphragm muscle is one of the most active skeletal muscles in the body with a duty cycle of ~0.4. However, it is likely that only type I and IIa fibers are active in sustaining ventilation (265, 266, 379, 383, 387). Presynaptic terminals at type I and IIa fibers in the diaphragm muscle have lower quantal content than terminals at type IIx and/or IIb fibers (100, 359). Compared to type IIx and IIb fibers, presynaptic terminals a type I and IIa fibers have a greater density of synaptic vesicles at each active zone, but the overall size of the RRP is proportional to the number of active zones within a presynaptic terminal (359). Thus, because presynaptic terminals at type IIx and IIb fibers are larger, there are more active zones and accordingly, the overall size of the RRP is greater. The larger initial quantal content at type IIx and IIb diaphragm muscle fibers is consistent with the larger overall RRP at these presynaptic terminals (359). The number of synaptic vesicles released per nerve impulse (quantal content) most likely depends on the number of vesicles available (size of the RRP), and the probability of vesicle release at each active zone (100, 342, 359, 474).

During repetitive activation of the presynaptic terminal, the ability to sustain neuromuscular transmission depends on the probability of synaptic vesicle release and the size of the RRP. The RRP is likely replenished through recruitment from other pools and/or the recycling of released vesicles (100, 258, 260, 359). The number of synaptic vesicles released with each repetitive stimulus (i.e., the quantal content) progressively decreases (100, 359). This decrease in quantal content results from depletion of the RRP (97, 140, 342, 359, 474), as well as a decrease in the probability of release (25, 72, 359). The relative contribution of RRP depletion versus decreased probability of release differs across presynaptic terminals innervating different muscle fiber types (359). At terminals innervating type IIx and/or IIb fibers in the rat diaphragm muscle, the initial rapid decline in quantal content that occurs during repetitive stimulation appears to predominantly result from the depletion of RRP vesicles with little change in the probability of release. At type I or IIa diaphragm fibers, the initial decline in quantal content during repetitive stimulation is more rapid and cannot be entirely explained by a depletion of RRP vesicles. Therefore, a decrease in the probability of vesicle release at type I and IIa presynaptic terminals also appears to contribute to the decease in quantal content during repetitive stimulation. Fiber type differences in the decline quantal content likely reflect differences in activation histories of these fibers and may underlie differences in susceptibility to neuromuscular transmission.

## Intrinsic muscle fatigue

Intrinsic muscle fatigue is defined as a decline in muscle force generation that is independent of the fidelity of neuromuscular transmission and/or excitation-contraction coupling. In this case, muscle fatigue is typically assessed by repetitive direct muscle stimulation rather than indirect nerve stimulation, where axonal propagation or neuromuscular transmission failure may occur (388). The timing and extent of muscle fatigue depends on stimulation parameters such as stimulation frequency and/or duty cycle (time muscle is active vs. relaxed) (205, 387). With increasing stimulation frequency, muscle fatigue occurs more rapidly and to a greater extent. Similarly, as duty cycle increases the rate of decline of muscle force is more rapid and the extent of fatigue is more pronounced.

**Relationship to motor unit fatigue—**Motor units comprise different muscle fibers that vary in their contractile protein composition, which underlies fiber type classification. Typically, motor units are homogeneous comprising a single muscle fiber type (Figure 4). Relevant to the discussion of the intrinsic fatigue properties of muscle fibers is the fact that motor units vary in their susceptibility to fatigue with repetitive stimulation, i.e., they are defined as fatigue resistant (type S and FR) and fatigable (type FInt and FF units). The

recruitment of motor units during different motor tasks is closely matched to their fatigability; thus, the intrinsic fatigue properties of muscle fibers comprising these motor units critically determine the efficacy of motor control.

**Relationship to muscle fiber metabolic capacity—**Intrinsic muscle fatigue depends on the balance between energy utilization (cross-bridge cycling rate and ATP consumption) and production (mitochondrial volume density and capacity for oxidative phosphorylation) within a single fiber. Within single muscle fibers, differences in MyHC isoform expression are associated with differences in cross-bridge cycling rate, ATP consumption, mitochondrial volume density, and the capacity for oxidative phosphorylation (98, 390). For instance, in muscle fibers expressing $MyHC_{2X}$ and/or $MyHC_{2B}$ isoforms ATP consumption rate is much higher compared to fibers expressing $MyHC_{Slow}$ and $MyHC_{2A}$ isoforms, even when normalized for differences in myosin concentration (174, 394, 399). Accordingly, it is not surprising that muscle fibers expressing $MyHC_{2X}$ and/or $MyHC_{2B}$ isoforms comprise fatigable motor units, whereas fibers expressing $MyHC_{Slow}$ and $MyHC_{2A}$ isoforms comprise fatigue resistant motor units (98, 390).

Metabolites produced during cross-bridge cycling may also influence force generation and contribute to fatigue. For example, during cross-bridge cycling and associated ATP hydrolysis, there is an accumulation of inorganic phosphate ($P_i$) and a decrease in pH. In studies using single, permeabilized muscle fibers, it has been shown that both increased $P_i$ and decreased pH reduce force generation (5, 471). In addition, increased $P_i$ and decreased pH reduce $Ca^{2+}$ sensitivity such that submaximal force generation is also reduced (304). This would affect the force-frequency relationship of muscle fibers. Repetitive activation of muscle fibers may also alter the availability of myoplasmic $Ca^{2+}$ by reducing $Ca^{2+}$ release from the sarcoplasmic reticulum (470). Thus, not only is there a reduction in $Ca^{2+}$ sensitivity but also a reduction in available myoplasmic $Ca^{2+}$.

Conditions that disproportionately affect the cross-sectional area of certain muscle fiber types (e.g., chronic obstructive pulmonary disease, corticosteroid treatment, hypothyroidism, sarcopenia) will impact the overall assessment of muscle fatigue under experimental conditions where supramaximal activation is used. For example, selective atrophy of type IIx and/or IIb diaphragm muscle fibers that comprise more fatigable motor units may lead to confusion about the impact of disease conditions on muscle fatigue. With selective atrophy of type IIx and/or IIb diaphragm muscle fibers, there would be a reduced contribution of more fatigable motor units to diaphragm muscle force. At the same time, there would be an apparent improvement in the fatigue resistance of the diaphragm muscle.

## Neuromotor Control of Respiratory Muscles

Motor units are recruited based on the size of motoneurons as reflected by axonal conduction velocity (179, 180, 284). Accordingly, motor units that are recruited first (i.e, lower threshold) display slower axonal conduction velocities compared to higher threshold units (i.e., recruited later during motor behaviors). Motor unit recruitment order thus corresponds with the mechanical and fatigue properties of the muscle fibers comprising these units. Type S motor units comprising type I fibers are recruited first, followed in rank order by type FR, FInt and FF units, comprising type IIa, IIx and/or IIb fibers, respectively (64, 285, 424). This orderly recruitment of motor units also exists in the diaphragm muscle (90, 202, 203, 371, 372).

A model of motor unit recruitment in the diaphragm muscle was developed to account for forces generated across a range of ventilatory and non-ventilatory behaviors. This model was based on a progressive recruitment of type S, FR, FInt and FF units, and the forces

contributed by each motor unit type (265, 266, 379, 387, 458). During ventilatory behaviors in several species, quiet breathing (eupnea) can be accomplished by the recruitment of only type S and FR motor units (265, 379, 383, 386). Even during more stressful ventilatory behaviors (e.g, following exposure to 10% $O_2$ and 5% $CO_2$), the necessary forces generated by the diaphragm can be accomplished primarily by the recruitment of type S and FR units with the possible additional recruitment of only a small number of type FInt units. Only during more forceful non-ventilatory behaviors (e.g., overcoming airway obstruction and during airway protective behaviors such as coughing or sneezing) would it be necessary to recruit the remaining more fatigable (type FInt and FF) motor units. Obviously it is more relevant to explore respiratory muscle activation under these behavioral conditions rather than during non-physiological conditions reflected in most studies using isolated nerve-muscle preparations. The model of motor unit recruitment has been used to evaluate the impact on motor performance of various pathophysiological conditions that may differentially affect muscle fibers comprising specific motor unit types (e.g, COPD or spinal cord injury) (266, 269, 270).

## Conclusion

Striated respiratory muscles serve as the pump for lung ventilation and in this respect they are equivalent to the heart in the cardiovascular system. Yet, in comparison to the heart, the respiratory muscles have received relatively little attention and there is much to be learned about their unique function and how they might fail in pulmonary disease. Striated respiratory muscles also serve to maintain the patency of the upper airway, and their dysfunction leads to highly prevalent diseases such as obstructive sleep apnea. Again, we have much to learn about the physiology and pathophysiology of the upper airway muscles.

As in other striated muscles, the sarcomere is the basic structural and functional element of respiratory muscles, and expression of sarcomeric proteins underlies the mechanical properties of muscle fibers. Cross-bridges form by the binding of MyHC to the actin filament, and are the elementary units of force generation and contraction. Passive mechanical properties of muscle fibers also relate to sarcomeric proteins as well as their interaction with the extracellular matrix. Categorization of different fiber types based on expression of different MyHC isoforms provides a conceptual framework to understand the physiological properties of respiratory muscles. The nervous system controls respiratory muscle contraction based on activation of motor units that comprise specific fiber types. These motor units vary in the contractile and fatigue properties and recruitment of specific motor unit types is well matched to accomplishing specific ventilatory and non-ventilatory functions of the respiratory muscles. Pathophysiology that results in respiratory muscle dysfunction will manifest differently depending on the impact on sarcomeric proteins and may vary across muscle fiber (motor unit) types. Recent attention to fiber type specific adaptations to injury and disease offer significant promise to the development of novel therapeutic strategies.

## Acknowledgments

This work was supported by NIH grants HL096750 and AG044615 (GCS and CBM), HL051173 (GCS), AR055974 (MBR), and HL098453 (LFF).

## References

1. Adelman WJ, Palti Y, Senft JP. Potassium ion accumulation in a periaxonal space and its effect on the measurement of membrane potassium ion conductance. J Membr Biol. 1973; 13:387–410. [PubMed: 4775518]

2. Aldrich TK, Shander A, Chaudhry I, Nagashima H. Fatigue of isolated rat diaphragm: role of impaired neuromuscular transmission. J Appl Physiol. 1986; 61:1077–1083. [PubMed: 3019989]
3. Aldrich TK. Transmission fatigue of the rabbit diaphragm. Respir Physiol. 1987; 69:307–319. [PubMed: 2821596]
4. Allan DW, Greer JJ. Embryogenesis of the phrenic nerve and diaphragm in the fetal rat. J Comp Neurol. 1997; 382:459–468. [PubMed: 9184993]
5. Allen DG. Skeletal muscle function: role of ionic changes in fatigue, damage and disease. Clin Exp Pharmacol Physiol. 2004; 31:485–493. [PubMed: 15298539]
6. Ameredes BT, Zhan W-Z, Vanderboom R, Prakash YS, Sieck GC. Power fatigue of the rat diaphragm muscle. J Appl Physiol. 2000; 89:2215–2219. [PubMed: 11090570]
7. Anderson J, Li Z, Goubel F. Passive stiffness is increased in soleus muscle of desmin knockout mouse. Muscle Nerve. 2001; 24:1090–1092. [PubMed: 11439386]
8. Argadine HM, Hellyer NJ, Mantilla CB, Zhan WZ, Sieck GC. The effect of denervation on protein synthesis and degradation in adult rat diaphragm muscle. J Appl Physiol. 2009; 107:438–444. [PubMed: 19520837]
9. Argadine HM, Mantilla CB, Zhan WZ, Sieck GC. Intracellular signaling pathways regulating net protein balance following diaphragm muscle denervation. Am J Physiol Cell Physiol. 2011; 300:C318–327. [PubMed: 21084642]
10. Baar K, Esser K. Phosphorylation of p70(S6k) correlates with increased skeletal muscle mass following resistance exercise. Am J Physiol Cell Physiol. 1999; 276:C120–127.
11. Babiuk RP, Zhang W, Clugston R, Allan DW, Greer JJ. Embryological origins and development of the rat diaphragm. J Comp Neurol. 2003; 455:477–487. [PubMed: 12508321]
12. Bagni MA, Cecchi G, Colomo F, Garzella P. Are weakly binding bridges present in resting intact muscle fibers? Biophys J. 1992; 63:1412–1415. [PubMed: 1477287]
13. Bagni MA, Cecchi G, Colomo F, Garzella P. Absence of mechanical evidence for attached weakly binding cross-bridges in frog relaxed muscle fibres. J Physiol. 1995; 482(Pt 2):391–400. [PubMed: 7714830]
14. Bang ML, Centner T, Fornoff F, Geach AJ, Gotthardt M, McNabb M, Witt CC, Labeit D, Gregorio CC, Granzier H, Labeit S. The complete gene sequence of titin, expression of an unusual approximately 700-kDa titin isoform, and its interaction with obscurin identify a novel Z-line to I-band linking system. Circ Res. 2001; 89:1065–1072. [PubMed: 11717165]
15. Bar A, Pette D. Three fast myosin heavy chains in adult rat skeletal muscle. FEBS Lett. 1988; 235:153–155. [PubMed: 3402594]
16. Barron DH, Matthews BHC. Intermittent conduction in the spinal cord. J Physiol (Lond). 1935; 85:73–103. [PubMed: 16994699]
17. Bartlett D Jr, Remmers JE, Gautier H. Laryngeal regulation of respiratory airflow. Respir Physiol. 1973; 18:194–204. [PubMed: 4730751]
18. Bartoo ML, Popov VI, Fearn LA, Pollack GH. Active tension generation in isolated skeletal myofibrils. J Muscle Res Cell Motil. 1993; 14:498–510. [PubMed: 8300845]
19. Baumeister W, Walz J, Zuhl F, Seemuller E. The proteasome: paradigm of a self-compartmentalizing protease. Cell. 1998; 92:367–380. [PubMed: 9476896]
20. Bazzy AR, Donnelly DF. Failure to generate action potentials in newborn diaphragms following nerve stimulation. Brain Res. 1993; 600:349–352. [PubMed: 8382101]
21. Bellemare F, Bigland-Ritchie B, Woods JJ. Contractile properties of the human diaphragm in vivo. J Appl Physiol. 1986; 61:1153–1161. [PubMed: 3759756]
22. Bellemare F, Bigland-Ritchie B. Central components of diaphragmatic fatigue assessed by phrenic nerve stimulation. J Appl Physiol. 1987; 62:1307–1316. [PubMed: 3571083]
23. Benard G, Karbowski M. Mitochondrial fusion and division: Regulation and role in cell viability. Semin Cell Dev Biol. 2009; 20:365–374. [PubMed: 19530306]
24. Berthier C, Blaineau S. Supramolecular organization of the subsarcolemmal cytoskeleton of adult skeletal muscle fibers. A review. Biol Cell. 1997; 89:413–434. [PubMed: 9561721]
25. Betz WJ. Depression of transmitter release at the neuromuscular junction of the frog. J Physiol. 1970; 206:629–644. [PubMed: 5498509]

26. Betz WJ, Ridge RM, Bewick GS. Comparison of FM1-43 staining patterns and electrophysiological measures of transmitter release at the frog neuromuscular junction. J Physiol Paris. 1993; 87:193–202. [PubMed: 7511018]
27. Bicknese S, Periasamy N, Shohet SB, Verkman AS. Cytoplasmic viscosity near the cell plasma membrane: measurement by evanescent field frequency-domain microfluorimetry. Biophys J. 1993; 65:1272–1282. [PubMed: 8241407]
28. Biggs WH 3rd, Meisenhelder J, Hunter T, Cavenee WK, Arden KC. Protein kinase B/Akt-mediated phosphorylation promotes nuclear exclusion of the winged helix transcription factor FKHR1. Proc Natl Acad Sci U S A. 1999; 96:7421–7426. [PubMed: 10377430]
29. Biggs WH 3rd, Cavenee WK, Arden KC. Identification and characterization of members of the FKHR (FOX O) subclass of winged-helix transcription factors in the mouse. Mamm Genome. 2001; 12:416–425. [PubMed: 11353388]
30. Bigland-Ritchie B, Jones DA, Woods JJ. Excitation frequency and muscle fatigue: electrical responses during human voluntary and stimulated contractions. Exp Neurol. 1979; 64:414–427. [PubMed: 428516]
31. Bigland-Ritchie B, Lippold OCJ. Changes in muscle activation during prolonged maximal voluntary contractions. J Physiol (Lond). 1979; 330:265–278. [PubMed: 6294288]
32. Bigland-Ritchie B, Donovan EF, Roussos CS. Conduction velocity and EMG power spectrum changes in fatigue of sustained maximal efforts. J Appl Physiol. 1981; 51:1300–1305. [PubMed: 7298467]
33. Bigland-Ritchie B, Kukulka CG, Lippold OCJ, Woods JJ. The absence of neuromuscular transmission failure in sustained maximal voluntary contractions. J Physiol. 1982; 330:265–278. [PubMed: 6294288]
34. Bittner GD. Differentiation of nerve terminals in the crayfish opener muscle and its functional significance. J Gen Physiol. 1968; 51:731–758. [PubMed: 4300149]
35. Blanco CE, Sieck GC, Edgerton VR. Quantitative histochemical determination of succinic dehydrogenase activity in skeletal muscle fibres. Histochem J. 1988; 20:230–243. [PubMed: 3209423]
36. Blanco CE, Fournier M, Sieck GC. Metabolic variability within individual fibres of the cat tibialis posterior and diaphragm muscles. Histochem J. 1991; 23:366–374. [PubMed: 1917565]
37. Blanco CE, Sieck GC. Quantitative determination of calcium-activated myosin adenosine triphosphatase activity in rat skeletal muscle fibres. Histochem J. 1992; 24:431–444. [PubMed: 1387125]
38. Bloch RJ, Gonzalez-Serratos H. Lateral force transmission across costameres in skeletal muscle. Exerc Sport Sci Rev. 2003; 31:73–78. [PubMed: 12715970]
39. Boczkowski J, Dureuil B, Branger C, Pavlovic D, Murciano D, Pariente R, Aubier M. Effects of sepsis on diaphragmatic function in rats. Am Rev Respir Dis. 1988; 138:260–265. [PubMed: 3195825]
40. Bodine SC, Latres E, Baumhueter S, Lai VK, Nunez L, Clarke BA, Poueymirou WT, Panaro FJ, Na E, Dharmarajan K, Pan ZQ, Valenzuela DM, DeChiara TM, Stitt TN, Yancopoulos GD, Glass DJ. Identification of ubiquitin ligases required for skeletal muscle atrophy. Science. 2001; 294:1704–1708. [PubMed: 11679633]
41. Bodine SC, Stitt TN, Gonzalez M, Kline WO, Stover GL, Bauerlein R, Zlotchenko E, Scrimgeour A, Lawrence JC, Glass DJ, Yancopoulos GD. Akt/mTOR pathway is a crucial regulator of skeletal muscle hypertrophy and can prevent muscle atrophy in vivo. Nat Cell Biol. 2001; 3:1014–1019. [PubMed: 11715023]
42. Bolster DR, Crozier SJ, Kimball SR, Jefferson LS. AMP-activated protein kinase suppresses protein synthesis in rat skeletal muscle through down-regulated mammalian target of rapamycin (mTOR) signaling. J Biol Chem. 2002; 277:23977–23980. [PubMed: 11997383]
43. Boriek AM, Rodarte JR. Inferences on passive diaphragm mechanics from gross anatomy. J Appl Physiol. 1994; 77:2065–2070. [PubMed: 7868417]
44. Boriek AM, Miller CC 3rd, Rodarte JR. Muscle fiber architecture of the dog diaphragm. J Appl Physiol. 1998; 84:318–326. [PubMed: 9451652]

45. Boriek AM, Kelly NG, Rodarte JR, Wilson TA. Biaxial constitutive relations for the passive canine diaphragm. J Appl Physiol. 2000; 89:2187–2190. [PubMed: 11090566]
46. Boriek AM, Capetanaki Y, Hwang W, Officer T, Badshah M, Rodarte J, Tidball JG. Desmin integrates the three-dimensional mechanical properties of muscles. Am J Physiol Cell Physiol. 2001; 280:C46–52. [PubMed: 11121375]
47. Boriek AM, Rodarte JR, Reid MB. Shape and tension distribution of the passive rat diaphragm. Am J Physiol Regul Integr Comp Physiol. 2001; 280:R33–41. [PubMed: 11124131]
48. Boriek AM, Zhu D, Zeller M, Rodarte JR. Inferences on force transmission from muscle fiber architecture of the canine diaphragm. Am J Physiol Regul Integr Comp Physiol. 2001; 280:R156–165. [PubMed: 11124147]
49. Boriek AM, Hwang W, Trinh L, Rodarte JR. Shape and tension distribution of the active canine diaphragm. Am J Physiol Regul Integr Comp Physiol. 2005; 288:R1021–1027. [PubMed: 15793029]
50. Bosco C, Komi PV. Potentiation of the mechanical behavior of the human skeletal muscle through prestretching. Acta Physiol Scand. 1979; 106:467–472. [PubMed: 495154]
51. Bracher A, Coleman R, Schnall R, Oliven A. Histochemical properties of upper airway muscles: comparison of dilator and nondilator muscles. Eur Respir J. 1997; 10:990–993. [PubMed: 9163636]
52. Brandt PW, Diamond MS, Rutchik JS, Schachat FH. Co-operative interactions between troponin-tropomyosin units extend the length of the thin filament in skeletal muscle. J Mol Biol. 1987; 195:885–896. [PubMed: 3656437]
53. Brenner B. Kinetics of the crossbridge cycle derived from measurements of force, rate of force development and isometric ATPase. J Muscle Res Cell Motil. 1986; 7:75–76.
54. Brenner B. The necessity of using two parameters to describe isotonic shortening velocity of muscle tissue: the effect of various interventions upon initial shortening velocity (vi) and curvature (b). Basic Res Cardiol. 1986; 81:54–69. [PubMed: 3487312]
55. Brenner B, Eisenberg E. Rate of force generation in muscle: Correlation with actomyosin ATPase activity in solution. Proc Nat Acad Sci USA. 1986; 83:3542–3546. [PubMed: 2939452]
56. Brooke MH, Kaiser KK. Muscle fiber types: how many and what kind? Arch Neurol. 1970; 23:369–379. [PubMed: 4248905]
57. Brooks SV, Faulkner JA. Contractile properties of skeletal muscles from young, adult and aged mice. J Physiol. 1988; 404:71–82. [PubMed: 3253447]
58. Brotto MA, Biesiadecki BJ, Brotto LS, Nosek TM, Jin JP. Coupled expression of troponin T and troponin I isoforms in single skeletal muscle fibers correlates with contractility. Am J Physiol Cell Physiol. 2006; 290:C567–576. [PubMed: 16192301]
59. Brown LM, Gonzalez-Serratos H, Huxley AF. Sarcomere and filament lengths in passive muscle fibres with wavy myofibrils. J Muscle Res Cell Motil. 1984; 5:293–314. [PubMed: 6611352]
60. Brunet A, Bonni A, Zigmond MJ, Lin MZ, Juo P, Hu LS, Anderson MJ, Arden KC, Blenis J, Greenberg ME. Akt promotes cell survival by phosphorylating and inhibiting a Forkhead transcription factor. Cell. 1999; 96:857–868. [PubMed: 10102273]
61. Buffelli M, Burgess RW, Feng G, Lobe CG, Lichtman JW, Sanes JR. Genetic evidence that relative synaptic efficacy biases the outcome of synaptic competition. Nature. 2003; 424:430–434. [PubMed: 12879071]
62. Bulbring E. Observations on the isolated phrenic nerve diaphragm preparation of the rat. Br J Pharmacol. 1946; 1:38–61.
63. Burke RE, Levine DN, Zajac FE 3rd. Mammalian motor units: physiological-histochemical correlation in three types in cat gastrocnemius. Science. 1971; 174:709–712. [PubMed: 4107849]
64. Burke RE, Levine DN, Tsairis P, Zajac FE 3rd. Physiological types and histochemical profiles in motor units of the cat gastrocnemius. J Physiol (Lond). 1973; 234:723–748. [PubMed: 4148752]
65. Cai D, Frantz JD, Tawa NE Jr, Melendez PA, Oh BC, Lidov HG, Hasselgren PO, Frontera WR, Lee J, Glass DJ, Shoelson SE. IKKbeta/NF-kappaB activation causes severe muscle wasting in mice. Cell. 2004; 119:285–298. [PubMed: 15479644]

66. Campbell KS, Lakie M. A cross-bridge mechanism can explain the thixotropic short-range elastic component of relaxed frog skeletal muscle. J Physiol. 1998; 510(Pt 3):941–962. [PubMed: 9660904]

67. Campbell KS, Moss RL. A thixotropic effect in contracting rabbit psoas muscle: prior movement reduces the initial tension response to stretch. J Physiol. 2000; 525(Pt 2):531–548. [PubMed: 10835052]

68. Campbell KS, Moss RL. History-dependent mechanical properties of permeabilized rat soleus muscle fibers. Biophys J. 2002; 82:929–943. [PubMed: 11806934]

69. Capetanaki Y, Bloch RJ, Kouloumenta A, Mavroidis M, Psarras S. Muscle intermediate filaments and their links to membranes and membranous organelles. Exp Cell Res. 2007; 313:2063–2076. [PubMed: 17509566]

70. Carrera M, Barbe F, Sauleda J, Tomas M, Gomez C, Agusti AG. Patients with obstructive sleep apnea exhibit genioglossus dysfunction that is normalized after treatment with continuous positive airway pressure. Am J Resp Crit Care Med. 1999; 159:1960–1966. [PubMed: 10351945]

71. Chandra M, Mamidi R, Ford S, Hidalgo C, Witt C, Ottenheijm C, Labeit S, Granzier H. Nebulin alters cross-bridge cycling kinetics and increases thin filament activation: a novel mechanism for increasing tension and reducing tension cost. J Biol Chem. 2009; 284:30889–30896. [PubMed: 19736309]

72. Christensen BN, Martin AR. Estimates of probability of transmitter release at the mammalian neuromuscular junction. J Physiol. 1970; 210:933–945. [PubMed: 4395959]

73. Claflin DR, Faulkner JA. Shortening velocity extrapolated to zero load and unloaded shortening velocity of whole rat skeletal muscle. J Physiol. 1985; 359:357–363. [PubMed: 3999042]

74. Claflin DR, Faulkner JA. The force-velocity relationship at high shortening velocities in the soleus muscle of the rat. J Physiol (London). 1989; 411:627–637. [PubMed: 2614737]

75. Clark KA, McElhinny AS, Beckerle MC, Gregorio CC. Striated muscle cytoarchitecture: an intricate web of form and function. Annu Rev Cell Dev Biol. 2002; 18:637–706. [PubMed: 12142273]

76. Clarke BA, Drujan D, Willis MS, Murphy LO, Corpina RA, Burova E, Rakhilin SV, Stitt TN, Patterson C, Latres E, Glass DJ. The E3 Ligase MuRF1 degrades myosin heavy chain protein in dexamethasone-treated skeletal muscle. Cell Metab. 2007; 6:376–385. [PubMed: 17983583]

77. Close RI. Dynamic properties of mammalian skeletal muscles. Physiol Rev. 1972; 52:129–197. [PubMed: 4256989]

78. Coirault C, Samuel JL, Chemla D, Pourny JC, Lambert F, Marotte F, Lecarpentier Y. Increased compliance in diaphragm muscle of the cardiomyopathic Syrian hamster. J Appl Physiol. 1998; 85:1762–1769. [PubMed: 9804579]

79. Cooke R. The actomyosin engine. FASEB J. 1995; 9:636–642. [PubMed: 7768355]

80. Corton JM, Gillespie JG, Hawley SA, Hardie DG. 5-aminoimidazole-4-carboxamide ribonucleoside. A specific method for activating AMP-activated protein kinase in intact cells? Eur J Biochem. 1995; 229:558–565. [PubMed: 7744080]

81. D'Antona G, Megighian A, Bortolotto S, Pellegrino MA, Marchese-Ragona R, Staffieri A, Bottinelli R, Reggiani C. Contractile properties and myosin heavy chain isoform composition in single fibre of human laryngeal muscles. J Muscle Res Cell Motil. 2002; 23:187–195. [PubMed: 12500898]

82. Damiani E, Margreth A. Characterization study of the ryanodine receptor and of calsequestrin isoforms of mammalian skeletal muscles in relation to fibre types. J Muscle Res Cell Motil. 1994; 15:86–101. [PubMed: 8051290]

83. Danjo W, Fujimura N, Ujike Y. Effect of pentoxifylline on diaphragmatic contractility in septic rats. Acta Med Okayama. 2008; 62:101–107. [PubMed: 18464886]

84. de Tombe PP, ter Keurs HE. An internal viscous element limits unloaded velocity of sarcomere shortening in rat myocardium. J Physiol. 1992; 454:619–642. [PubMed: 1474506]

85. De Troyer A, Sampson M, Sigrist S, Macklem PT. The diaphragm: two muscles. Science. 1981; 213:237–238. [PubMed: 7244632]

86. De Troyer A, Sampson M, Sigrist S, Macklem PT. Action of costal and crural parts of the diaphragm on the rib cage in dog. J Appl Physiol. 1982; 53(1):30–39. [PubMed: 7118646]

87. Dempsey JA, Veasey SC, Morgan BJ, O'Donnell CP. Pathophysiology of sleep apnea. Physiol Rev. 2010; 90:47–112. [PubMed: 20086074]

88. Deval C, Mordier S, Obled C, Bechet D, Combaret L, Attaix D, Ferrara M. Identification of cathepsin L as a differentially expressed message associated with skeletal muscle wasting. Biochem J. 2001; 360:143–150. [PubMed: 11696001]

89. Diaz PT, Brownstein E, Clanton TL. Effects of N-acetylcysteine on in vitro diaphragm function are temperature dependent. J Appl Physiol. 1994; 77:2434–2439. [PubMed: 7868466]

90. Dick TE, Kong FJ, Berger AJ. Correlation of recruitment order with axonal conduction velocity for supraspinally driven diaphragmatic motor units. J Neurophysiol. 1987; 57:245–259. [PubMed: 3559674]

91. Diffee GM, Greaser ML, Reinach FC, Moss RL. Effects of a non-divalent cation binding mutant of myosin regulatory light chain on tension generation in skinned skeletal muscle fibers. Biophys J. 1995; 68:1443–1452. [PubMed: 7787030]

92. Eccles JC, Sherrington CS. Numbers and contraction values of individual motor units examined in some muscles of the limb. Am J Physiol. 1930; 253:210–218.

93. Eddinger TJ, Moss RL. Mechanical properties of skinned single fibers of identified types from rat diaphragm. Am J Physiol. 1987; 253:C210–C218. [PubMed: 3303962]

94. Edman KAP. The velocity of unloaded shortening and its relation to sarcomere length and isometric force in vertebrate muscle fibres. J Physiol. 1979; 291:143–159. [PubMed: 314510]

95. Edwards RH. Human muscle function and fatigue. CIBA Found Symp. 1981; 82:1–18. [PubMed: 6117420]

96. Ellisman MH, Rash JE, Staehelin LA, Porter KR. Studies of excitable membranes. II. A comparison of specializations at neuromuscular junctions and nonjunctional sarcolemmas of mammalian fast and slow twitch muscle fibers. J Cell Biol. 1976; 68:752–774. [PubMed: 1030710]

97. Elmqvist D, Quastel DM. A quantitative study of end-plate potentials in isolated human muscle. J Physiol. 1965; 178:505–529. [PubMed: 5827910]

98. Enad JG, Fournier M, Sieck GC. Oxidative capacity and capillary density of diaphragm motor units. J Appl Physiol. 1989; 67:620–627. [PubMed: 2529236]

99. Enright PL, Kronmal RA, Manolio TA, Schenker MB, Hyatt RE. Respiratory muscle strength in the elderly. Correlates and reference values. Cardiovascular Health Study Research Group. Am J Respir Crit Care Med. 1994; 149:430–438. [PubMed: 8306041]

100. Ermilov LG, Mantilla CB, Rowley KL, Sieck GC. Safety factor for neuromuscular transmission at type-identified diaphragm fibers. Muscle Nerve. 2007; 35:800–803. [PubMed: 17286272]

101. Ermilov LG, Pulido JN, Atchison FW, Zhan WZ, Ereth MH, Sieck GC, Mantilla CB. Impairment of diaphragm muscle force and neuromuscular transmission after normothermic cardiopulmonary bypass: effect of low dose inhaled CO. Am J Physiol Regul Integr Comp Physiol. 2010; 298:R784–789. [PubMed: 20089713]

102. Farkas GA, Roussos C. Diaphragm in emphysematous hamsters: sarcomere adaptability. J Appl Physiol. 1983; 54:1635–1640. [PubMed: 6874487]

103. Farkas GA, Decramer M, Rochester DF, De Troyer A. Contractile properties of intercostal muscles and their functional significance. J Appl Physiol. 1985; 59:528–535. [PubMed: 4030606]

104. Farkas GA, Rochester DF. Contractile characteristics and operating lengths of canine neck inspiratory muscles. J Appl Physiol. 1986; 61:220–226. [PubMed: 3733607]

105. Farkas GA, Rochester DF. Functional characteristics of canine costal and crural diaphragm. J Appl Physiol. 1988; 65:2253–2260. [PubMed: 3209568]

106. Farkas GA, Rochester DF. Characteristics and functional significance of canine abdominal muscles. J Appl Physiol. 1988; 65:2427–2433. [PubMed: 2975277]

107. Farkas GA. Mechanical properties of respiratory muscles in primates. Respir Physiol. 1991; 86:41–50. [PubMed: 1759052]

108. Faulkner JA, Maxwell LC, Ruff GL, White TP. The diaphragm as a muscle. Am Rev Respir Dis. 1979; 119:89–92. [PubMed: 570813]

109. Faulkner JA, Jones DA, Round JM. Injury to skeletal muscles of mice by forced lengthening during contractions. Q J Exp Physiol. 1989; 74:661–670. [PubMed: 2594927]

110. Fenn WO. A quantitative comparison between the energy liberated and the work performed by the isolated sartorius muscle of the frog. J Physiol (London). 1923; 58:175–203. [PubMed: 16993652]

111. Fenn WO. The relation between the work performed and the energy liberated in muscular contraction. J Physiol (Lond). 1924; 58:373–395. [PubMed: 16993634]

112. Fenn, WO.; Rhan, H., editors. Respiration. Washington, DC: American Physiological Society; 1964.

113. Ferreira LF, Gilliam LA, Reid MB. L-2-Oxothiazolidine-4-carboxylate reverses glutathione oxidation and delays fatigue of skeletal muscle in vitro. J Appl Physiol. 2009; 107:211–216. [PubMed: 19407260]

114. Ferreira LF, Moylan JS, Gilliam LA, Smith JD, Nikolova-Karakashian M, Reid MB. Sphingomyelinase stimulates oxidant signaling to weaken skeletal muscle and promote fatigue. Am J Physiol Cell Physiol. 2010; 299:C552–560. [PubMed: 20519448]

115. Flucher BE, Franzini-Armstrong C. Formation of junctions involved in excitation-contraction coupling in skeletal and cardiac muscle. Proc Natl Acad Sci U S A. 1996; 93:8101–8106. [PubMed: 8755610]

116. Fournier M, Sieck GC. Mechanical properties of muscle units in the cat diaphragm. J Neurophysiol. 1988; 59:1055–1066. [PubMed: 3367195]

117. Fournier M, Sieck GC. Somatotopy in the segmental innervation of the cat diaphragm. J Appl Physiol. 1988; 64:291–298. [PubMed: 3356649]

118. Fournier M, Alula M, Sieck GC. Neuromuscular transmission failure during postnatal development. Neurosci Lett. 1991; 125:34–36. [PubMed: 1649983]

119. Franzini-Armstrong C. Studies of the triad. I. Structure of the junction in frog twitch fibers. J Cell Biol. 1970; 47:488–499. [PubMed: 19866746]

120. Franzini-Armstrong C, Jorgensen AO. Structure and development of E-C coupling units in skeletal muscle. Annu Rev Physiol. 1994; 56:509–534. [PubMed: 8010750]

121. Freiburg A, Trombitas K, Hell W, Cazorla O, Fougerousse F, Centner T, Kolmerer B, Witt C, Beckmann JS, Gregorio CC, Granzier H, Labeit S. Series of exon-skipping events in the elastic spring region of titin as the structural basis for myofibrillar elastic diversity. Circ Res. 2000; 86:1114–1121. [PubMed: 10850961]

122. Froemming GR, Murray BE, Harmon S, Pette D, Ohlendieck K. Comparative analysis of the isoform expression pattern of Ca(2+)- regulatory membrane proteins in fast-twitch, slow-twitch, cardiac, neonatal and chronic low-frequency stimulated muscle fibers. Biochim Biophys Acta. 2000; 1466:151–168. [PubMed: 10825439]

123. Fujita H, Labeit D, Gerull B, Labeit S, Granzier HL. Titin isoform-dependent effect of calcium on passive myocardial tension. Am J Physiol Heart Circ Physiol. 2004; 287:H2528–2534. [PubMed: 15548726]

124. Fukuda N, Wu Y, Nair P, Granzier HL. Phosphorylation of titin modulates passive stiffness of cardiac muscle in a titin isoform-dependent manner. J Gen Physiol. 2005; 125:257–271. [PubMed: 15738048]

125. Fukuda N, Granzier HL, Ishiwata S, Kurihara S. Physiological functions of the giant elastic protein titin in mammalian striated muscle. J Physiol Sci. 2008; 58:151–159. [PubMed: 18477421]

126. Fuller DD, Fregosi RF. Fatiguing contractions of tongue protrudor and retractor muscles: influence of systemic hypoxia. J Appl Physiol. 2000; 88:2123–2130. [PubMed: 10846026]

127. Furuno K, Goodman MN, Goldberg AL. Role of different proteolytic systems in the degradation of muscle proteins during denervation atrophy. J Biol Chem. 1990; 265:8550–8557. [PubMed: 2187867]

128. Gautsch TA, Anthony JC, Kimball SR, Paul GL, Layman DK, Jefferson LS. Availability of eIF4E regulates skeletal muscle protein synthesis during recovery from exercise. Am J Physiol. 1998; 274:C406–414. [PubMed: 9486130]

129. Gea J, Zhu E, Galdiz JB, Comtois N, Salazkin I, Fiz JA, Grassino A. Functional consequences of eccentric contractions of the diaphragm. Arch Bronconeumol. 2009; 45:68–74. [PubMed: 19232267]
130. Geiger PC, Cody MJ, Sieck GC. Force-calcium relationship depends on myosin heavy chain and troponin isoforms in rat diaphragm muscle fibers. J Appl Physiol. 1999; 87:1894–1900. [PubMed: 10562634]
131. Geiger PC, Cody MJ, Macken RL, Sieck GC. Maximum specific force depends on myosin heavy chain content in rat diaphragm muscle fibers. J Appl Physiol. 2000; 89:695–703. [PubMed: 10926656]
132. Geiger PC, Cody MJ, Macken RL, Bayrd ME, Sieck GC. Mechanisms underlying increased force generation by rat diaphragm muscle fibers during development. J Appl Physiol. 2001; 90:380–388. [PubMed: 11133931]
133. Geiger PC, Cody MJ, Macken RL, Bayrd ME, Sieck GC. Effect of unilateral denervation on maximum specific force in rat diaphragm muscle fibers. J Appl Physiol. 2001; 90:1196–1204. [PubMed: 11247914]
134. Geiger PC, Cody MJ, Han YS, Hunter LW, Zhan WZ, Sieck GC. Effects of hypothyroidism on maximum specific force in rat diaphragm muscle fibers. J Appl Physiol. 2002; 92:1506–1514. [PubMed: 11896017]
135. Geiger PC, Bailey JP, Zhan WZ, Mantilla CB, Sieck GC. Denervation-induced changes in myosin heavy chain expression in the rat diaphragm muscle. J Appl Physiol. 2003; 95:611–619. [PubMed: 12704093]
136. Geiger PC, Bailey JP, Mantilla CB, Zhan WZ, Sieck GC. Mechanisms underlying myosin heavy chain expression during development of the rat diaphragm muscle. J Appl Physiol. 2006; 101:1546–1555. [PubMed: 16873604]
137. Gertler RA, Robbins N. Differences in neuromuscular transmission in red and white muscles. Brain Res. 1978; 142:160–164. [PubMed: 203368]
138. Gilliam LA, Ferreira LF, Bruton JD, Moylan JS, Westerblad H, St Clair DK, Reid MB. Doxorubicin acts through tumor necrosis factor receptor subtype 1 to cause dysfunction of murine skeletal muscle. J Appl Physiol. 2009; 107:1935–1942. [PubMed: 19779154]
139. Glass DJ. Molecular mechanisms modulating muscle mass. Trends Mol Med. 2003; 9:344–350. [PubMed: 12928036]
140. Glavinovic MI. Change of statistical parameters of transmitter release during various kinetic tests in unparalysed voltage-clamped rat diaphragm. J Physiol. 1979; 290:481–497. [PubMed: 224173]
141. Goffart M, Ritchie JM. The effect of adrenaline on the contraction of mammalian skeletal muscle. J Physiol. 1952; 116:357–371. [PubMed: 14939184]
142. Goldman, YE.; Homsher, E. Molecular physiology of the cross-bridge cycle. In: Engel, A.; Franzini-Armstrong, C., editors. Myology: Basic and Clinical. New York, NY: McGraw-Hill; 2004. p. 187-202.
143. Goldstein SS, Rall W. Changes of action potential shape and velocity for changing core conductor geometry. Biophys J. 1974; 14:731–757. [PubMed: 4420585]
144. Gomes MD, Lecker SH, Jagoe RT, Navon A, Goldberg AL. Atrogin-1, a muscle-specific F-box protein highly expressed during muscle atrophy. Proc Natl Acad Sci U S A. 2001; 98:14440–14445. [PubMed: 11717410]
145. Goodman C, Patterson M, Stephenson G. MHC-based fiber type and E-C coupling characteristics in mechanically skinned muscle fibers of the rat. Am J Physiol Cell Physiol. 2003; 284:C1448–1459. [PubMed: 12734106]
146. Gordon AM, Huxley AF, Julian FJ. The variation in isometric tension with sarcomere length in vertebrate muscle fibres. J Physiol. 1966; 184:170–192. [PubMed: 5921536]
147. Gordon DC, Hammond CG, Fisher JT, Richmond FJ. Muscle-fiber architecture, innervation, and histochemistry in the diaphragm of the cat. J Morphol. 1989; 201:131–143. [PubMed: 2474663]
148. Gorza L, Gundersen K, Lomo T, Schiaffino S, Westgaard RH. Slow-to-fast transformation of denervated soleus muscles by chronic high-frequency stimulation in the rat. J Physiol. 1988; 402:627–649. [PubMed: 3236251]

149. Gorza L. Identification of a novel type 2 fiber population in mammalian skeletal muscle by combined use of histochemical myosin ATPase and anti-myosin monoclonal antibodies. J Histochem Cytochem. 1990; 38:257–265. [PubMed: 2137154]

150. Gosselin LE, Martinez DA, Vailas AC, Sieck GC. Interstitial space and collagen alterations of the developing rat diaphragm. J Appl Physiol. 1993; 74:2450–2455. [PubMed: 7687597]

151. Gosselin LE, Johnson BD, Sieck GC. Age-related changes in diaphragm muscle contractile properties and myosin heavy chain isoforms. Am J Respir Crit Care Med. 1994; 150:174–178. published erratum appears in Am J Respir Crit Care Med 1994 Sep;150(3):879. [PubMed: 8025746]

152. Gosselin LE, Martinez DA, Vailas AC, Sieck GC. Passive length-force properties of senescent diaphragm: relationship with collagen characteristics. J Appl Physiol. 1994; 76:2680–2685. [PubMed: 7928900]

153. Gosselin LE, Sieck GC, Aleff RA, Martinez DA, Vailas AC. Changes in diaphragm muscle collagen gene expression after acute unilateral denervation. J Appl Physiol. 1995; 79:1249–1254. [PubMed: 8567569]

154. Gosselin LE, Zhan WZ, Sieck GC. Hypothyroid-mediated changes in adult rat diaphragm muscle contractile properties and MHC isoform expression. J Appl Physiol. 1996; 80:1934–1939. [PubMed: 8806897]

155. Gosselin LE, Williams JE, Personius K, Farkas GA. A comparison of factors associated with collagen metabolism in different skeletal muscles from dystrophic (mdx) mice: impact of pirfenidone. Muscle Nerve. 2007; 35:208–216. [PubMed: 17058274]

156. Gransee HM, Mantilla CB, Sieck GC. Respiratory Muscle Plasticity. Compr Physiol. 2012; 2:1441–1462. [PubMed: 23798306]

157. Granzier H, Labeit S. Structure-function relations of the giant elastic protein titin in striated and smooth muscle cells. Muscle Nerve. 2007; 36:740–755. [PubMed: 17763461]

158. Granzier HL, Wang K. Passive tension and stiffness of vertebrate skeletal and insect flight muscles: the contribution of weak cross-bridges and elastic filaments. Biophys J. 1993; 65:2141–2159. [PubMed: 8298040]

159. Granzier HL, Irving TC. Passive tension in cardiac muscle: contribution of collagen, titin, microtubules, and intermediate filaments. Biophys J. 1995; 68:1027–1044. [PubMed: 7756523]

160. Granzier HL, Labeit S. The giant protein titin: a major player in myocardial mechanics, signaling, and disease. Circ Res. 2004; 94:284–295. [PubMed: 14976139]

161. Greenberg MJ, Mealy TR, Watt JD, Jones M, Szczesna-Cordary D, Moore JR. The molecular effects of skeletal muscle myosin regulatory light chain phosphorylation. Am J Physiol Regul Integr Comp Physiol. 2009; 297:R265–274. [PubMed: 19458282]

162. Greenberg MJ, Mealy TR, Jones M, Szczesna-Cordary D, Moore JR. The direct molecular effects of fatigue and myosin regulatory light chain phosphorylation on the actomyosin contractile apparatus. Am J Physiol Regul Integr Comp Physiol. 2010; 298:R989–996. [PubMed: 20089714]

163. Greer EL, Dowlatshahi D, Banko MR, Villen J, Hoang K, Blanchard D, Gygi SP, Brunet A. An AMPK-FOXO pathway mediates longevity induced by a novel method of dietary restriction in C. elegans. Curr Biol. 2007; 17:1646–1656. [PubMed: 17900900]

164. Greer EL, Oskoui PR, Banko MR, Maniar JM, Gygi MP, Gygi SP, Brunet A. The energy sensor AMP-activated protein kinase directly regulates the mammalian FOXO3 transcription factor. J Biol Chem. 2007; 282:30107–30119. [PubMed: 17711846]

165. Greer JJ, Allan DW, Martin-Caraballo M, Lemke RP. An overview of phrenic nerve and diaphragm muscle development in the perinatal rat. J Appl Physiol. 1999; 86:779–786. [PubMed: 10066685]

166. Gregorevic P, Plant DR, Leeding KS, Bach LA, Lynch GS. Improved contractile function of the mdx dystrophic mouse diaphragm muscle after insulin-like growth factor-I administration. Am J Pathol. 2002; 161:2263–2272. [PubMed: 12466140]

167. Greising SM, Gransee HM, Mantilla CB, Sieck GC. Systems biology of skeletal muscle: fiber type as an organizing principle. Wiley Interdiscip Rev Syst Biol Med. 2012; 4:457–473. [PubMed: 22811254]

168. Griffiths RI, Shadwick RE, Berger PJ. Functional importance of a highly elastic ligament on the mammalian diaphragm. Proc Biol Sci. 1992; 249:199–204. [PubMed: 1360681]

169. Griffiths RI, Berger PJ. Functional development of the sheep diaphragmatic ligament. J Physiol. 1996; 492(Pt 3):913–919. [PubMed: 8735001]

170. Grob D. Muscular disease. Bull NY Acad Med. 1961; 37:809–834.

171. Grossman Y, Parnas I, Spira ME. Differential conduction block in branches of a bifurcating axon. J Physiol. 1979; 295:283–305. [PubMed: 521937]

172. Gulati AK, Reddi AH, Zalewski AA. Changes in the basement membrane zone components during skeletal muscle fiber degeneration and regeneration. J Cell Biol. 1983; 97:957–962. [PubMed: 6225786]

173. Guyton, AC.; Hall, JE. Textbook of Medical Physiology. Philadelphia, PA: W.B. Saunders Co.; 1999.

174. Han YS, Geiger PC, Cody MJ, Macken RL, Sieck GC. ATP consumption rate per cross bridge depends on myosin heavy chain isoform. J Appl Physiol. 2003; 94:2188–2196. [PubMed: 12588786]

175. Hardin BJ, Campbell KS, Smith JD, Arbogast S, Smith J, Moylan JS, Reid MB. TNF-alpha acts via TNFR1 and muscle-derived oxidants to depress myofibrillar force in murine skeletal muscle. J Appl Physiol. 2008; 104:694–699. [PubMed: 18187611]

176. Hatt H, Smith DO. Synaptic depression related to presynaptic axon conduction block. J Physiol. 1976; 259:367–393. [PubMed: 182964]

177. Hebb, DO. The Organization of Behavior. New York: John Wiley & Sons; 1949.

178. Hellyer NJ, Mantilla CB, Park EW, Zhan WZ, Sieck GC. Neuregulin-dependent protein synthesis in C2C12 myotubes and rat diaphragm muscle. Am J Physiol Cell Physiol. 2006; 291:C1056–1061. [PubMed: 16790500]

179. Henneman E, Olson CB. Relations between structure and function in the design of skeletal muscles. J Neurophysiol. 1965; 28:581–598. [PubMed: 14328455]

180. Henneman E, Somjen G, Carpenter DO. Functional significance of cell size in spinal motoneurons. J Neurophysiol. 1965; 28:560–580. [PubMed: 14328454]

181. Hill AV. The heat of shortening and the dynamic constants of muscle. Proc R Soc Lond. 1938; 126:136–195.

182. Hill DK. Tension due to interaction between the sliding filaments in resting striated muscle. The effect of stimulation. J Physiol. 1968; 199:637–684. [PubMed: 5710425]

183. Hisa Y, Malmgren LT, Lyon MJ. Quantitative histochemical studies on the cat infrahyoid muscles. Otolaryngol Head Neck Surg. 1990; 103:723–732. [PubMed: 2148971]

184. Hlastala, MP.; Berger, AJ. Physiology of Respiration. New York, NY: Oxford University Press; 2001.

185. Homma I, Hagbarth KE. Thixotropy of rib cage respiratory muscles in normal subjects. J Appl Physiol. 2000; 89:1753–1758. [PubMed: 11053322]

186. Horowits R. The physiological role of titin in striated muscle. Rev Physiol Biochem Pharmacol. 1999; 138:57–96. [PubMed: 10396138]

187. Hubmayr RD, Farkas GA, Tao HY, Sieck GC, Margulies SS. Diaphragm mechanics in dogs with unilateral emphysema. J Clin Invest. 1993; 91:1598–1603. [PubMed: 8473503]

188. Huijing PA. Muscle as a collagen fiber reinforced composite: a review of force transmission in muscle and whole limb. J Biomech. 1999; 32:329–345. [PubMed: 10213024]

189. Hunter RB, Stevenson E, Koncarevic A, Mitchell-Felton H, Essig DA, Kandarian SC. Activation of an alternative NF-kappaB pathway in skeletal muscle during disuse atrophy. FASEB J. 2002; 16:529–538. [PubMed: 11919155]

190. Hunter RB, Kandarian SC. Disruption of either the Nfkb1 or the Bcl3 gene inhibits skeletal muscle atrophy. J Clin Invest. 2004; 114:1504–1511. [PubMed: 15546001]

191. Huxley AF, Niedergerke R. Structural changes in muscle during contraction; interference microscopy of living muscle fibres. Nature. 1954; 173:971–973. [PubMed: 13165697]

192. Huxley AF. Muscle structure and theories of contraction. Prog Biophysics Biophys Chem. 1957; 7:255–318.

193. Huxley AF, Taylor RE. Local activation of striated muscle fibres. J Physiol (Lond). 1958; 144:426–441. [PubMed: 13621406]

194. Huxley AF, Simmons RM. Proposed mechanism of force generation in striated muscle. Nature. 1971; 233:533–538. [PubMed: 4939977]

195. Huxley H, Hanson J. Changes in the cross-striations of muscle during contraction and stretch and their structural interpretation. Nature. 1954; 173:973–976. [PubMed: 13165698]

196. Hwang W, Kelly NG, Boriek AM. Passive mechanics of muscle tendinous junction of canine diaphragm. J Appl Physiol. 2005; 98:1328–1333. [PubMed: 15772060]

197. Isaza R, Behnke BJ, Bailey JK, McDonough P, Gonzalez NC, Poole DC. Arterial blood gas control in the upright versus recumbent Asian elephant. Respir Physiol Neurobiol. 2003; 134:169–176. [PubMed: 12609483]

198. Izumizaki M, Shibata M, Homma I. Factors contributing to thixotropy of inspiratory muscles. Respir Physiol Neurobiol. 2004; 140:257–264. [PubMed: 15186787]

199. Izumizaki M, Iwase M, Ohshima Y, Homma I. Acute effects of thixotropy conditioning of inspiratory muscles on end-expiratory chest wall and lung volumes in normal humans. J Appl Physiol. 2006; 101:298–306. [PubMed: 16575018]

200. Jannapureddy SR, Patel ND, Hwang W, Boriek AM. Genetic Models in Applied Physiology. Merosin deficiency leads to alterations in passive and active skeletal muscle mechanics. J Appl Physiol. 2003; 94:2524–2533. discussion 2523. [PubMed: 12736195]

201. Jenkins RR. Free radial chemistry --relationship to exercise. Sports Med. 1988; 5:156–170. [PubMed: 3285435]

202. Jodkowski JS, Viana F, Dick TE, Berger AJ. Electrical properties of phrenic motoneurons in the cat: correlation with inspiratory drive. J Neurophysiol. 1987; 58:105–124. [PubMed: 3039077]

203. Jodkowski JS, Viana F, Dick TE, Berger AJ. Repetitive firing properties of phrenic motoneurons in the cat. J Neurophysiol. 1988; 60:687–702. [PubMed: 3171647]

204. Johnson BD, Sieck GC. Activation-induced reduction of SDH activity in diaphragm muscle fibers. J Appl Physiol. 1993; 75:2689–2695. [PubMed: 8125891]

205. Johnson BD, Sieck GC. Differential susceptibility of diaphragm muscle fibers to neuromuscular transmission failure. J Appl Physiol. 1993; 75:341–348. [PubMed: 8397179]

206. Johnson BD, Wilson LE, Zhan WZ, Watchko JF, Daood MJ, Sieck GC. Contractile properties of the developing diaphragm correlate with myosin heavy chain phenotype. J Appl Physiol. 1994; 77:481–487. [PubMed: 7961272]

207. Judge AR, Koncarevic A, Hunter RB, Liou HC, Jackman RW, Kandarian SC. Role for IkappaBalpha, but not c-Rel, in skeletal muscle atrophy. Am J Physiol Cell Physiol. 2007; 292:C372–382. [PubMed: 16928772]

208. Keens TG, Bryan AC, Levison H, Ianuzzo CD. Developmental pattern of muscle fiber types in human ventilatory muscles. J Appl Physiol. 1978; 44:909–913. [PubMed: 149779]

209. Kellermayer MS, Smith SB, Bustamante C, Granzier HL. Mechanical fatigue in repetitively stretched single molecules of titin. Biophys J. 2001; 80:852–863. [PubMed: 11159452]

210. Kelly NG, McCarter RJ, Barnwell GM. Respiratory muscle stiffness is age- and muscle-specific. Aging. 1993; 5:229–238. [PubMed: 8399468]

211. Kelsen SG, Nochomovitz ML. Fatigue of the mammalian diaphragm in vitro. J Appl Physiol. 1982; 53:440–447. [PubMed: 6288638]

212. Kelsen SG, Supinski GS, Oliven A. Diaphragm structure and function in elastase-induced emphysema. Chest. 1984; 85:55S–58S. [PubMed: 6562957]

213. Kernell D, Monster AW. Time course and properties of late adaptation in spinal motoneurones of the cat. Exp Brain Res. 1982; 46:191–196. [PubMed: 6284539]

214. Kernell D, Monster AW. Motoneurone properties and motor fatigue. An intracellular study of gastrocnemius motoneurones of the cat. Exp Brain Res. 1982; 46:197–204. [PubMed: 6284540]

215. Khawli FA, Reid MB. N-acetylcysteine depresses contractile function and inhibits fatigue of diaphragm in vitro. J Appl Physiol. 1994; 77:317–324. [PubMed: 7961253]

216. Kim MJ, Druz WS, Danon J, Machnach W, Sharp JT. Mechanics of the canine diaphragm. J Appl Physiol. 1976; 41:369–382. [PubMed: 965306]

217. Kjaer M. Role of extracellular matrix in adaptation of tendon and skeletal muscle to mechanical loading. Physiol Rev. 2004; 84:649–698. [PubMed: 15044685]
218. Kleijn M, Scheper GC, Voorma HO, Thomas AA. Regulation of translation initiation factors by signal transduction. Eur J Biochem. 1998; 253:531–544. [PubMed: 9654048]
219. Kobzik L, Reid MB, Bredt DS, Stamler JS. Nitric oxide in skeletal muscle. Nature. 1994; 372:546–548. [PubMed: 7527495]
220. Koo BB, Strohl KP, Gillombardo CB, Jacono FJ. Ventilatory patterning in a mouse model of stroke. Respir Physiol Neurobiol. 2010; 172:129–135. [PubMed: 20472101]
221. Krnjevic K, Miledi R. Failure of neuromuscular propagation in rats. J Physiol. 1958; 140:440–461. [PubMed: 13514717]
222. Krnjevic K, Miledi R. Presynaptic failure of neuromuscular propagation in rats. J Physiol (Lond). 1959; 149:1–22. [PubMed: 14412088]
223. Kruger M, Linke WA. Protein kinase-A phosphorylates titin in human heart muscle and reduces myofibrillar passive tension. J Muscle Res Cell Motil. 2006; 27:435–444. [PubMed: 16897574]
224. Kuchler G, Patzak A, Schubert E. Muscle elasticity: effect of muscle length and temperature. Biomed Biochim Acta. 1990; 49:1209–1225. [PubMed: 2094225]
225. Kuei JH, Shadmehr R, Sieck GC. Relative contribution of neurotransmission failure to diaphragm fatigue. J Appl Physiol. 1990; 68:174–180. [PubMed: 2155900]
226. Kulakowski SA, Parker SD, Personius KE. Reduced TrkB expression results in precocious age-like changes in neuromuscular structure, neurotransmission, and muscle function. J Appl Physiol. 2011; 111:844–852. [PubMed: 21737823]
227. Kulke M, Fujita-Becker S, Rostkova E, Neagoe C, Labeit D, Manstein DJ, Gautel M, Linke WA. Interaction between PEVK-titin and actin filaments: origin of a viscous force component in cardiac myofibrils. Circ Res. 2001; 89:874–881. [PubMed: 11701614]
228. Kumar A, Khandelwal N, Malya R, Reid MB, Boriek AM. Loss of dystrophin causes aberrant mechanotransduction in skeletal muscle fibers. FASEB J. 2004; 18:102–113. [PubMed: 14718391]
229. Labeit D, Watanabe K, Witt C, Fujita H, Wu Y, Lahmers S, Funck T, Labeit S, Granzier H. Calcium-dependent molecular spring elements in the giant protein titin. Proc Natl Acad Sci U S A. 2003; 100:13716–13721. [PubMed: 14593205]
230. Labeit S, Kolmerer B. Titins: giant proteins in charge of muscle ultrastructure and elasticity. Science. 1995; 270:293–296. [PubMed: 7569978]
231. LaFramboise WA, Daood MJ, Guthrie RD, Butler-Browne GS, Whalen RG, Ontell M. Myosin isoforms in neonatal rat extensor digitorum longus, diaphragm, and soleus muscles. Am J Physiol. 1990; 259:L116–L122. [PubMed: 2382729]
232. LaFramboise WA, Daood MJ, Guthrie RD, Schiaffino S, Moretti P, Brozanski B, Ontell MP, Butler-Browne GS, Whalen RG, Ontell M. Emergence of the mature myosin phenotype in the rat diaphragm muscle. Dev Biol. 1991; 144:1–15. [PubMed: 1995390]
233. Lakie M, Robson LG. Thixotropy in frog single muscle fibres. Exp Physiol. 1990; 75:123–125. [PubMed: 2310557]
234. Lecker SH, Jagoe RT, Gilbert A, Gomes M, Baracos V, Bailey J, Price SR, Mitch WE, Goldberg AL. Multiple types of skeletal muscle atrophy involve a common program of changes in gene expression. FASEB J. 2004; 18:39–51. [PubMed: 14718385]
235. Levine S, Kaiser L, Leferovich J, Tikunov B. Cellular adaptations in the diaphragm in chronic obstructive pulmonary disease. N Engl J Med. 1997; 337:1799–1806. [PubMed: 9400036]
236. Lewis MI, Sieck GC, Fournier M, Belman MJ. Effect of nutritional deprivation on diaphragm contractility and muscle fiber size. J Appl Physiol. 1986; 60:596–603. [PubMed: 3949661]
237. Lewis MI, Monn SA, Sieck GC. Effect of corticosteroids on diaphragm fatigue, SDH activity, and muscle fiber size. J Appl Physiol. 1992; 72:293–301. [PubMed: 1537729]
238. Lewis MI, Zhan WZ, Sieck GC. Adaptations of the diaphragm in emphysema. J Appl Physiol. 1992; 72:934–943. [PubMed: 1568989]
239. Lewis MI, Monn SA, Zhan WZ, Sieck GC. Interactive effects of emphysema and malnutrition on diaphragm structure and function. J Appl Physiol. 1994; 77:947–955. [PubMed: 8002552]

240. Lewis MI, LoRusso TJ, Zhan W-Z, Sieck GC. Interactive effects of denervation and malnutrition on diaphragm structure and function. J Appl Physiol. 1996; 81:2165–2172. [PubMed: 8941542]

241. Lewis MI, Fournier M, Yeh AY, Micevych PE, Sieck GC. Alterations in diaphragm contractility after nandrolone administration: an analysis of potential mechanisms. J Appl Physiol. 1999; 86:985–992. [PubMed: 10066714]

242. Lewis MI, Li H, Huang ZS, Biring MS, Cercek B, Fournier M. Influence of varying degrees of malnutrition on IGF-I expression in the rat diaphragm. J Appl Physiol. 2003; 95:555–562. [PubMed: 12704096]

243. Lewis MI, Bodine SC, Kamangar N, Xu X, Da X, Fournier M. Effect of severe short-term malnutrition on diaphragm muscle signal transduction pathways influencing protein turnover. J Appl Physiol. 2006; 100:1799–1806. [PubMed: 16484360]

244. Li Z, Mericskay M, Agbulut O, Butler-Browne G, Carlsson L, Thornell LE, Babinet C, Paulin D. Desmin is essential for the tensile strength and integrity of myofibrils but not for myogenic commitment, differentiation, and fusion of skeletal muscle. J Cell Biol. 1997; 139:129–144. [PubMed: 9314534]

245. Liddell EGT, Sherrington CS. Recruitment and some other factors of reflex inhibition. Proc Roy Soc Lond (Biol). 1925; 97:488–518.

246. Light N, Champion AE. Characterization of muscle epimysium, perimysium and endomysium collagens. Biochem J. 1984; 219:1017–1026. [PubMed: 6743238]

247. Lloyd JS, Brozanski BS, Daood M, Watchko JF. Developmental transitions in the myosin heavy chain phenotype of human respiratory muscle. Biol Neonate. 1996; 69:67–75. [PubMed: 8713651]

248. Lopez MA, Mayer U, Hwang W, Taylor T, Hashmi MA, Jannapureddy SR, Boriek AM. Force transmission, compliance, and viscoelasticity are altered in the alpha7-integrin-null mouse diaphragm. Am J Physiol Cell Physiol. 2005; 288:C282–289. [PubMed: 15643051]

249. Luby-Phelps K. Cytoarchitecture and physical properties of cytoplasm: volume, viscosity, diffusion, intracellular surface area. Int Rev Cytol. 2000; 192:189–221. [PubMed: 10553280]

250. Luff AR. Dynamic properties of the inferior rectus, extensor digitorum longus, diaphragm and soleus muscles of the mouse. J Physiol. 1981; 313:161–171. [PubMed: 7277215]

251. Lynch GS, Fary CJ, Williams DA. Quantitative measurement of resting skeletal muscle [Ca2+]i following acute and long-term downhill running exercise in mice. Cell Calcium. 1997; 22:373–383. [PubMed: 9448944]

252. MacIntosh, BR.; Gardiner, PF.; McComas, AJ. Skeletal Muscle Form and Function. Champaign, IL: Human Kinetics; 2006.

253. Macklem, PT.; Mead, J., editors. Mechanics of Breathing. Washington, DC: American Physiological Society; 1986.

254. Macklem, PT. The Thorax; Part A: Physiology, Chapter 15 The Act of Breathing. New York, NY: Marcel Dekker, Inc.; 1995.

255. Magid A, Law DJ. Myofibrils bear most of the resting tension in frog skeletal muscle. Science. 1985; 230:1280–1282. [PubMed: 4071053]

256. Mammucari C, Milan G, Romanello V, Masiero E, Rudolf R, Del Piccolo P, Burden SJ, Di Lisi R, Sandri C, Zhao J, Goldberg AL, Schiaffino S, Sandri M. FoxO3 controls autophagy in skeletal muscle in vivo. Cell Metab. 2007; 6:458–471. [PubMed: 18054315]

257. Mann EA, Burnett T, Cornell S, Ludlow CL. The effect of neuromuscular stimulation of the genioglossus on the hypopharyngeal airway. Laryngoscope. 2002; 112:351–356. [PubMed: 11889396]

258. Mantilla CB, Rowley KL, Fahim MA, Zhan WZ, Sieck GC. Synaptic vesicle cycling at type-identified diaphragm neuromuscular junctions. Muscle Nerve. 2004; 30:774–783. [PubMed: 15478121]

259. Mantilla CB, Zhan WZ, Sieck GC. Neurotrophins improve neuromuscular transmission in the adult rat diaphragm. Muscle Nerve. 2004; 29:381–386. [PubMed: 14981737]

260. Mantilla CB, Rowley KL, Zhan WZ, Fahim MA, Sieck GC. Synaptic vesicle pools at diaphragm neuromuscular junctions vary with motoneuron soma, not axon terminal, inactivity. Neuroscience. 2007; 146:178–189. [PubMed: 17346898]

261. Mantilla CB, Sieck GC. Key aspects of phrenic motoneuron and diaphragm muscle development during the perinatal period. J Appl Physiol. 2008; 104:1818–1827. [PubMed: 18403452]
262. Mantilla CB, Sill RV, Aravamudan B, Zhan WZ, Sieck GC. Developmental effects on myonuclear domain size of rat diaphragm fibers. J Appl Physiol. 2008; 104:787–794. [PubMed: 18187618]
263. Mantilla, CB.; Dow, DE.; Sieck, GC. Skeletal muscle changes in hypothyroidism. In: Preedy, VR.; Burrow, GN.; Watson, RR., editors. Comprehensive Handbook of Iodine. Oxford: Academic Press; 2009. p. 1087-1101.
264. Mantilla CB, Sieck GC. Neuromuscular adaptations to respiratory muscle inactivity. Respir Physiol Neurobiol. 2009; 169:133–140. [PubMed: 19744580]
265. Mantilla CB, Seven YB, Zhan WZ, Sieck GC. Diaphragm motor unit recruitment in rats. Respir Physiol Neurobiol. 2010; 173:101–106. [PubMed: 20620243]
266. Mantilla CB, Sieck GC. Phrenic motor unit recruitment during ventilatory and non-ventilatory behaviors. Respir Physiol Neurobiol. 2011; 179:57–63. [PubMed: 21763470]
267. Mantilla, CB.; Sieck, GC. Age-related remodeling of neuromuscular junctions. In: Lynch, GS., editor. Sarcopenia - age-related muscle wasting and weakness. Netherlands: Springer; 2011. p. 37-54.
268. Mantilla CB, Ermilov LG. The novel TrkB receptor agonist 7,8-dihydroxyflavone enhances neuromuscular transmission. Muscle Nerve. 2012; 45:274–276. [PubMed: 22246885]
269. Mantilla CB, Greising SM, Zhan WZ, Seven YB, Sieck GC. Prolonged C2 spinal hemisection-induced inactivity reduces diaphragm muscle specific force with modest, selective atrophy of type IIx and/or IIb fibers. J Appl Physiol. 2013; 114:380–386. [PubMed: 23195635]
270. Mantilla CB, Sieck GC. Neuromotor Control in Chronic Obstructive Pulmonary Disease. J Appl Physiol. 2013
271. Maquirriain J, Ghisi JP, Kokalj AM. Rectus abdominis muscle strains in tennis players. Br J Sports Med. 2007; 41:842–848. [PubMed: 17957025]
272. Mardini IA, McCarter RJ. Contractile properties of the shortening rat diaphragm in vitro. J Appl Physiol. 1987; 62:1111–1116. [PubMed: 3571068]
273. Margulies SS, Farkas GA, Rodarte JR. Effects of body position and lung volume on in situ operating length of canine diaphragm. J Appl Physiol. 1990; 69:1702–1708. [PubMed: 2272964]
274. Margulies SS, Lei GT, Farkas GA, Rodarte JR. Finite-element analysis of stress in the canine diaphragm. J Appl Physiol. 1994; 76:2070–2075. [PubMed: 8063670]
275. Martin TP, Vailas AC, Durivage JB, Edgerton VR, Castleman KR. Quantitative histochemical determination of muscle enzymes: biochemical verification. J Histochem Cytochem. 1985; 33:1053–1059. [PubMed: 4045183]
276. Matsui T, Nagoshi T, Rosenzweig A. Akt and PI 3-kinase signaling in cardiomyocyte hypertrophy and survival. Cell Cycle. 2003; 2:220–223. [PubMed: 12734428]
277. Mayock DE, Standaert TA, Murphy TD, Woodrum DE. Diaphragmatic force and substrate reponse to resistive loaded breathing in the piglet. J Appl Physiol. 1991; 70:70–76. [PubMed: 2010411]
278. McArdle A, van der Meulen JH, Catapano M, Symons MC, Faulkner JA, Jackson MJ. Free radical activity following contraction-induced injury to the extensor digitorum longus muscles of rats. Free Radic Biol Med. 1999; 26:1085–1091. [PubMed: 10381177]
279. McCully KK, Faulkner JA. Length-tension relationship of mammalian diaphragm muscles. J Appl Physiol. 1983; 54:1681–1686. [PubMed: 6874493]
280. McCully KK, Faulkner JA. Injury to skeletal muscle fibers of mice following lengthening contractions. J Appl Physiol. 1985; 59:119–126. [PubMed: 4030553]
281. McKenzie DK, Bigland-Ritchie B, Gorman RB, Gandevia SC. Central and peripheral fatigue of human diaphragm and limb muscles assessed by twitch interpolation. J Physiol. 1992; 454:643–656. [PubMed: 1335508]
282. McKenzie DK, Allen GM, Butler JE, Gandevia SC. Task failure with lack of diaphragm fatigue during inspiratory resistive loading in human subjects. J Appl Physiol. 1997; 82:2011–2019. [PubMed: 9173971]

283. McKinsey TA, Zhang CL, Olson EN. Signaling chromatin to make muscle. Curr Opin Cell Biol. 2002; 14:763–772. [PubMed: 12473352]

284. McPhedran AM, Wuerker RB, Henneman E. Properties of motor units in a homogeneous red muscle (soleus) of the cat. J Neurophysiol. 1965; 28:71–84. [PubMed: 14244797]

285. Mendell LM. The size principle: a rule describing the recruitment of motoneurons. J Neurophysiol. 2005; 93:3024–3026. [PubMed: 15914463]

286. Merton PA. Voluntary strength and fatigue. J Physiol. 1954; 123:553–564. [PubMed: 13152698]

287. Metzger JM, Scheidt KB, Fitts RH. Histochemical and physiological characteristics of the rat diaphragm. J Appl Physiol. 1985; 58:1085–1091. [PubMed: 3988665]

288. Millar AG, Bradacs H, Charlton MP, Atwood HL. Inverse relationship between release probability and readily releasable vesicles in depressing and facilitating synapses. J Neurosci. 2002; 22:9661–9667. [PubMed: 12427821]

289. Minajeva A, Kulke M, Fernandez JM, Linke WA. Unfolding of titin domains explains the viscoelastic behavior of skeletal myofibrils. Biophys J. 2001; 80:1442–1451. [PubMed: 11222304]

290. Miyata H, Zhan WZ, Prakash YS, Sieck GC. Myoneural interactions affect diaphragm muscle adaptations to inactivity. J Appl Physiol. 1995; 79:1640–1649. [PubMed: 8594024]

291. Mizushima N, Yamamoto A, Matsui M, Yoshimori T, Ohsumi Y. In vivo analysis of autophagy in response to nutrient starvation using transgenic mice expressing a fluorescent autophagosome marker. Mol Biol Cell. 2004; 15:1101–1111. [PubMed: 14699058]

292. Monti RJ, Roy RR, Hodgson JA, Edgerton VR. Transmission of forces within mammalian skeletal muscles. J Biomech. 1999; 32:371–380. [PubMed: 10213027]

293. Moore AJ, Stubbings A, Swallow EB, Dusmet M, Goldstraw P, Porcher R, Moxham J, Polkey MI, Ferenczi MA. Passive properties of the diaphragm in COPD. J Appl Physiol. 2006; 101:1400–1405. [PubMed: 16840573]

294. Moore BJ, Feldman HA, Reid MB. Developmental changes in diaphragm contractile properties. J Appl Physiol. 1993; 75:522–526. [PubMed: 8226448]

295. Moss RL, Halpern W. Elastic and viscous properties of resting frog skeletal muscle. Biophys J. 1977; 17:213–228. [PubMed: 300253]

296. Moss RL, Lauer MR, Giulian GG, Greaser ML. Altered $Ca^{2+}$ dependence of tension development in skinned skeletal muscle fibers following modification of troponin by partial substitution with cardiac troponin C. J Biol Chem. 1986; 261:6096–6099. [PubMed: 3700385]

297. Mutungi G, Ranatunga KW. The viscous, viscoelastic and elastic characteristics of resting fast and slow mammalian (rat) muscle fibres. J Physiol. 1996; 496(Pt 3):827–836. [PubMed: 8930847]

298. Mutungi G, Ranatunga KW. Do cross-bridges contribute to the tension during stretch of passive muscle? A response. J Muscle Res Cell Motil. 2000; 21:301–302. [PubMed: 10952178]

299. Mutungi G. The effects of inorganic phosphate and arsenate on both passive muscle visco-elasticity and maximum Ca2+ activated tension in chemically skinned rat fast and slow twitch muscle fibres. J Muscle Res Cell Motil. 2003; 24:65–75. [PubMed: 12953837]

300. Naess K, Storm-Mathisen A. Fatigue of sustained tetanic contractions. Acta Physiologica Scandinavica. 1955; 44:363–383.

301. Nakashima K, Yakabe Y. AMPK activation stimulates myofibrillar protein degradation and expression of atrophy-related ubiquitin ligases by increasing FOXO transcription factors in C2C12 myotubes. Biosci Biotechnol Biochem. 2007; 71:1650–1656. [PubMed: 17617726]

302. Nelson, DL.; Cox, MM. Lehniger - Principles of Biochemistry. New York, NY: W.H. Freeman and Co.; 2005.

303. Nguyen T, Shrager J, Kaiser L, Mei L, Daood M, Watchko J, Rubinstein N, Levine S. Developmental myosin heavy chains in the adult human diaphragm: coexpression patterns and effect of COPD. J Appl Physiol. 2000; 88:1446–1456. [PubMed: 10749841]

304. Nosek TM, Fender KY, Godt RE. It is diprotonated inorganic phosphate that depresses force in skinned skeletal muscle fibers. Science. 1987; 236:191–193. [PubMed: 3563496]

305. Nystrom GJ, Lang CH. Sepsis and AMPK Activation by AICAR Differentially Regulate FoxO-1, -3 and -4 mRNA in Striated Muscle. Int J Clin Exp Med. 2008; 1:50–63. [PubMed: 19079687]

306. Oliven A, Carmi N, Coleman R, Odeh M, Silbermann M. Age-related changes in upper airway muscles morphological and oxidative properties. Exp Gerontol. 2001; 36:1673–1686. [PubMed: 11672988]

307. Oliven A, Odeh M, Geitini L, Oliven R, Steinfeld U, Schwartz AR, Tov N. Effect of coactivation of tongue protrusor and retractor muscles on pharyngeal lumen and airflow in sleep apnea patients. J Appl Physiol. 2007; 103:1662–1668. [PubMed: 17673558]

308. Oliven A, Tov N, Geitini L, Steinfeld U, Oliven R, Schwartz AR, Odeh M. Effect of genioglossus contraction on pharyngeal lumen and airflow in sleep apnoea patients. Eur Respir J. 2007; 30:748–758. [PubMed: 17567673]

309. Osborne S, Road JD. Diaphragm and phrenic nerve activities during inspiratory loading in anesthetized rabbits. Respir Physiol. 1995; 99:321–330. [PubMed: 7770667]

310. Osmond, DG. The Thorax; Part A: Physiology, Chapter 14 Functional Anatomy of the Chest Wall. New York, NY: Marcel Dekker, Inc.; 1995.

311. Ottenheijm CA, Heunks LM, Sieck GC, Zhan WZ, Jansen SM, Degens H, de Boo T, Dekhuijzen PN. Diaphragm dysfunction in chronic obstructive pulmonary disease. Am J Respir Crit Care Med. 2005; 172:200–205. [PubMed: 15849324]

312. Ottenheijm CA, Heunks LM, Hafmans T, van der Ven PF, Benoist C, Zhou H, Labeit S, Granzier HL, Dekhuijzen PN. Titin and diaphragm dysfunction in chronic obstructive pulmonary disease. Am J Respir Crit Care Med. 2006; 173:527–534. [PubMed: 16339921]

313. Ottenheijm CA, Heunks LM, Hafmans T, van der Ven PF, Benoist C, Zhou H, Labeit S, Granzier HL, Dekhuijzen PN. Titin and diaphragm dysfunction in chronic obstructive pulmonary disease. Am J Resp Crit Care Med. 2006; 173:527–534. [PubMed: 16339921]

314. Ottenheijm CA, Knottnerus AM, Buck D, Luo X, Greer K, Hoying A, Labeit S, Granzier H. Tuning passive mechanics through differential splicing of titin during skeletal muscle development. Biophys J. 2009; 97:2277–2286. [PubMed: 19843460]

315. Pandorf CE, Jiang W, Qin AX, Bodell PW, Baldwin KM, Haddad F. Regulation of an antisense RNA with the transition of neonatal to IIb myosin heavy chain during postnatal development and hypothyroidism in rat skeletal muscle. Am J Physiol Regul Integr Comp Physiol. 2012; 302:R854–867. [PubMed: 22262309]

316. Pardo JV, Siliciano JD, Craig SW. Vinculin is a component of an extensive network of myofibril-sarcolemma attachment regions in cardiac muscle fibers. J Cell Biol. 1983; 97:1081–1088. [PubMed: 6413511]

317. Parnas I. Differential block at high frequency of branches of a single axon innervating two muscles. J Neurophysiol. 1972; 35:903–914. [PubMed: 4347420]

318. Passerieux E, Rossignol R, Letellier T, Delage JP. Physical continuity of the perimysium from myofibers to tendons: involvement in lateral force transmission in skeletal muscle. J Struct Biol. 2007; 159:19–28. [PubMed: 17433715]

319. Patel JR, Diffee GM, Moss RL. Myosin regulatory light chain modulates the Ca2+ dependence of the kinetics of tension development in skeletal muscle fibers. Biophys J. 1996; 70:2333–2340. [PubMed: 9172757]

320. Patel ND, Jannapureddy SR, Hwang W, Chaudhry I, Boriek AM. Altered muscle force and stiffness of skeletal muscles in alpha-sarcoglycan-deficient mice. Am J Physiol Cell Physiol. 2003; 284:C962–968. [PubMed: 12620894]

321. Patel TJ, Lieber RL. Force transmission in skeletal muscle: from actomyosin to external tendons. Exerc Sport Sci Rev. 1997; 25:321–363. [PubMed: 9213097]

322. Pereon Y, Dettbarn C, Lu Y, Westlund KN, Zhang JT, Palade P. Dihydropyridine receptor isoform expression in adult rat skeletal muscle. Pflugers Arch. 1998; 436:309–314. [PubMed: 9644210]

323. Periasamy M, Kalyanasundaram A. SERCA pump isoforms: their role in calcium transport and disease. Muscle Nerve. 2007; 35:430–442. [PubMed: 17286271]

324. Perrie WT, Smillie LB, Perry SB. A phosphorylated light-chain component of myosin from skeletal muscle. Biochem J. 1973; 35:151–164. [PubMed: 4776866]

325. Peter JB, Barnard RJ, Edgerton VR, Gillespie CA, Stempel KE. Metabolic profiles of three fiber types of skeletal muscle in guinea pigs and rabbits. Biochemistry. 1972; 11:2627–2633. [PubMed: 4261555]
326. Pickart CM. Ubiquitin in chains. Trends Biochem Sci. 2000; 25:544–548. [PubMed: 11084366]
327. Pieribone VA, Shupliakov O, Brodin L, Hilfiker-Rothenfluh S, Czernik AJ, Greengard P. Distinct pools of synaptic vesicles in neurotransmitter release. Nature. 1995; 375:493–497. [PubMed: 7777058]
328. Polkey MI, Duguet A, Luo Y, Hughes PD, Hart N, Hamnegard CH, Green M, Similowski T, Moxham J. Anterior magnetic phrenic nerve stimulation: laboratory and clinical evaluation. Intensive Care Med. 2000; 26:1065–1075. [PubMed: 11030162]
329. Prado LG, Makarenko I, Andresen C, Kruger M, Opitz CA, Linke WA. Isoform diversity of giant proteins in relation to passive and active contractile properties of rabbit skeletal muscles. J Gen Physiol. 2005; 126:461–480. [PubMed: 16230467]
330. Prakash YS, Fournier M, Sieck GC. Effects of prenatal undernutrition on developing rat diaphragm. J Appl Physiol. 1993; 75:1044–1052. [PubMed: 8226510]
331. Prakash YS, Sieck GC. Age-related remodeling of neuromuscular junctions on type-identified diaphragm fibers. Muscle Nerve. 1998; 21:887–895. [PubMed: 9626248]
332. Prakash YS, Miyata H, Zhan WZ, Sieck GC. Inactivity-induced remodeling of neuromuscular junctions in rat diaphragmatic muscle. Muscle Nerve. 1999; 22:307–319. [PubMed: 10086891]
333. Pringle JW, Tregear RT. Mechanical properties of insect fibrillar muscle at large amplitudes of oscillation. Proc R Soc Lond B Biol Sci. 1969; 174:33–50. [PubMed: 4390451]
334. Proske U, Morgan DL. Do cross-bridges contribute to the tension during stretch of passive muscle? J Muscle Res Cell Motil. 1999; 20:433–442. [PubMed: 10555062]
335. Purslow PP, Trotter JA. The morphology and mechanical properties of endomysium in series-fibred muscles: variations with muscle length. J Muscle Res Cell Motil. 1994; 15:299–308. [PubMed: 7929795]
336. Puxkandl R, Zizak I, Paris O, Keckes J, Tesch W, Bernstorff S, Purslow P, Fratzl P. Viscoelastic properties of collagen: synchrotron radiation investigations and structural model. Philos Trans R Soc Lond B Biol Sci. 2002; 357:191–197. [PubMed: 11911776]
337. Rack PM, Westbury DR. The effects of length and stimulus rate on tension in the isometric cat soleus muscle. J Physiol. 1969; 204:443–460. [PubMed: 5824646]
338. Ranatunga KW. Sarcomeric visco-elasticity of chemically skinned skeletal muscle fibres of the rabbit at rest. J Muscle Res Cell Motil. 2001; 22:399–414. [PubMed: 11964066]
339. Rayment I, Holden HM, Whittaker M, Yohn CB, Lorenz M, Holmes KC, Milligan RA. Structure of the actin-myosin complex and its implications for muscle contraction. Science. 1993; 261:58–65. [PubMed: 8316858]
340. Rayment I, Holden HM, Sellers JR, Fananapazir L, Epstein ND. Three-dimensional structure of myosin subfragment-1: a molecular motor. Science. 1995; 261:50–58. [PubMed: 8316857]
341. Reed SA, Senf SM, Cornwell EW, Kandarian SC, Judge AR. Inhibition of IkappaB kinase alpha (IKKalpha) or IKKbeta (IKKbeta) plus forkhead box O (Foxo) abolishes skeletal muscle atrophy. Biochem Biophys Res Commun. 2011; 405:491–496. [PubMed: 21256828]
342. Reid B, Slater CR, Bewick GS. Synaptic vesicle dynamics in rat fast and slow motor nerve terminals. J Neurosci. 1999; 19:2511–2521. [PubMed: 10087065]
343. Reid MB, Feldman HA, Miller MJ. Isometric contractile properties of diaphragm strips from alcoholic rats. J Appl Physiol. 1987; 63:1156–1164. [PubMed: 3654462]
344. Reid MB, Miller MJ. Theophylline does not increase maximal tetanic force or diaphragm endurance in vitro. J Appl Physiol. 1989; 67:1655–1661. [PubMed: 2676958]
345. Reid MB, Haack KE, Franchek KM, Valberg PA, Kobzik L, West MS. Reactive oxygen in skeletal muscle: I. Intracellular oxidant kinetics and fatigue in vitro. J Appl Physiol. 1992; 73:1797–1804. [PubMed: 1474054]
346. Reid MB, Khawli FA, Moody MA. Reactive oxygen in skeletal muscle: III. Contractility of unfatigued muscle. J Appl Physiol. 1993; 75:1081–1087. [PubMed: 8226515]

347. Reid MB. Role of nitric oxide in skeletal muscle: synthesis, distribution and functional importance. Acta Physiol Scand. 1998; 162:401–409. [PubMed: 9578386]
348. Reid MB, Kobzik L, Bredt DS, Stamler JS. Nitric oxide modulates excitation-contraction coupling in the diaphragm. Comp Biochem Physiol A Mol Integr Physiol. 1998; 119:211–218. [PubMed: 11253787]
349. Reiser PJ, Moss RL, Giulian GG, Greaser ML. Shortening velocity in single fibers from adult rabbit soleus muscles is correlated with myosin heavy chain composition. J Biol Chem. 1985; 260:9077–9080. [PubMed: 4019463]
350. Richards DA, Guatimosim C, Rizzoli SO, Betz WJ. Synaptic vesicle pools at the frog neuromuscular junction. Neuron. 2003; 39:529–541. [PubMed: 12895425]
351. Ritchie JM. The relation between force and velocity of shortening in rat muscle. J Physiol. 1954; 123:633–639. [PubMed: 13152703]
352. Rizzoli SO, Betz WJ. The structural organization of the readily releasable pool of synaptic vesicles. Science. 2004; 303:2037–2039. [PubMed: 15044806]
353. Road J, Newman S, Derenne JP, Grassino A. In vivo length-force relationship of canine diaphragm. J Appl Physiol. 1986; 60:63–70. [PubMed: 3944047]
354. Romanello V, Guadagnin E, Gomes L, Roder I, Sandri C, Petersen Y, Milan G, Masiero E, Del Piccolo P, Foretz M, Scorrano L, Rudolf R, Sandri M. Mitochondrial fission and remodelling contributes to muscle atrophy. EMBO J. 2010; 29:1774–1785. [PubMed: 20400940]
355. Rommel C, Clarke BA, Zimmermann S, Nunez L, Rossman R, Reid K, Moelling K, Yancopoulos GD, Glass DJ. Differentiation stage-specific inhibition of the Raf-MEK-ERK pathway by Akt. Science. 1999; 286:1738–1741. [PubMed: 10576741]
356. Rommel C, Bodine SC, Clarke BA, Rossman R, Nunez L, Stitt TN, Yancopoulos GD, Glass DJ. Mediation of IGF-1-induced skeletal myotube hypertrophy by PI(3)K/Akt/mTOR and PI(3)K/Akt/GSK3 pathways. Nat Cell Biol. 2001; 3:1009–1013. [PubMed: 11715022]
357. Rowe J, Chen Q, Domire ZJ, McCullough MB, Sieck G, Zhan WZ, An KN. Effect of collagen digestion on the passive elastic properties of diaphragm muscle in rat. Med Eng Phys. 2010; 32:90–94. [PubMed: 19945332]
358. Rowley KL, Mantilla CB, Sieck GC. Respiratory muscle plasticity. Respir Physiol Neurobiol. 2005; 147:235–251. [PubMed: 15871925]
359. Rowley KL, Mantilla CB, Ermilov LG, Sieck GC. Synaptic vesicle distribution and release at rat diaphragm neuromuscular junctions. J Neurophysiol. 2007; 98:478–487. [PubMed: 17493926]
360. Sanchez J, Medrano G, Debesse B, Riquet M, Derenne JP. Muscle fibre types in costal and crural diaphragm in normal men and in patients with moderate chronic respiratory disease. Bull Eur Physiopathol Respir. 1985; 21:351–356. [PubMed: 4041660]
361. Sandercock TG, Faulkner JA, Albers JW, Abbrecht PH. Single motor unit and fiber action potentials during fatigue. J Appl Physiol. 1985; 58:1073–1079. [PubMed: 3988664]
362. Sandri M, Sandri C, Gilbert A, Skurk C, Calabria E, Picard A, Walsh K, Schiaffino S, Lecker SH, Goldberg AL. Foxo transcription factors induce the atrophy-related ubiquitin ligase atrogin-1 and cause skeletal muscle atrophy. Cell. 2004; 117:399–412. [PubMed: 15109499]
363. Sandri M. Signaling in muscle atrophy and hypertrophy. Physiology (Bethesda). 2008; 23:160–170. [PubMed: 18556469]
364. Sassoon CS, Caiozzo VJ, Manka A, Sieck GC. Altered diaphragm contractile properties with controlled mechanical ventilation. J Appl Physiol. 2002; 92:2585–2595. [PubMed: 12015377]
365. Schiaffino S, Gorza L, Sartore S, Saggin L, Ausoni S, Vianello M, Gundersen K, Lomo T. Three myosin heavy chain isoforms in type 2 skeletal muscle fibres. J Muscle Res Cell Motil. 1989; 10:197–205. [PubMed: 2547831]
366. Schiaffino, S.; Gorza, L.; Ausoni, S. Muscle fiber types expressing different myosin heavy chain isoforms. Their functional properties and adaptive capacity. In: Pette, D., editor. The Dynamic State of Muscle Fibers. Berlin: De Gruyter; 1990. p. 329-341.
367. Schiaffino S, Reggiani C. Molecular diversity of myofibrillar proteins: Gene regulation and functional significance. Physiol Rev. 1996; 76:371–423. [PubMed: 8618961]

368. Schnall RP, Pillar G, Kelsen SG, Oliven A. Dilatory effects of upper airway muscle contraction induced by electrical stimulation in awake humans. J Appl Physiol. 1995; 78:1950–1956. [PubMed: 7649934]
369. Schoenberg M. Equilibrium muscle cross-bridge behavior. Theoretical considerations. Biophys J. 1985; 48:467–475. [PubMed: 4041539]
370. Senf SM, Dodd SL, McClung JM, Judge AR. Hsp70 overexpression inhibits NF-kappaB and Foxo3a transcriptional activities and prevents skeletal muscle atrophy. FASEB J. 2008; 22:3836–3845. [PubMed: 18644837]
371. Seven YB, Mantilla CB, Zhan WZ, Sieck GC. Frequency-domain analysis of diaphragm muscle EMG activity across ventilatory and non-ventilatory motor behaviors. FASEB J. 2011; 25:1111.1124.
372. Seven YB, Mantilla CB, Zhan WZ, Sieck GC. Non-stationarity and power spectral shifts in EMG activity reflect motor unit recruitment in rat diaphragm muscle. Respir Physiol Neurobiol. 2013
373. Shindoh C, DiMarco A, Thomas A, Manubay P, Supinski G. Effect of N-acetylcysteine on diaphragm fatigue. J Appl Physiol. 1990; 68:2107–2113. [PubMed: 2361912]
374. Sieck DC, Zhan WZ, Fang YH, Ermilov LG, Sieck GC, Mantilla CB. Structure-activity relationships in rodent diaphragm muscle fibers vs. neuromuscular junctions. Respir Physiol Neurobiol. 2012; 180:88–96. [PubMed: 22063925]
375. Sieck GC, Roy RR, Powell P, Blanco C, Edgerton VR, Harper RM. Muscle fiber type distribution and architecture of the cat diaphragm. J Appl Physiol. 1983; 55:1386–1392. [PubMed: 6643176]
376. Sieck GC, Trelease RB, Harper RM. Sleep influences on diaphragmatic motor unit discharge. Exp Neurol. 1984; 85:316–335. [PubMed: 6745377]
377. Sieck GC, Sacks RD, Blanco CE, Edgerton VR. SDH activity and cross-sectional area of muscle fibers in cat diaphragm. J Appl Physiol. 1986; 60:1284–1292. [PubMed: 2939051]
378. Sieck GC. Diaphragm muscle: structural and functional organization. Clin Chest Med. 1988; 9:195–210. [PubMed: 3292123]
379. Sieck GC, Fournier M. Diaphragm motor unit recruitment during ventilatory and nonventilatory behaviors. J Appl Physiol. 1989; 66:2539–2545. [PubMed: 2745316]
380. Sieck GC, Fournier M, Enad JG. Fiber type composition of muscle units in the cat diaphragm. Neurosci Lett. 1989; 97:29–34. [PubMed: 2521928]
381. Sieck GC, Lewis MI, Blanco CE. Effects of undernutrition on diaphragm fiber size, SDH activity, and fatigue resistance. J Appl Physiol. 1989; 66:2196–2205. [PubMed: 2745285]
382. Sieck GC, Fournier M. Changes in diaphragm motor unit EMG during fatigue. J Appl Physiol. 1990; 68:1917–1926. [PubMed: 2163376]
383. Sieck GC. Neural control of the inspiratory pump. NIPS. 1991; 6:260–264.
384. Sieck GC. Diaphragm motor units and their response to altered use. Sem Respir Med. 1991; 12:258–269.
385. Sieck, GC.; Fournier, M. Developmental aspects of diaphragm muscle cells: Structural and functional organization. In: Haddad, GG.; Farber, JP., editors. Developmental Neurobiology of Breathing. New York: Marcel Dekker; 1991. p. 375-428.
386. Sieck GC. Physiological effects of diaphragm muscle denervation and disuse. Clin Chest Med. 1994; 15:641–659. [PubMed: 7867280]
387. Sieck, GC. Organization and recruitment of diaphragm motor units. In: Roussos, C., editor. The Thorax. New York, NY: Marcel Dekker; 1995. p. 783-820.
388. Sieck GC, Prakash YS. Fatigue at the neuromuscular junction. Branch point vs. presynaptic vs. postsynaptic mechanisms. Adv Exp Med Biol. 1995; 384:83–100. [PubMed: 8585479]
389. Sieck GC, Zhan WZ, Prakash YS, Daood MJ, Watchko JF. SDH and actomyosin ATPase activities of different fiber types in rat diaphragm muscle. J Appl Physiol. 1995; 79:1629–1639. [PubMed: 8594023]
390. Sieck GC, Fournier M, Prakash YS, Blanco CE. Myosin phenotype and SDH enzyme variability among motor unit fibers. J Appl Physiol. 1996; 80:2179–2189. [PubMed: 8806928]
391. Sieck, GC.; Prakash, YS. The diaphragm muscle. In: Miller, AD.; Bianchi, AL.; Bishop, BP., editors. Neural Control of the Respiratory Muscles. Boca Raton: CRC Press; 1996. p. 7-20.

392. Sieck GC, Wilson LE, Johnson BD, Zhan WZ. Hypothyroidism alters diaphragm muscle development. J Appl Physiol. 1996; 81:1965–1972. [PubMed: 8941517]
393. Sieck, GC.; Prakash, YS. The diaphragm muscle. In: Miller, AD.; Bianchi, AL.; Bishop, BP., editors. Neural Control of the Respitatory Muscles. Boca Raton, FL: CRC Press; 1997. p. 7-20.
394. Sieck GC, Prakash YS. Cross bridge kinetics in respiratory muscles. Eur Respir J. 1997; 10:2147–2158. [PubMed: 9311518]
395. Sieck GC, Han YS, Prakash YS, Jones KA. Cross-bridge cycling kinetics, actomyosin ATPase activity and myosin heavy chain isoforms in skeletal and smooth respiratory muscles. Comp Biochem Physiol. 1998; 119:435–450.
396. Sieck GC, Van Balkom RH, Prakash YS, Zhan WZ, Dekhuijzen PN. Corticosteroid effects on diaphragm neuromuscular junctions. J Appl Physiol. 1999; 86:114–122. [PubMed: 9887121]
397. Sieck GC, Zhan WZ. Denervation alters myosin heavy chain expression and contractility of developing rat diaphragm muscle. J Appl Physiol. 2000; 89:1106–1113. [PubMed: 10956357]
398. Sieck GC, Regnier M. Plasticity and energetic demands of contraction in skeletal and cardiac muscle. J Appl Physiol. 2001; 90:1158–1164. [PubMed: 11181631]
399. Sieck GC, Prakash YS, Han YS, Fang YH, Geiger PC, Zhan WZ. Changes in actomyosin ATP consumption rate in rat diaphragm muscle fibers during postnatal development. J Appl Physiol. 2003; 94:1896–1902. [PubMed: 12562672]
400. Sieck GC, Zhan WZ, Han YS, Prakash YS. Effect of denervation on ATP consumption rate of diaphragm muscle fibers. J Appl Physiol. 2007; 103:858–866. [PubMed: 17556500]
401. Sieck, GC.; Mantilla, CB. Neuromuscular Junction (NMJ): Aging. In: Hof, PR.; Mobbs, CV., editors. Handbook of the Neuroscience of Aging. London, UK, Burlington, MA, San Diego, CA: Elsevier Academic Press; 2009. p. 223-228.
402. Skurk C, Maatz H, Kim HS, Yang J, Abid MR, Aird WC, Walsh K. The Akt-regulated forkhead transcription factor FOXO3a controls endothelial cell viability through modulation of the caspase-8 inhibitor FLIP. J Biol Chem. 2004; 279:1513–1525. [PubMed: 14551207]
403. Smith DO. Mechanisms of action potential propagation failure at sites of axon branching in the crayfish. J Physiol (Lond). 1980; 301:243–259. [PubMed: 7411430]
404. Smith DO. Axon conduction failure under *in vivo* conditions in crayfish. J Physiol. 1983; 344:327–333. [PubMed: 6655584]
405. Smith IJ, Alamdari N, O'Neal P, Gonnella P, Aversa Z, Hasselgren PO. Sepsis increases the expression and activity of the transcription factor Forkhead Box O 1 (FOXO1) in skeletal muscle by a glucocorticoid-dependent mechanism. Int J Biochem Cell Biol. 2010; 42:701–711. [PubMed: 20079455]
406. Solomon V, Goldberg AL. Importance of the ATP-ubiquitin-proteasome pathway in the degradation of soluble and myofibrillar proteins in rabbit muscle extracts. J Biol Chem. 1996; 271:26690–26697. [PubMed: 8900146]
407. Somerville LL, Wang K. Sarcomere matrix of striated muscle: in vivo phosphorylation of titin and nebulin in mouse diaphragm muscle. Arch Biochem Biophys. 1988; 262:118–129. [PubMed: 3355162]
408. Staib JL, Swoap SJ, Powers SK. Diaphragm contractile dysfunction in MyoD gene-inactivated mice. Am J Physiol Regul Integr Comp Physiol. 2002; 283:R583–590. [PubMed: 12184991]
409. Stephens JA, Taylor A. Fatigue of maintained voluntary muscle contractions in man. J Physiol (Lond). 1972; 220:1–18. [PubMed: 5059236]
410. Stephens TJ, Chen ZP, Canny BJ, Michell BJ, Kemp BE, McConell GK. Progressive increase in human skeletal muscle AMPKalpha2 activity and ACC phosphorylation during exercise. Am J Physiol Endocrinol Metab. 2002; 282:E688–694. [PubMed: 11832374]
411. Stevens CF, Wesseling JF. Activity-dependent modulation of the rate at which synaptic vesicles become available to undergo exocytosis. Neuron. 1998; 21:415–424. [PubMed: 9728922]
412. Stienen GJ, Kiers JG, Bottinelli R, Reggiani C. Myofibrillar ATPase activity in skinned human skeletal muscle fibres: fibre type and temperature dependence. J Physiol. 1996; 493:299–309. [PubMed: 8782097]
413. Stitt TN, Drujan D, Clarke BA, Panaro F, Timofeyva Y, Kline WO, Gonzalez M, Yancopoulos GD, Glass DJ. The IGF-1/PI3K/Akt pathway prevents expression of muscle atrophy-induced

ubiquitin ligases by inhibiting FOXO transcription factors. Mol Cell. 2004; 14:395–403. [PubMed: 15125842]

414. Stockbridge N. Differential conduction at axonal bifurcations. II. Theoretical basis. J Neurophysiol. 1988; 59:1286–1295. [PubMed: 3373278]
415. Stockbridge N, Stockbridge LL. Differential conduction at axonal bifurcations. I. Effect of electrotonic length. J Neurophysiol. 1988; 59:1277–1285. [PubMed: 3373277]
416. Street SF. Lateral transmission of tension in frog myofibers: a myofibrillar network and transverse cytoskeletal connections are possible transmitters. J Cell Physiol. 1983; 114:346–364. [PubMed: 6601109]
417. Stromer MH. Immunocytochemistry of the muscle cell cytoskeleton. Microsc Res Tech. 1995; 31:95–105. [PubMed: 7655091]
418. Strumpf RK, Humphrey JD, Yin FC. Biaxial mechanical properties of passive and tetanized canine diaphragm. Am J Physiol. 1993; 265:H469–475. [PubMed: 8368350]
419. Sudhof TC. The synaptic vesicle cycle. Annu Rev Neurosci. 2004; 27:509–547. [PubMed: 15217342]
420. Supinski GS, Kelsen SG. Effect of elastase-induced emphysema on the force-generating ability of the diaphragm. J Clin Invest. 1982; 70:978–988. [PubMed: 6922866]
421. Supinski GS, Kelsen SG. Effect of elastase-induced emphysema on the force-generating ability of the diaphragm. J Clin Invest. 1982; 70:978–988. [PubMed: 6922866]
422. Swadlow HA, Kocsis JD, Waxman SG. Modulation of impulse conduction along the axonal tree. Annu Rev Biophys Bioeng. 1980; 9:143–179. [PubMed: 6994588]
423. Syme DA. Passive viscoelastic work of isolated rat, Rattus norvegicus, diaphragm muscle. J Physiol. 1990; 424:301–315. [PubMed: 2391652]
424. Sypert GW, Munson JB. Basis of segmental motor control: Motoneuron size or motor unit type? Neurosurg. 1981; 8:608–621.
425. Takada F, Vander Woude DL, Tong HQ, Thompson TG, Watkins SC, Kunkel LM, Beggs AH. Myozenin: an alpha-actinin- and gamma-filamin-binding protein of skeletal muscle Z lines. Proc Natl Acad Sci U S A. 2001; 98:1595–1600. [PubMed: 11171996]
426. Takahashi A, Kureishi Y, Yang J, Luo Z, Guo K, Mukhopadhyay D, Ivashchenko Y, Branellec D, Walsh K. Myogenic Akt signaling regulates blood vessel recruitment during myofiber growth. Mol Cell Biol. 2002; 22:4803–4814. [PubMed: 12052887]
427. Tatsumi R, Maeda K, Hattori A, Takahashi K. Calcium binding to an elastic portion of connectin/titin filaments. J Muscle Res Cell Motil. 2001; 22:149–162. [PubMed: 11519738]
428. Tawa NE Jr, Odessey R, Goldberg AL. Inhibitors of the proteasome reduce the accelerated proteolysis in atrophying rat skeletal muscles. J Clin Invest. 1997; 100:197–203. [PubMed: 9202072]
429. Taylor SR, Rudel R. Striated muscle fibers: inactivation of contraction induced by shortening. Science. 1970; 167:882–884. [PubMed: 5410851]
430. Termin A, Staron RS, Pette D. Myosin heavy chain isoforms in histochemically defined fiber types of rat muscle. Histochemistry. 1989; 92:453–457. [PubMed: 2530196]
431. Thornell LE, Price MG. The cytoskeleton in muscle cells in relation to function. Biochem Soc Trans. 1991; 19:1116–1120. [PubMed: 1794471]
432. Tidball JG. Energy stored and dissipated in skeletal muscle basement membranes during sinusoidal oscillations. Biophys J. 1986; 50:1127–1138. [PubMed: 3801573]
433. Timpl R. Proteoglycans of basement membranes. EXS. 1994; 70:123–144. [PubMed: 8298244]
434. Timpl R, Brown JC. The laminins. Matrix Biol. 1994; 14:275–281. [PubMed: 7827749]
435. Tong JF, Yan X, Zhu MJ, Du M. AMP-activated protein kinase enhances the expression of muscle-specific ubiquitin ligases despite its activation of IGF-1/Akt signaling in C2C12 myotubes. J Cell Biochem. 2009; 108:458–468. [PubMed: 19639604]
436. Topulos GP, Reid MB, Leith DE. Pliometric activity of inspiratory muscles: maximal pressure-flow curves. J Appl Physiol. 1987; 62:322–327. [PubMed: 3558191]

437. Trombitas K, Greaser M, French G, Granzier H. PEVK extension of human soleus muscle titin revealed by immunolabeling with the anti-titin antibody 9D10. J Struct Biol. 1998; 122:188–196. [PubMed: 9724620]

438. Trombitas K, Wu Y, McNabb M, Greaser M, Kellermayer MS, Labeit S, Granzier H. Molecular basis of passive stress relaxation in human soleus fibers: assessment of the role of immunoglobulin-like domain unfolding. Biophys J. 2003; 85:3142–3153. [PubMed: 14581214]

439. Trotter JA, Richmond FJ, Purslow PP. Functional morphology and motor control of series-fibered muscles. Exerc Sport Sci Rev. 1995; 23:167–213. [PubMed: 7556350]

440. Truong XT. Viscoelastic wave propagation and rheologic properties of skeletal muscle. Am J Physiol. 1974; 226:256–264. [PubMed: 4544064]

441. Tskhovrebova L, Trinick J, Sleep JA, Simmons RM. Elasticity and unfolding of single molecules of the giant muscle protein titin. Nature. 1997; 387:308–312. [PubMed: 9153398]

442. Tuck SA, Remmers JE. Mechanical properties of the passive pharynx in Vietnamese pot-bellied pigs. I. Statics. J Appl Physiol. 2002; 92:2229–2235. [PubMed: 12015331]

443. Tuck SA, Remmers JE. Mechanical properties of the passive pharynx in Vietnamese pot-bellied pigs. II. Dynamics. J Appl Physiol. 2002; 92:2236–2244. [PubMed: 12015332]

444. Tzelepis GE, Zakynthinos S, Mandros C, Tzelepis E, Roussos C. Respiratory muscle performance with stretch-shortening cycle manoeuvres: maximal inspiratory pressure-flow curves. Acta Physiol Scand. 2005; 185:251–256. [PubMed: 16218930]

445. van Balkom RHH, Zhan WZ, Prakash YS, Dekhuijzen PNR, Sieck GC. Corticosteroid effects on isotonic contractile properties of rat diaphragm muscle. J Appl Physiol. 1997; 83:1062–1067. [PubMed: 9338411]

446. Van Gammeren D, Damrauer JS, Jackman RW, Kandarian SC. The IkappaB kinases IKKalpha and IKKbeta are necessary and sufficient for skeletal muscle atrophy. FASEB J. 2009; 23:362–370. [PubMed: 18827022]

447. van Lunteren E, Strohl KP. The muscles of the upper airways. Clin Chest Med. 1986; 7:171–188. [PubMed: 3522067]

448. van Lunteren E, Haxhiu MA, Cherniack NS. Mechanical function of hyoid muscles during spontaneous breathing in cats. J Appl Physiol. 1987; 62:582–590. [PubMed: 3558217]

449. van Lunteren E, Salomone RJ, Manubay P, Supinski GS, Dick TE. Contractile and endurance properties of geniohyoid and diaphragm muscles. J Appl Physiol. 1990; 69:1992–1997. [PubMed: 2076992]

450. van Lunteren E, Dick TE. Intrinsic properties of pharyngeal and diaphragmatic respiratory motoneurons and muscles. J Appl Physiol. 1992; 73:787–800. [PubMed: 1400039]

451. van Lunteren E, Manubay P. Contractile properties of feline genioglossus, sternohyoid, and sternothyroid muscles. J Appl Physiol. 1992; 72:1010–1015. [PubMed: 1568954]

452. van Lunteren E, Martin RJ. Pharyngeal dilator muscle contractile and endurance properties in neonatal piglets. Respir Physiol. 1993; 92:65–75. [PubMed: 8511409]

453. van Lunteren E, Vafaie H, Salomone RJ. Comparative effects of aging on pharyngeal and diaphragm muscles. Respir Physiol. 1995; 99:113–125. [PubMed: 7740199]

454. van Lunteren E, Spiegler S, Moyer M. Differential expression of lipid and carbohydrate metabolism genes in upper airway versus diaphragm muscle. Sleep. 2010; 33:363–370. [PubMed: 20337195]

455. Verheul AJ, Mantilla CB, Zhan WZ, Bernal M, Dekhuijzen PN, Sieck GC. Influence of corticosteroids on myonuclear domain size in the rat diaphragm muscle. J Appl Physiol. 2004; 97:1715–1722. [PubMed: 15234958]

456. Vivanco I, Sawyers CL. The phosphatidylinositol 3-Kinase AKT pathway in human cancer. Nat Rev Cancer. 2002; 2:489–501. [PubMed: 12094235]

457. Volz LM, Mann LB, Russell JA, Jackson MA, Leverson GE, Connor NP. Biochemistry of anterior, medial, and posterior genioglossus muscle in the rat. Dysphagia. 2007; 22:210–214. [PubMed: 17458585]

458. Walmsley B, Hodgson JA, Burke RE. Forces produced by medial gastrocnemius and soleus muscles during locomotion in freely moving cats. J Neurophysiol. 1978; 41:1203–1216. [PubMed: 702192]

459. Wang K, Wright J. Architecture of the sarcomere matrix of skeletal muscle: immunoelectron microscopic evidence that suggests a set of parallel inextensible nebulin filaments anchored at the Z line. J Cell Biol. 1988; 107:2199–2212. [PubMed: 3058720]

460. Wang K, McCarter R, Wright J, Beverly J, Ramirez-Mitchell R. Viscoelasticity of the sarcomere matrix of skeletal muscles. The titin-myosin composite filament is a dual-stage molecular spring. Biophys J. 1993; 64:1161–1177. [PubMed: 8494977]

461. Wang K, Forbes JG, Jin AJ. Single molecule measurements of titin elasticity. Prog Biophys Mol Biol. 2001; 77:1–44. [PubMed: 11473785]

462. Wang R, Li Q, Tang DD. Role of vimentin in smooth muscle force development. Am J Physiol Cell Physiol. 2006; 291:C483–489. [PubMed: 16571866]

463. Wang X, Proud CG. The mTOR pathway in the control of protein synthesis. Physiology (Bethesda). 2006; 21:362–369. [PubMed: 16990457]

464. Watchko JF, Brozanski BS, O'Day TL, Guthrie RD, Sieck GC. Contractile properties of the rat external abdominal oblique and diaphragm muscles during development. J Appl Physiol. 1992; 72:1432–1436. [PubMed: 1592735]

465. Watchko JF, Daood MJ, Vazquez RL, Brozanski BS, LaFramboise WA, Guthrie RD, Sieck GC. Postnatal expression of myosin isoforms in an expiratory muscle--external abdominal oblique. J Appl Physiol. 1992; 73:1860–1866. [PubMed: 1474062]

466. Watchko JF, Sieck GC. Respiratory muscle fatigue resistance relates to myosin phenotype and SDH activity during development. J Appl Physiol. 1993; 75:1341–1347. [PubMed: 8226549]

467. Watchko JF, Johnson BD, Gosselin LE, Prakash YS, Sieck GC. Age-related differences in diaphragm muscle injury after lengthening activations. J Appl Physiol. 1994; 77:2125–2133. [PubMed: 7868424]

468. Watchko JF, Daood MJ, Sieck GC. Myosin heavy chain transitions during development. Functional implications for the respiratory musculature. Comp Biochem Physiol. 1998; 119:459–470.

469. Waxman SG. Integrative properties and design principles of axons. Int Rev Neurobiol. 1975; 18:1–40. [PubMed: 1107245]

470. Westerblad H, Allen DG. Changes of myoplasmic calcium concentration during fatigue in single mouse muscle fibers. J Gen Physiol. 1991; 98:615–635. [PubMed: 1761971]

471. Westerblad H, Dahlstedt AJ, Lannergren J. Mechanisms underlying reduced maximum shortening velocity during fatigue of intact, single fibers of mouse muscle. J Physiol. 1998; 510:269–277. [PubMed: 9625883]

472. Wiegand DA, Latz B. Effect of geniohyoid and sternohyoid muscle contraction on upper airway resistance in the cat. J Appl Physiol. 1991; 71:1346–1354. [PubMed: 1757357]

473. Wilcox P, Osborne S, Bressler B. Monocyte inflammatory mediators impair in vitro hamster diaphragm contractility. Am Rev Respir Dis. 1992; 146:462–466. [PubMed: 1489141]

474. Wilson DF. Depression, facilitation, and mobilization of transmitter at the rat diaphragm neuromuscular junction. Am J Physiol. 1979; 237:C31–C37. [PubMed: 37741]

475. Wilson DF, Cardaman RC. Age-associated changes in neuromuscular transmission in the rat. Am J Physiol. 1984; 247:C288–292. [PubMed: 6089579]

476. Wood SJ, Slater CR. The contribution of postsynaptic folds to the safety factor for neuromuscular transmission in rat fast- and slow-twitch muscles. J Physiol. 1997; 500:165–176. [PubMed: 9097941]

477. Xu W, Baribault H, Adamson ED. Vinculin knockout results in heart and brain defects during embryonic development. Development. 1998; 125:327–337. [PubMed: 9486805]

478. Yamasaki R, Berri M, Wu Y, Trombitas K, McNabb M, Kellermayer MS, Witt C, Labeit D, Labeit S, Greaser M, Granzier H. Titin-actin interaction in mouse myocardium: passive tension modulation and its regulation by calcium/S100A1. Biophys J. 2001; 81:2297–2313. [PubMed: 11566799]

479. Yan S, Gauthier AP, Similowski T, Faltus R, Macklem PT, Bellemare F. Force-frequency relationships of in vivo human and in vitro rat diaphragm using paired stimuli. Eur Respir J. 1993; 6:211–218. [PubMed: 8444292]

480. Yarom R, Sagher U, Havivi Y, Peled IJ, Wexler MR. Myofibers in tongues of Down's syndrome. J Neurol Sci. 1986; 73:279–287. [PubMed: 2941522]

481. Yasuda K, Anazawa T, Ishiwata S. Microscopic analysis of the elastic properties of nebulin in skeletal myofibrils. Biophys J. 1995; 68:598–608. [PubMed: 7696512]

482. Yu ZB, Gao F, Feng HZ, Jin JP. Differential regulation of myofilament protein isoforms underlying the contractility changes in skeletal muscle unloading. Am J Physiol Cell Physiol. 2007; 292:C1192–1203. [PubMed: 17108008]

483. Zhan WZ, Farkas GA, Schroeder MA, Gosselin LE, Sieck GC. Regional adaptations of rabbit diaphragm muscle fibers to unilateral denervation. J Appl Physiol. 1995; 79:941–950. [PubMed: 8567538]

484. Zhan WZ, Miyata H, Prakash YS, Sieck GC. Metabolic and phenotypic adaptations of diaphragm muscle fibers with inactivation. J Appl Physiol. 1997; 82:1145–1153. [PubMed: 9104851]

485. Zhan WZ, Watchko JF, Prakash YS, Sieck GC. Isotonic contractile and fatigue properties of developing rat diaphragm muscle. J Appl Physiol. 1998; 84:1260–1268. [PubMed: 9516192]

486. Zhao J, Brault JJ, Schild A, Cao P, Sandri M, Schiaffino S, Lecker SH, Goldberg AL. FoxO3 coordinately activates protein degradation by the autophagic/lysosomal and proteasomal pathways in atrophying muscle cells. Cell Metab. 2007; 6:472–483. [PubMed: 18054316]

487. Zucker RS, Regehr WG. Short-term synaptic plasticity. Annu Rev Physiol. 2002; 64:355–405. [PubMed: 11826273]

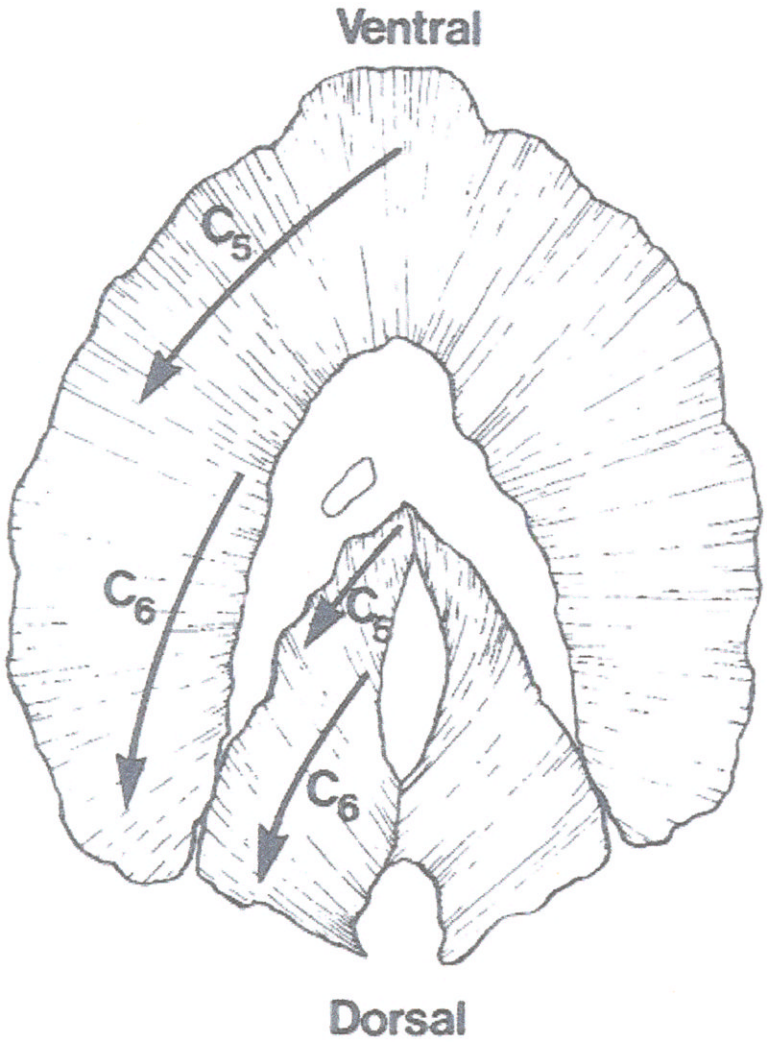


**Figure 1.**
Innervation of the cat diaphragm muscle. Phrenic nerve axons derived from the C4 segment of the cervical spinal cord innervate ventral aspects of the costal and crural regions of the diaphragm muscle, whereas axons derived from C6 innervate more dorsal aspects. Reproduced from ref. (378); used with permission.

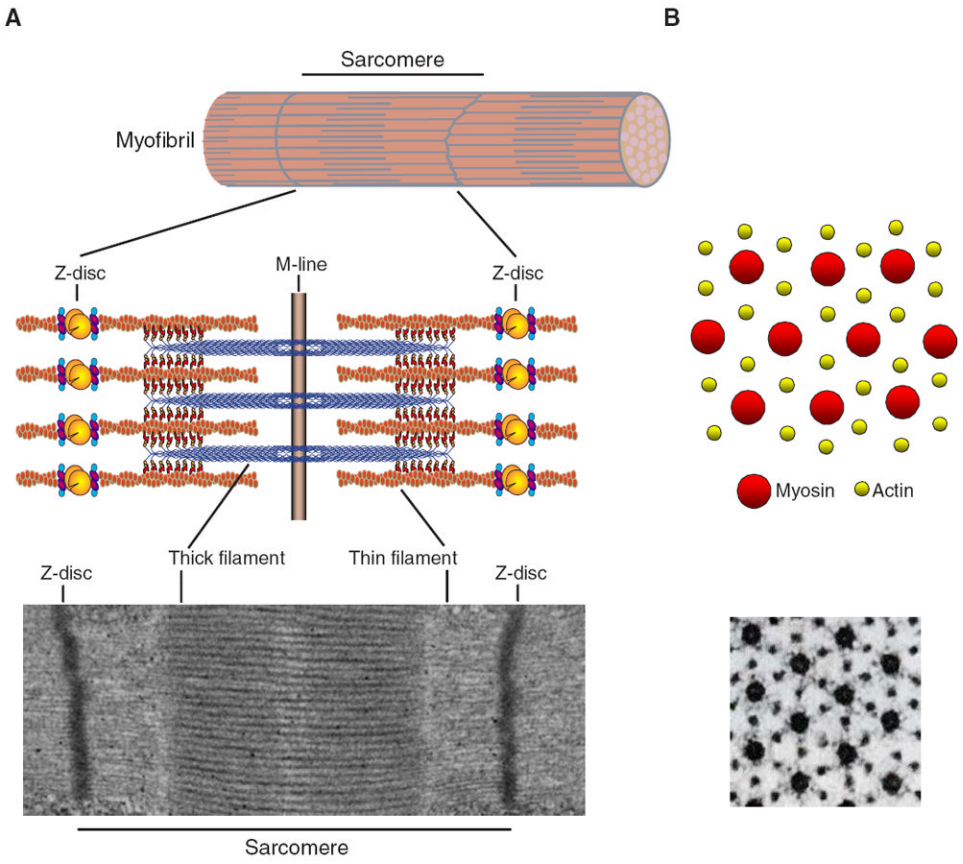


**Figure 2.**
Muscle fibers contain myofibrils (a), each comprising sarcomeres arranged in series which give muscle a striated appearance visible also in transmission electron micrographs. Thick and thin filaments in the sarcomere are composed of myosin (red) and actin (yellow), respectively, and their interaction provides the basis for force generation and contraction. In cross section, myosin and actin filaments are organized in a myofilament lattice, clearly visible with electron microscopy. Reproduced from ref. (167); used with permission.

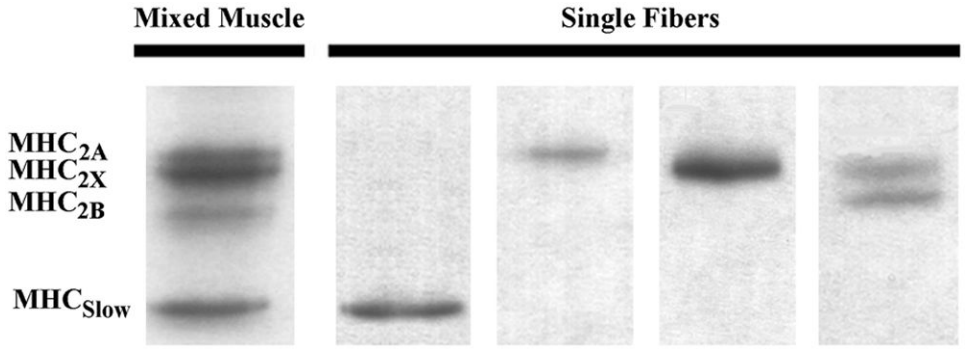


**Figure 3.**
Muscle fibers from the rat diaphragm muscle express a single myosin heavy chain (MyHC) isoform with the exception of $MyHC_{2X}$ and $MyHC_{2B}$ in some fibers. Modified from ref. (130)

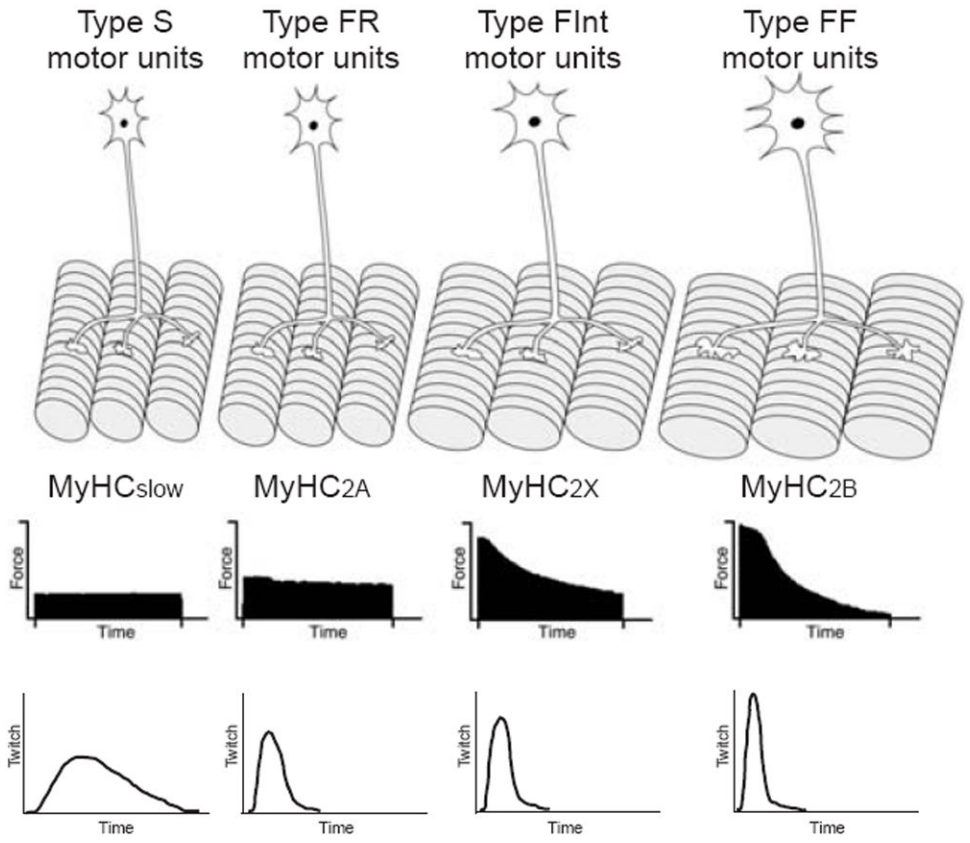


**Figure 4.**

Motor units are classified according to their contractile and fatigue properties as slow-twitch (type S) and as fast-twitch units, which display fatigue-resistant (type FR), fatigue-intermediate (type FInt) and fatigable (type FF) characteristics. Expression of MyHC isoforms by muscle fibers corresponds with motor unit properties. Contraction speeds also vary across motor unit types. Reproduced from ref. (156); used with permission.

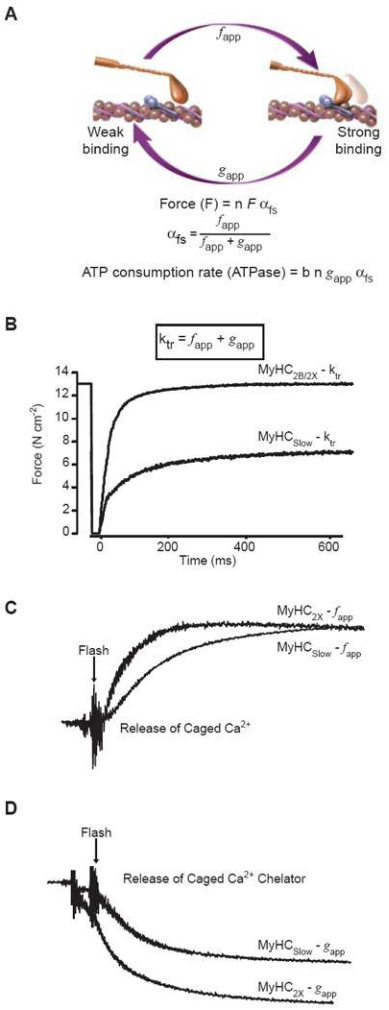


**Figure 5.**

Cross-bridges cycle between a strongly bound and an unbound state during force generation and contraction. Cross-bridge cycling determines rates of cross-bridge attachment ($f_{app}$) and detachment ($g_{app}$). Illustration copyrighted by the Mayo Clinic and Foundation and reproduced from ref. (398) with permission.

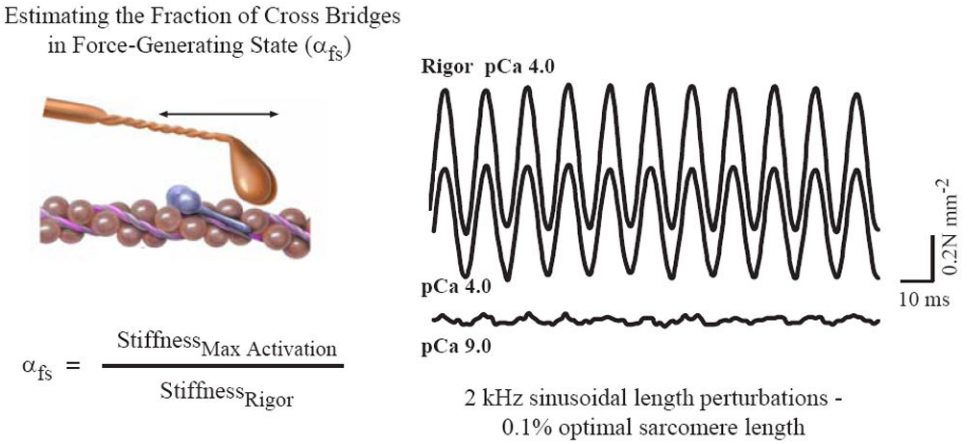


**Figure 6.**

Force measurements in single muscle fibers during maximal activation in rigor solution (without ATP and with free ionized $Ca^{2+}$ concentration of 100 μM, i.e., pCa 4.0), pCa4.0 solution (with ATP) and pCa9.0 solution (free ionized $Ca^{2+}$ concentration of 1 nM). Resting and activated stiffness were determined by imposing sinusoidal length oscillations (0.2% $L_o$) at 2kHz. Reproduced from ref. (174); used with permission.

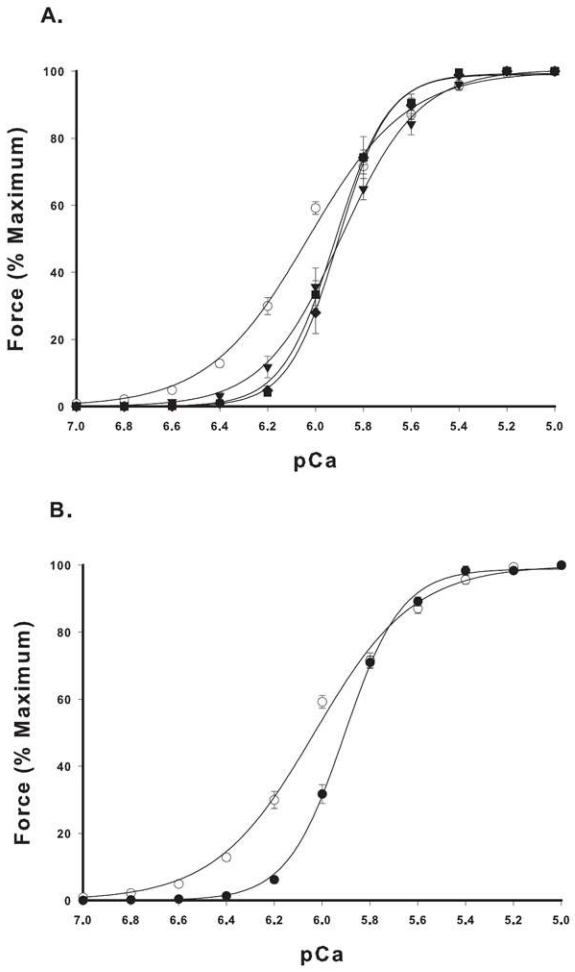


**Figure 7.**

Force development in single diaphragm muscle fibers expressing slow (open symbol) and fast (closed symbols – in A: $MyHC_{2A}$: ▼, $MyHC_{2X}$: ■, $MyHC_{2B}$ and/or $MyHC_{2X}$: ◆) isoforms of MyHC. Force depends on myoplasmic $Ca^{2+}$ concentrations (pCa; -log[$Ca^{2+}$]). Reproduced with permission from ref. (130).

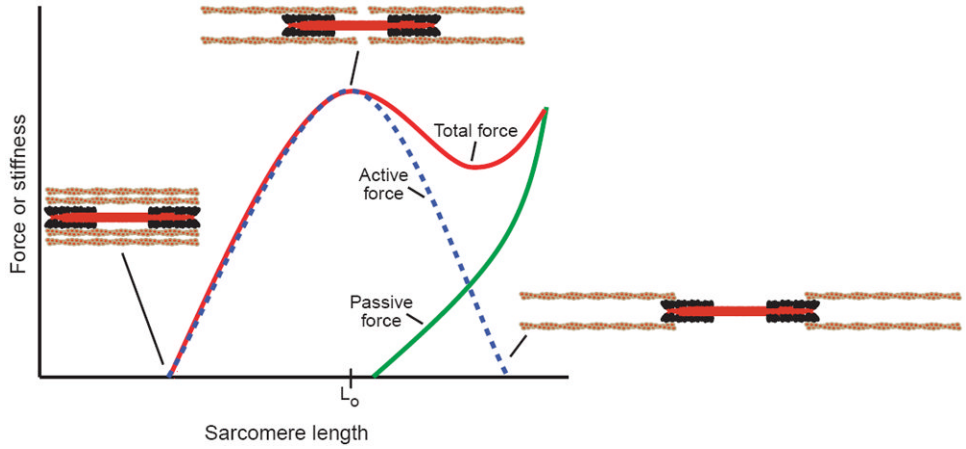


**Figure 8.**
Muscle force generation depends on sarcomere length and the overlap between thick and thin filaments, which determines the fraction of cross-bridges that can form ($\alpha_{fs}$). Reproduced from ref. (167); used with permission.

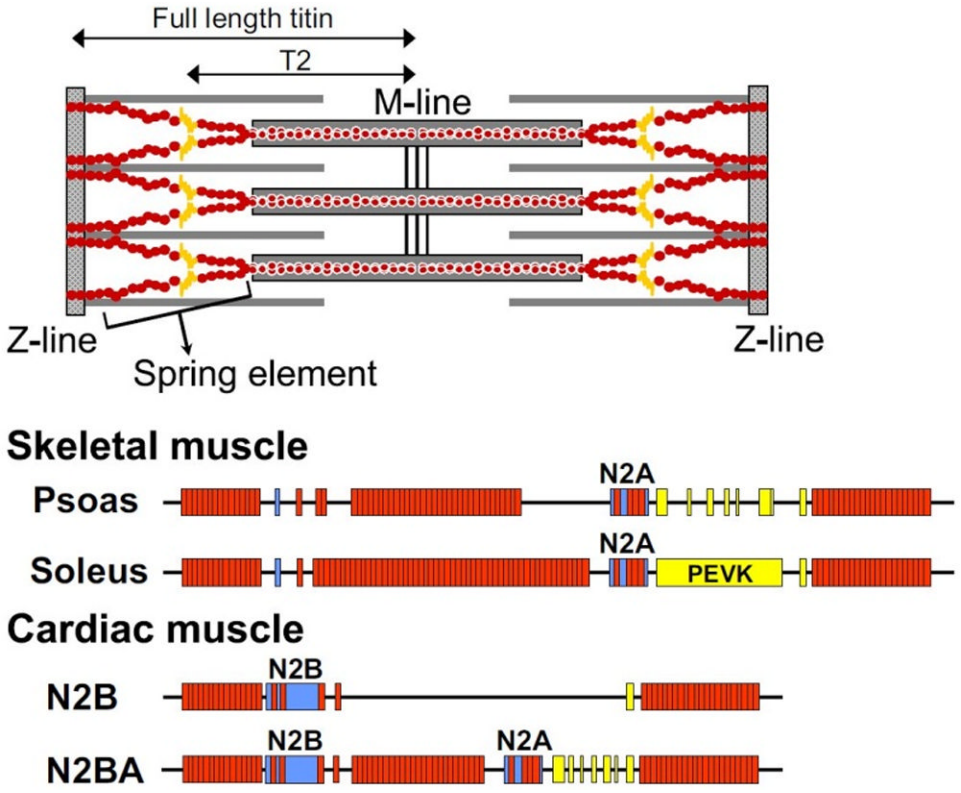


**Figure 9.**

Titin cDNA sequences for splice variants expressed in rabbit psoas and soleus muscles. Sequences predict differences in the I-band region of titin. Estimated protein molecular weight is show on the right. The longer segments in soleus contribute to lower titin-based passive tension. Titin-based passive tension is similar for diaphragm and soleus (329). Thus, we anticipate similar titin sequences for both muscles. Reproduced from ref. (125); used with permission from Springer®.

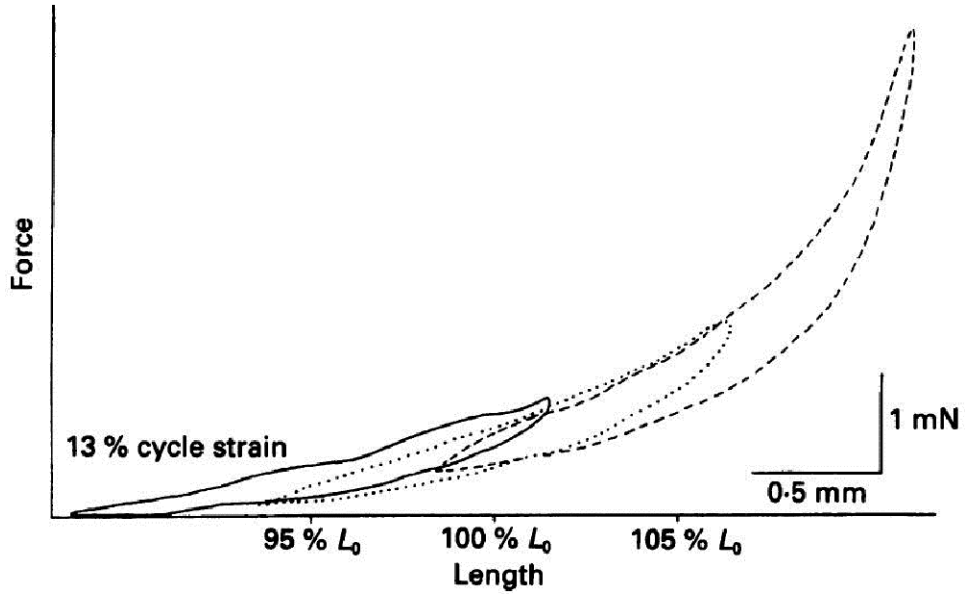


**Figure 10.**

Force-length relationship of rat diaphragm muscle during lengthening and shortening cycles. Results are from cycles of sinusoidal oscillations at 2 Hz and loops are displayed in clockwise orientation. $L_o$ is optimal length and cycle strain is the amplitude of oscillations as percentage of $L_o$. Note that passive force during lengthening is higher than during shortening (hysteresis). The amount of hysteresis depends on resting length of the diaphragm. Viscous work (area within each loop) increases at longer lengths. Reproduced from ref. (423); used with permission.

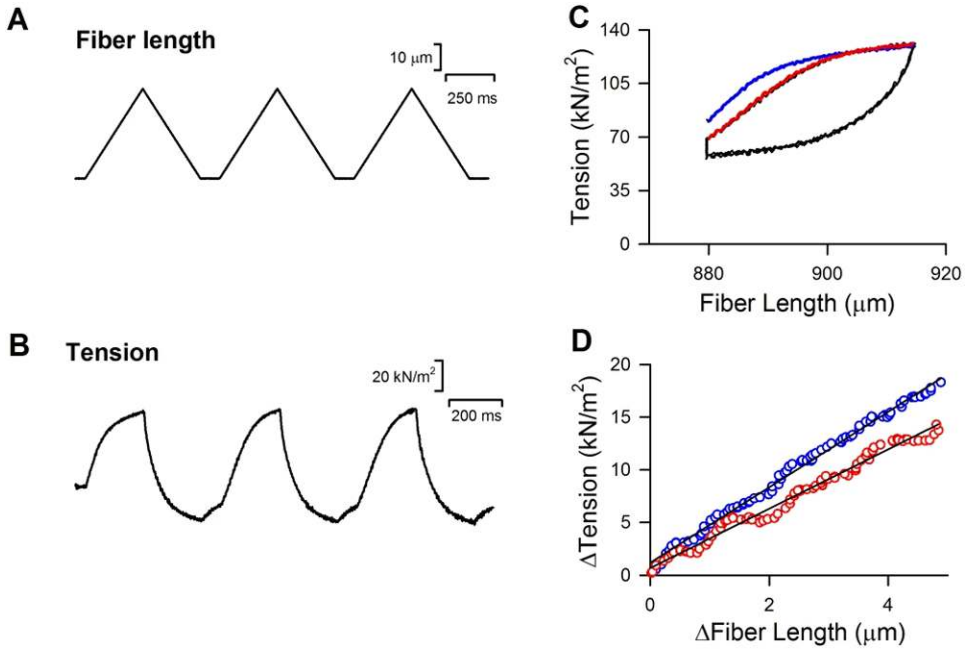


**Figure 11.**

Movement history-dependence (thixotropy) of length-tension relationship in diaphragm single fibers. Raw tracings of fiber length (*A*) and tension (*B*) in a chemically permeabilized fiber from mouse diaphragm (LF Ferreira, KS Campbell, and MB Reid; unpublished observations). Data collected during maximal calcium activation (pCa 4.5) at 15°C. Fiber was stretched by 35 μm from the optimal fiber length (879 μm; sarcomere length 2.586 μm). *C*) Relationship between tension and fiber length – data re-plotted from panel A. Hysteresis is greater in the first lengthening-shortening cycle than in subsequent cycles. The initial portions of the first and second cycles are traced by blue and red lines, respectively. *D*, Relationship between changes (Δ) in tension and fiber length shows a decrease in stiffness with a prior lengthening-shortening cycle, i.e., slope of relationship for second cycle (red circles) is approximately 30% lower than slope of first cycle (blue circles). Solid black lines are best fit from linear regression. For details on protocol and methods see Campbell & Moss (68) and Hardin et al. (175).

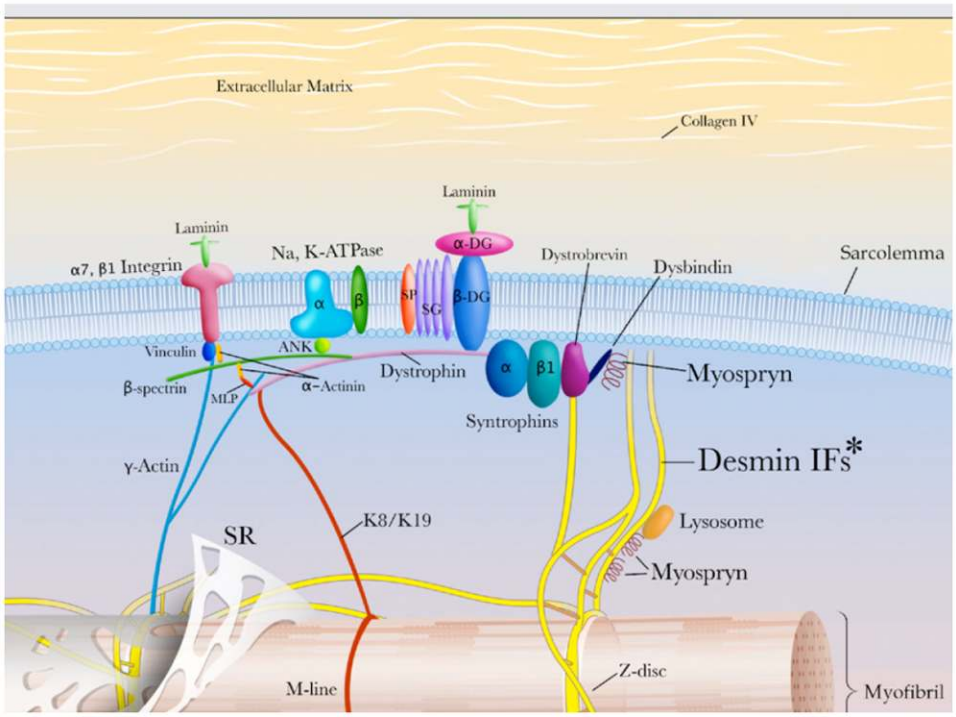


**Figure 12.**

Schematic illustration of proteins of the extracellular matrix, costamere, and intermediate filaments. The extracellular matrix and basement membrane include laminin, collagen IV, and intermediate filament (IF) proteins which include desmin (yellow) and keratins (K8/K19; red) plus other proteins not shown (synemin, paranemin, syncoilin). Desmin surrounds the Z-disks connecting myofibrils to each other and to the sarcolemma. Most IF proteins are linked to costameric proteins; keratin-containing IF are located around the M-line and also link to costameres. Ank, ankyrin; ANT, adenine nucleotide translocator; CK, creatine kinase; DG, dystroglycan; K, keratin; MLP, striated muscle-specific LIM protein; SP, sarcospan; SG, sarcoglycan; SR, sarcoplasmic reticulum. Reproduced from ref. (69); used with permission from Elsevier.

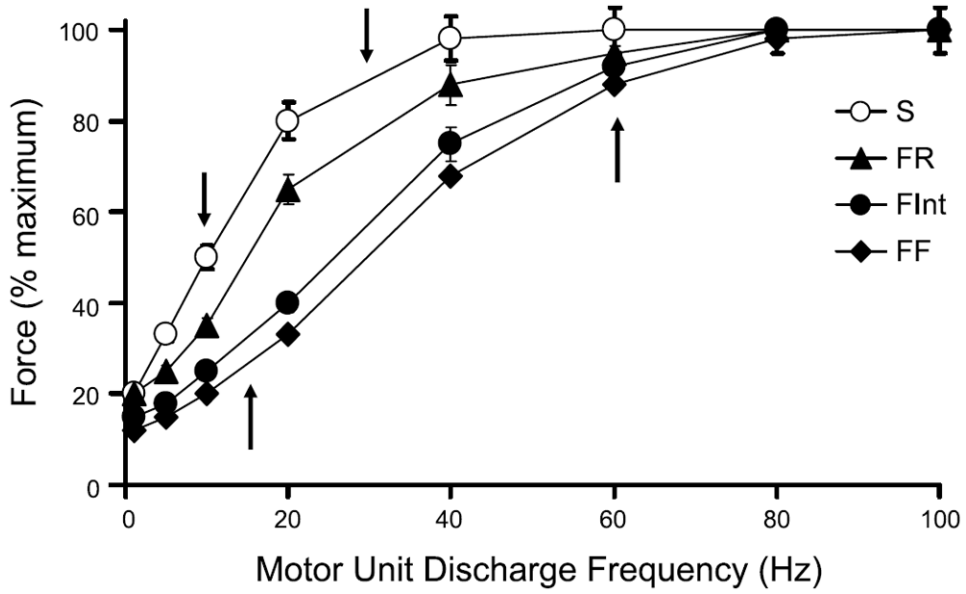


**Figure 13.**

Force (normalized to percent maximum tetanic force) generated by cat diaphragm motor units at different frequencies of stimulation. Results are for individual motor units classified by their contractile and fatigue properties (see text for details). The steepest portion of the force-frequency curve occurs between 10 and 30 Hz for all types of motor units in the diaphragm muscle (116), consistent with onset and peak discharge frequencies of ~8 Hz and ~25 Hz respectively for type S and FR units (top arrows) and ~15 Hz and ~60 Hz respectively for type FInt and FF units (bottom arrows), reported in (376).

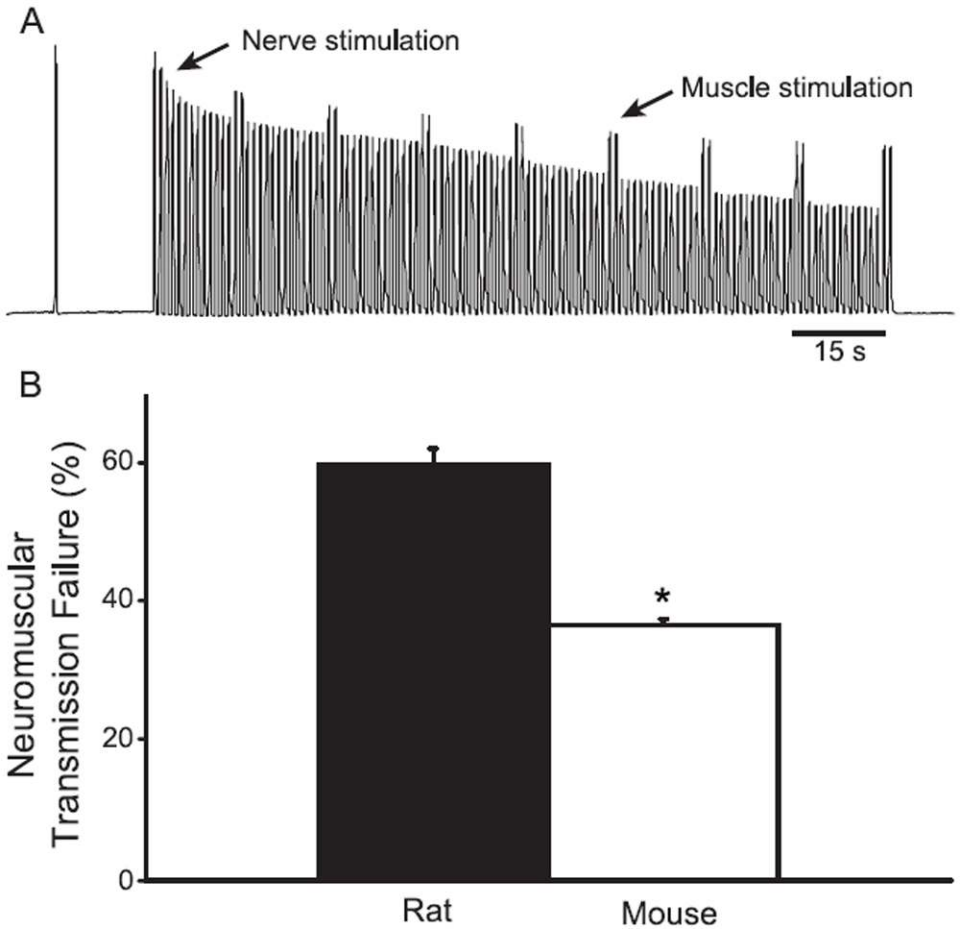


**Figure 14.**

Contribution of neuromuscular transmission failure to diaphragm muscle fatigue. Diaphragm muscle-phrenic nerve preparations are stimulated electrically every 1 s via a suction electrode to the phrenic nerve (40 Hz in 330-ms trains) and direct muscle stimulation via plate electrodes is superimposed intermittently every 15 s. A. Representative measurement of force developed by a mouse diaphragm muscle with repetitive stimulation. Reduced force generation by the diaphragm muscle reflects fatigue. The difference in force elicited by nerve and muscle stimulation reflects neuromuscular transmission failure. B. Neuromuscular transmission failure (mean ± SE) measured in diaphragm muscles from adult rats and mice. *, statistically significant difference. Reproduced from ref. (374); used with permission.

**Table 1**

Diaphragm muscle twitch characteristics at 35-37°C.

| | TPT (ms) | ½RT (ms) | $P_t$ (N/cm$^2$) | $P_t$:$P_o$ (%) | References |
|---|---|---|---|---|---|
| mouse | 10-15 | 10-15 | 5-8 | 20 - 30 | (113, 138, 175, 250, 408) |
| rat | 20-30 | 25-40 | 5-8 | 20 - 30 | (89, 215, 279, 287, 344, 346, 348) |
| cat | 30-70 | 40 | 10 | 25-40 | (116, 279) |
| dog | 50-60 | 60-70 | 6.5 | 30 | (105, 187, 279) |
| monkey | 30-40 | 30-40 | 6.5 | 30 | (107, 279) |
| human | 80-100 | 60-80 | 30-50** | 20 | (21, 328, 479) |

TPT, time to peak twitch force; ½ RT, relaxation time from maximum to half-maximum twitch force, $P_t$:$P_O$, twitch to tetanus force ratio

*Also, twitch force of 4.0 N/cm$^2$ were measured in rabbit diaphragm bundles in situ (373);

**twitch force reported as cm $H_2O$, not N/cm$^2$.